



## Review Paper

## Global review and synthesis of trends in observed terrestrial near-surface wind speeds: Implications for evaporation

Tim R. McVicar<sup>a,\*</sup>, Michael L. Roderick<sup>b</sup>, Randall J. Donohue<sup>a</sup>, Ling Tao Li<sup>a</sup>, Thomas G. Van Niel<sup>c</sup>, Axel Thomas<sup>d</sup>, Jürgen Grieser<sup>e</sup>, Deepak Jhajharia<sup>f</sup>, Youcef Himri<sup>g</sup>, Natalie M. Mahowald<sup>h</sup>, Anna V. Mescherskaya<sup>i</sup>, Andries C. Kruger<sup>j</sup>, Shafiqur Rehman<sup>k</sup>, Yagob Dinpashoh<sup>l</sup>

<sup>a</sup>CSIRO Land and Water, GPO Box 1666, Canberra, 2601 ACT, Australia

<sup>b</sup>Research School of Earth Sciences and Research School of Biology, The Australian National University, Canberra, 0200 ACT, Australia

<sup>c</sup>CSIRO Land and Water, Private Bag No. 5, Wembley, 6913 WA, Australia

<sup>d</sup>GIS-Service GmbH, Am Graben 1, 55263 Wackernheim, Germany and Institute of Geography, Johannes Gutenberg University, 55099 Mainz, Germany

<sup>e</sup>Risk Management Solutions, Peninsular House, 30 Monument Street, London EC3R 8NB, United Kingdom

<sup>f</sup>Department of Agricultural Engineering, North Eastern Regional Institute of Science & Technology (Deemed University), Nirjuli, Itanagar-791109, Arunachal Pradesh, India

<sup>g</sup>Société Nationale d'Electricité et du Gaz (SONELGAZ), Béchar, Algeria

<sup>h</sup>Department of Earth and Atmospheric Sciences, Cornell University, Snee 2140, Ithaca, NY 14853, USA

<sup>i</sup>Voikov Main Geophysical Observatory, 194021, St. Petersburg, Karbyshev 7, Russia

<sup>j</sup>South African Weather Service, Private Bag X097, Pretoria 0001, South Africa

<sup>k</sup>Center for Engineering Research, Research Institute, King Fahd University of Petroleum and Minerals, Dhahran 31261, Saudi Arabia

<sup>l</sup>Department of Water Engineering, Faculty of Agriculture, University of Tabriz, Tabriz, Iran

## ARTICLE INFO

## Article history:

Received 20 April 2011

Received in revised form 6 September 2011

Accepted 19 October 2011

Available online 29 October 2011

This manuscript was handled by Andras

Bardossy, Editor-in-Chief, with the

assistance of Efrat Morin, Associate Editor

## Keywords:

Climate change

Stilling

Evaporation paradox

Pan evaporation

Reference evapotranspiration

Trends

## SUMMARY

In a globally warming climate, observed rates of atmospheric evaporative demand have declined over recent decades. Several recent studies have shown that declining rates of evaporative demand are primarily governed by trends in the aerodynamic component (primarily being the combination of the effects of wind speed ( $u$ ) and atmospheric humidity) and secondarily by changes in the radiative component. A number of these studies also show that declining rates of observed near-surface  $u$  (termed 'stilling') is the primary factor contributing to declining rates of evaporative demand. One objective of this paper was to review and synthesise the literature to assess whether stilling is a globally widespread phenomenon. We analysed 148 studies reporting terrestrial  $u$  trends from across the globe (with uneven and incomplete spatial distribution and differing periods of measurement) and found that the average trend was  $-0.014 \text{ m s}^{-1} \text{ a}^{-1}$  for studies with more than 30 sites observing data for more than 30 years, which confirmed that stilling was widespread. Assuming a linear trend this constitutes a  $-0.7 \text{ m s}^{-1}$  change in  $u$  over 50 years. A second objective was to confirm the declining rates of evaporative demand by reviewing papers reporting trends in measured pan evaporation ( $E_{\text{pan}}$ ) and estimated crop reference evapotranspiration ( $ET_0$ ); average trends were  $-3.19 \text{ mm a}^{-2}$  ( $n = 55$ ) and  $-1.31 \text{ mm a}^{-2}$  ( $n = 26$ ), respectively. A third objective was to assess the contribution to evaporative demand trends that the four primary meteorological variables (being  $u$ ; atmospheric humidity; radiation; and air temperature) made. The results from 36 studies highlighted the importance of  $u$  trends. We also quantified the sensitivity of rates of evaporative demand to changes in  $u$  and how the relative contributions of the aerodynamic and radiative components change seasonally over the globe. Our review: (i) shows that terrestrial stilling is widespread across the globe; (ii) confirms declining rates of evaporative demand; and (iii) highlights the contribution  $u$  has made to these declining evaporative rates. Hence we advocate that assessing evaporative demand trends requires consideration of all four primary meteorological variables (being  $u$ , atmospheric humidity, radiation and air temperature). This is particularly relevant for long-term water resource assessment because changes in  $u$  exert greater influence on energy-limited water-yielding catchments than water-limited ones.

Crown Copyright © 2011 Published by Elsevier B.V. All rights reserved.

\* Corresponding author. Tel.: +61 2 6246 5741; fax: +61 2 6246 5800.

E-mail address: [tim.mcvicar@csiro.au](mailto:tim.mcvicar@csiro.au) (T.R. McVicar).

## Contents

1. Introduction	183
2. Trends of near-surface terrestrial wind speed	184
2.1. Global terrestrial review	184
2.2. Global terrestrial meta-analysis	185
2.3. Global (terrestrial and oceanic) synthesis	189
2.4. Possible causes of stilling	190
2.5. Implications for other disciplines	193
3. Trends in evaporative demand	194
4. Importance of wind speed to the evaporative process	197
4.1. Sensitivity analysis	197
4.2. Relative importance of aerodynamics on evaporation trends	198
5. Conclusion	199
Acknowledgements	201
Appendix A. Supplementary material	201
References	201

## 1. Introduction

Why in a globally warming climate have rates of observed pan evaporation ( $E_{\text{pan}}$ ) and estimated rates of fully physically-based models of both potential evapotranspiration ( $ET_p$ ) and crop reference evapotranspiration ( $ET_o$ ) declined at many sites over recent decades? The answer is that the evaporative process is primarily driven by radiative and aerodynamic components (the latter primarily being the combination of the effects of wind speed and atmospheric humidity). So, in addition to considering air temperature trends, which influence both the radiative and aerodynamic components, following the physically-based combination equation of evaporation set out by Penman (1948), trends in wind speed, atmospheric humidity and the radiative balance must also be considered to fully understand trends of  $E_{\text{pan}}$ ,  $ET_p$  or  $ET_o$  in a changing climate (e.g., Donohue et al., 2010; McKenney and Rosenberg, 1993).

The term ‘fully physically-based’ means that formulations of  $ET_p$  or  $ET_o$  must capture long-term trends of the four primary meteorological variables governing the evaporative process: wind speed ( $u$ ); atmospheric humidity; radiation; and air temperature. This is achieved by these four variables being explicitly used in the formulation. Using  $ET_p$  as an example, some formulations (e.g., Morton, 1983; Priestley and Taylor, 1972; Thornthwaite, 1948) are independent of  $u$ . As such, these models of  $ET_p$  imply that near-surface  $u$  is non-trending (meaning that a variable exhibits no long-term trend), and are therefore not considered to be fully physically-based in this paper. In contrast, other  $ET_p$  formulations (e.g., Penman, 1948) include  $u$  as a variable, so long-term  $u$  trends will explicitly influence assessment of long-term trends of Penman’s  $ET_p$  (see e.g., Donohue et al., 2010; McVicar et al., 2007 and the references therein for further discussion).

The concept of water-limited and energy-limited evaporation has long been used to understand the role of evaporation in the water balance at both hydroclimatologic (Budyko, 1974; Donohue et al., 2007) and agronomic (Philip, 1957; Ritchie, 1972) space and time scales. The hydroclimatologic terms ‘energy-limited’ and ‘water-limited’ are used here in preference to the equivalent agronomic terms of ‘constant rate stage (stage 1)’ and ‘falling rate stage (stage 2)’, respectively. This is, because the energy-limit – akin to the concept of  $ET_p$  – is not constant as it is both temporally variable (e.g., influenced by both seasonal variability and climate-change related trends Donohue et al., 2010) and spatially variable (e.g., related to topographic position McVicar et al., 2007). In the current paper the term ‘evaporation’ applies to: (i)  $E_{\text{pan}}$ ; (ii)  $ET_p$ ; (iii)  $ET_o$ ; and (iv) **may** apply to actual evapotranspiration ( $ET_a$ ) depending on water availability. For  $ET_a$  we say **may**, as if an area is severely water-limited (e.g., a dryland farm in drought) then

changing atmospheric conditions may negligibly change  $ET_a$  rates – as in this case  $ET_a$  rates are already limited by water availability (e.g., Kalma et al., 2008; Roderick et al., 2009). Whereas if assessing  $ET_a$  following irrigation, rainfall or in a climatologically moist headwater catchment (all energy-limited conditions, where the rate of energy supply, not water supply, limits  $ET_a$ ) then changing atmospheric conditions are important. Such energy-limited landscapes and catchments are significant (e.g., Viviroli et al., 2007; Viviroli et al., 2011). Irrigated areas produce ~40% of the world’s food (Postel, 1998; Postel et al., 1996), and over half the global population live in river catchments that originate in energy-limited landscapes (Beniston, 2005); this water supports about 25% of the global gross domestic product (Barnett et al., 2005). Hence it is important to understand how changes in  $u$  will impact the evaporative process in energy-limited landscapes and headwater catchments, especially as changes in  $ET_a$  effectively translate to changes in streamflow from these catchments (Donohue et al., 2011). In such catchments a decrease in  $ET_a$  results in increasing streamflow, and vice versa. The location of the climatological annual-average energy-limited landscapes is shown in Fig. 1 and the percentage area by continent and country which are energy-limited are provided in Table 1. Of course, the dynamics of areas considered to be water-limited depends on both evaporative demand and precipitation.

Given the role of  $u$  influencing evaporation (which is usually the largest extractive term of the water balance) and that declining near-surface  $u$  trends (termed ‘stilling’ Roderick et al., 2007) has recently been shown to be an important factor explaining the ‘pan evaporation paradox’ (e.g., Roderick et al., 2007; Zheng et al., 2009) our first objective was to perform a comprehensive review of observed terrestrial  $u$  trends from across the globe. Our second objective was to confirm how widespread declining rates of evaporative demand were, by reviewing papers reporting  $E_{\text{pan}}$  and  $ET_o$  trends. Our third objective was to illustrate, by review and modeling, the importance  $u$  trends have on the evaporative process. To address these three objectives the remainder of this paper is structured as follows:

- (i) we (a) illustrate the widespread nature of stilling by reviewing observed  $u$  changes, (b) perform meta-analysis, (c) synthesise a general global (terrestrial and oceanic) pattern, (d) discuss the likely causes of stilling, and (e) identify terrestrially-based disciplines, other than hydrology, that are likely to be affected by declining  $u$  (Section 2);
- (ii) we review studies that report trends in  $E_{\text{pan}}$  and  $ET_o$ , and review papers that assess the relative contributions of the four primary meteorological variables to observed evaporative trends (Section 3);

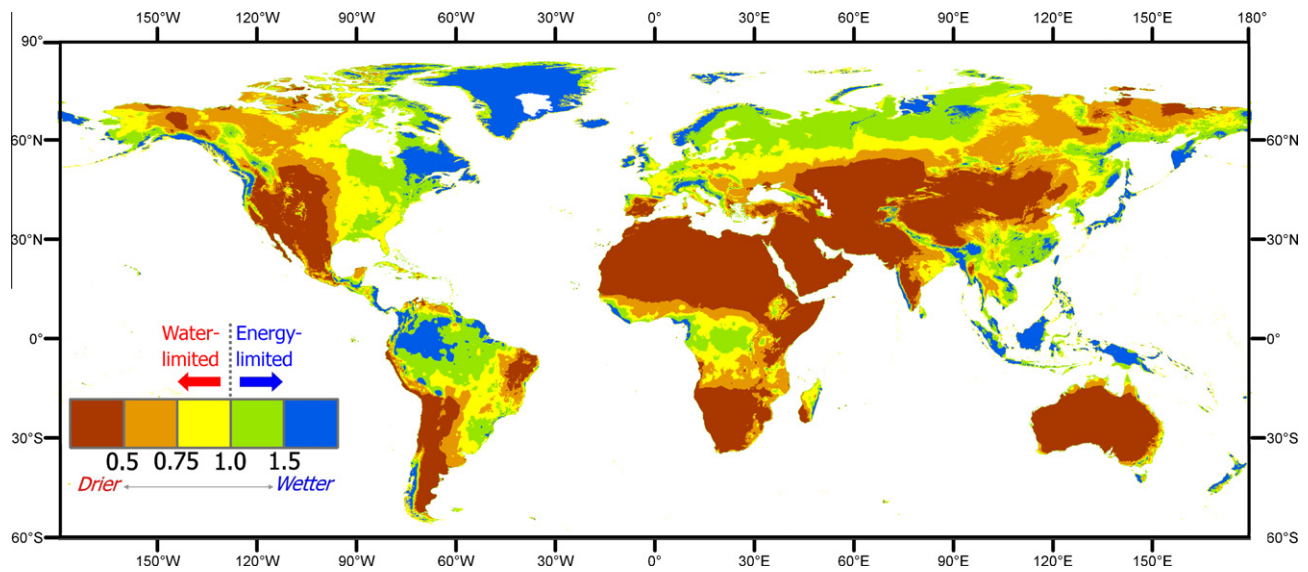


**Fig. 1.** Global distribution of energy-limited and water-limited areas. The long-term (1950–2000) annual average  $P$ /annual average  $ET_p$  ratio is shown. Assuming that precipitation is the only source of water, areas where this ratio is  $>1.0$  are described as energy-limited (as  $ET_a$  is limited by energy, not water) and areas where the ratio is  $<1.0$  are termed water-limited ( $ET_a$  is limited by water, not energy). See Donohue et al. (2007, and the references therein) for an introduction to the Budyko framework. Precipitation data are from Hijmans et al. (2005) and the evaporation data are from Zomer et al. (2008); both have a spatial resolution of 30 arc-seconds ( $\sim 1$  km at the equator).

- (iii) we quantify the sensitivity of  $E_{pan}$ ,  $ET_p$ , and  $ET_o$  rates to changes in  $u$  (Section 4); and
- (iv) finally conclusions are made (Section 5).

## 2. Trends of near-surface terrestrial wind speed

### 2.1. Global terrestrial review

In this sub-section we review 148 regional studies that present linear trends of  $u$ , as measured by terrestrial anemometers (see Table 2). Their spatial distribution over the global land-surface is shown in Fig. 2, and the temporal periods of measurement are illustrated in Fig. 3. As the vast majority of studies we review provide no information on the anemometer type, or its calibration, we

were unable to report on these. We strongly encourage future studies reporting observed  $u$  trends to provide this information, as an indication of the reliability of the results. The linear trends are calculated using ordinary linear regression (OLR), with year as the abscissa (or X-axis) and annual average  $u$  as the ordinate (or Y-axis), the resulting trends have units of  $m\ s^{-1}\ a^{-1}$  (units: metres per second per annum). While it could be argued that using OLR (a parametric test) to quantify trends is problematic, due to the inherent assumption that the annual average  $u$  series are temporally independent, and therefore a statistical test accounting for temporal autocorrelation may be better suited to  $u$  trend detection, we use OLR for two reasons. Firstly, our paper reviews existing studies that report trends observed in terrestrial  $u$  from across the globe; the majority of which have only reported trends using

**Table 1**  
Percent areas of continents and the 10-largest countries (in descending order of size) that are climatologically energy-limited (i.e., moist). The water-limited areas are the complement, i.e., water limited areas can be calculated as  $100 - \text{energy-limited percent area}$ . Similar analyses for all 169 countries  $>5000\ km^2$  are provided as Supplementary material Table 1. The energy-limited areas are where long-term (1950–2000) annual average  $P$ /annual average  $ET_p$  is  $>1.0$ , using  $P$  and  $ET_p$  data from Hijmans et al. (2005) and Zomer et al. (2008), respectively. Ann represents the annual time-step, with DJF referring to the season defined by December, January and February (and so on for the remaining seasons), and the 12 months are listed. Values assume that precipitation is the only source of water and do not account for water storage dynamics. The continents are abbreviated as: As = Asia; NA = North America; Eu = Europe; Af = Africa; SA = South America; Oc = Oceania (including Australia), with Antarctica not shown.

	ANN	DJF	MAM	JJA	SON	Jan	Feb	Mar	Apr	May	Jun	Jul	Aug	Sep	Oct	Nov	Dec
<i>Continents</i>																	
As	28	66	22	18	52	68	64	48	31	12	14	19	25	44	52	59	66
NA	43	87	39	18	79	87	84	79	49	20	15	16	31	64	76	85	88
Eu	55	99	19	5	83	99	98	80	22	6	4	4	16	57	84	99	100
Af	7	18	12	18	13	17	17	18	15	12	12	18	21	18	13	13	18
SA	43	50	53	34	27	50	52	52	53	45	41	34	26	22	29	41	46
Oc	8	12	10	15	6	13	16	13	9	14	17	16	12	8	5	4	6
<i>Countries</i>																	
Russia	42	100	27	3	93	100	100	88	47	3	1	3	16	67	93	100	100
Canada	40	100	37	5	94	100	100	95	56	8	2	3	19	75	93	99	100
USA	22	75	15	3	52	77	68	60	19	3	2	3	15	27	45	69	79
China	18	30	12	30	14	36	28	12	12	15	24	34	32	23	12	16	26
Brazil	53	77	64	23	26	77	78	76	63	42	30	22	14	13	30	54	69
Australia	3	9	5	10	1	11	14	9	4	9	13	11	7	3	1	1	3
India	17	6	7	67	26	7	6	5	5	10	28	75	73	69	24	5	6
Kazakhstan	0	90	1	0	2	91	77	6	1	0	0	0	0	0	14	71	95
Argentina	3	0	15	23	1	1	1	5	18	29	39	28	10	4	3	0	0
Sudan	0	0	0	20	0	0	0	0	0	3	8	27	34	9	2	0	0

OLR (with different start- and end-dates and with an uneven and incomplete coverage of the global land-surface). Secondly, when annual average  $u$  is the dependent variable, several studies have shown that there are negligible differences between resultant  $u$  trends calculated with OLR or those where temporal autocorrelation is accounted for (see Table 3). Additionally, in Table 2 we do not report results of significance testing of  $u$  trends as: (i) not all previous studies report this; (ii) if performed, methods of significance testing are not standardised; and (iii) if performed, the probability level to determine significance (or not) is arbitrarily selected and usually there is no discussion of how this threshold relates to process significance (or not); see Nicholls (2001, and the references therein for more discussion of this issue).

It should be noted that the values presented in Table 2 are long-term linear  $u$  trends, which may mask spatial and temporal variability. Firstly, when averages for entire countries, even continents, are reported these figures can mask the  $u$  increases in some regions. As examples: (i) while the contiguous-USA  $u$  trend has declined, Pryor and Ledolter (2010) show an increase for the western USA; and (ii) McVicar et al. (2008) reported increasing  $u$  trend in southeast Queensland/northeast New South Wales, and southern Victoria and Tasmania though most of Australia had experienced stilling. Secondly, as the trends are the rate of change of annual average  $u$ , this means seasonal changes in  $u$  trends are masked (e.g., Guo et al., 2011; McVicar et al., 2010). Analysing data from across the contiguous United States from 1961 to 1990 at ~180 stations Klink (1999, Table 5) showed that while the average trend of mean monthly  $u$  was declining ( $-0.004 \text{ m s}^{-1} \text{ a}^{-1}$ ), the average trend for mean monthly  $u$  maxima was increasing ( $+0.004 \text{ m s}^{-1} \text{ a}^{-1}$ ). In contrast from 1979 through 2008 Vautard et al. (2010, Fig. 2) show that strong winds (i.e.,  $u > 9 \text{ m s}^{-1}$ ) have rapidly declined in both Central Asia and Eastern Asia, slowly declined in Europe, and were non-trending for North America. Also note the differences in  $u$  trends calculated at Blue Hill Observatory for the two time periods by comparing records 15 and 16 in Table 2.

In addition to the studies summarised in Table 2 (where average  $u$  trends with units of  $\text{m s}^{-1} \text{ a}^{-1}$  have been reported or can be derived) several other studies report different  $u$  metrics also showing decreases, including:

- (i) Groisman et al. (2004, Section 4i, p. 77) report a change of  $\sim 0.1\% \text{ a}^{-1}$  of  $u$  observed at 10 m using  $\sim 1300$  stations over the contiguous USA for 1950–2000;
- (ii) Pryor et al. (2007, Fig. 3) report that over the contiguous USA the annual 50th percentile of  $u$  decreased significantly ( $P = 0.1$ ) for 118 (out of 157) stations for 1973–2005;
- (iii) Burn and Hesch (2007, Table 1) for southern-central Canada from 1951–2000 report that  $u$  significantly ( $P = 0.1$ ) decreased for the warm season (i.e., April through October) at 73% (or 22) of the 30 sites (and  $u$  only increased significantly ( $P = 0.1$ ) at one site – for the remaining seven sites there was no significant ( $P = 0.1$ )  $u$  trend);
- (iv) Xu et al. (2005, Table V) report that over all of East Asia from 1971–2000 that 27 of 32 stations exhibited stilling;
- (v) Wang et al. (2007, Fig. 3) show significant (99% confidence level) declining  $u$  trends for 115 stations from 1961–2000 for the entire Yangtze River Basin, China;
- (vi) Jhajharia et al. (2009, Table 6) document that 8 of 11 stations from  $\sim 1970$ – $\sim 2000$  in north-east India exhibited stilling at an annual time-step;
- (vii) Smits et al. (2005, Fig. 5) show that the frequency of weak, moderate and severe storm events at 13 Dutch stations for 1962–2002 decreased by approximately 10% decade $^{-1}$ ;
- (viii) Cabalar Fuentes (2005) report less frequent storms (decreasing from  $\sim 5$  to  $\sim 4$  events  $\text{a}^{-1}$ ; their Fig. 2) having shorter durations (decreasing from  $\sim 5$  to  $\sim 4$  days event $^{-1}$ ; their Fig. 3) yet with a non-trending change in the average maximum  $u$  over the rain-storm events ( $\sim 83 \text{ km/h}$ ; their Table 3) at three Atlantic coastal stations near Galicia, north-western Spain from 1961–2001;
- (ix) Mescherskaya et al. (2006, Table 1) using 23 stations located in northern Russia (i.e.,  $>60^\circ\text{N}$ ) from 1936–2000 report a 20–40% increase in the frequency of light  $u$  (i.e.,  $2$ – $5 \text{ m s}^{-1}$ ) with an associated decrease of stronger  $u$  (except for the coastal stations located on the Arctic Ocean and the Sea of Okhotsk);
- (x) Sweeney (2000, Table 3) reports a declining trend of  $-1.4$  days decade $^{-1}$  for days with gusts exceeding  $30 \text{ m s}^{-1}$  at Dublin from 1910–1999;
- (xi) Hewston and Dorling (2011, their Conclusions) from across the UK for 43 sites from 1980–2005 report that daily maximum  $u$  gusts (DMuG) declined by  $-0.02 \text{ m s}^{-1} \text{ a}^{-1}$ , and that ‘extreme DMuG’ (defined as the 98th percentile of the DMuG population, i.e., a 190-day subset of the 26-year record) declined by  $-0.08 \text{ m s}^{-1} \text{ a}^{-1}$ ; and
- (xii) Fujibe (2011, Section 5) reports that for 327 stations covering Japan from 1979–2008 the average  $u$  declined by  $-3\% \text{ decade}^{-1}$ .

In contrast with the above studies that report declining trends using various  $u$  metrics, several other studies report increasing trends using various  $u$  metrics, including:

- (i) Fujii (2007, Section 7, p. 275) analysed peak  $u$  gusts from 150 stations from Japan from 1966–2005 and show that the incidence of the 10-min mean  $u$  greater than  $20 \text{ m s}^{-1}$  increased 1.5-fold from 1976–1985 to 1996–2005, and the incidence of  $u$  greater than  $35 \text{ m s}^{-1}$  almost doubled over the same period;
- (ii) Kruger et al. (2010, Table 1) in South Africa, from 1993–2008, report that the 4-station average annual maximum  $u$  gust increased by  $+0.009 \text{ m s}^{-1} \text{ a}^{-1}$ ; and
- (iii) Cusack (2011, Fig. 2 and pers. comm.) from 1910–2010 for Holland report a 5-station trend of the annual daily maximum  $u$  values of  $+0.0004 \text{ m s}^{-1} \text{ a}^{-1}$ .

These increases in maximum  $u$  gusts are likely associated with cyclonic, frontal and thunderstorm activity (i.e., when large amounts of energy are released due to latent heat of condensation) that are apparently associated with the intensification of the hydrological cycle (Huntington, 2006).

## 2.2. Global terrestrial meta-analysis

We performed a meta-analysis on the 148 regional terrestrial studies presented in Table 2 by calculating the mean  $u$  trend for various thresholds describing the number of sites and the length of record. This style of meta-analysis was selected as it is impossible to standardise the start-year and end-year for the  $u$  trends when drawing upon as many studies as presented in Table 2. It should be noted that using different periods of analysis will likely impact the magnitude of the calculated  $u$  trends, and in some instances may even change the sign of the  $u$  trend (e.g., McVicar et al., 2010, Auxiliary Fig. S2). The results, provided in Table 4, show that for all 148 studies the average stilling was  $-0.017 \text{ m s}^{-1} \text{ a}^{-1}$ . When using 10 as the threshold value for the number of sites and number of years the average  $u$  trend was  $-0.012 \text{ m s}^{-1} \text{ a}^{-1}$  ( $n = 75$ ); changing marginally to  $-0.014 \text{ m s}^{-1} \text{ a}^{-1}$  ( $n = 30$ ) when 30 was the value used for both thresholds. The resultant  $u$  trends ranged between  $-0.009 \text{ m s}^{-1} \text{ a}^{-1}$  to  $-0.017 \text{ m s}^{-1} \text{ a}^{-1}$  for nearly all threshold combinations (Table 4).

**Table 2**  
Global summary of observed near-surface wind speed trends. Data are grouped by continental regions and studies are ordered from north to south by the site latitude or the central latitude of the site domain. The anemometer height above ground-level is specified in parenthesis in the 'Study Details' column, with n/s meaning 'not specified'.

Study number	Trend $\text{m s}^{-1} \text{a}^{-1}$	Location (site position/domain)	Study details	Source
<b>North America</b>				
1	+0.005	USA, Alaska, Barrow (71°N, 157°W)	1921–2001, 1 site, (10 m since the 1990s, various heights prior to this and standardised to this height using a log transform pers. comm.)	Lynch et al. (2004, Table 3)
2	+0.015	USA, Alaska, Barrow (71°N, 157°W)	1951–2001, 1 site, (10 m since the 1990s, various heights prior to this and standardised to this height using a log transform pers. comm.)	Hartmann and Wendler (2005, Table 5)
3	+0.003	Canada, Central Arctic (59–83°N, 62–105°W)	1953–2006, 8 sites, (10 m)	Wan et al. (2010, Table 3)
4	−0.008	Alaska and northern Canada (55–75°N, 68–156°W)	1953–1993, 14 sites, early to mid afternoon wind speeds from April to October, (n/s m)	Keimig and Bradley (2002, Table 1)
5	+0.020	Canada, Yukon, (60–62°N, 134–137°W)	1956–2005, 3 sites, (10 m)	Pinard (2007, Fig. 3)
6	−0.005	USA, Alaska, non-Arctic (55–67°N, 132–170°W)	1951–2001, 18 sites, (10 m since the 1990s, various heights prior to this and standardised to this height using a log transform pers. comm.)	Hartmann and Wendler (2005, Table 5)
7	−0.005	Canada, non-Central Arctic (42–71°N, 53–136°W)	1953–2006, 109 sites, regional trends vary from $-0.007 \text{ m s}^{-1} \text{a}^{-1}$ to $-0.001 \text{ m s}^{-1} \text{a}^{-1}$ , (10 m)	Wan et al. (2010, Table 3)
8	−0.007	North America (30–75°N, 50–170°W)	1979–2008, 170 sites, (10 m)	Vautard et al. (2010, Supplementary Table 1, Row 10)
9	−0.009	Canada, Southern Prairies (49–51°N, 101–114°W)	1953–2006, 6 sites, (10 m)	St. George and Wolfe (2009, corrected Table S1)
10	−0.017	Canada, West Coast (48–52°N, 123–131°W)	~1950–~1995, 4 sites (~12.5 m)	Tuller (2004, Fig. 3)
11	−0.025	Pacific North West (45–52°N, 121–129°W)	1950–2008, 53 stations, (n/s m), there are another 37 coastal sites that have a cyclic pattern of wind speed	Griffin et al. (2010, Section 4)
12	−0.005	USA, states of Minnesota, South and North Dakota (44–49°N, 92–98°W)	~1962–~1993, 7 sites, (~8 m)	Klink (2002, Table 3)
13	−0.051	USA, Wisconsin, Sparkling Lake (46°N, 90°W)	1989–1998, 1 site, (2 m, pers. comm.)	Lenters et al. (2005, Fig. 6c)
14	−0.001	USA, Idaho, south west (43°N, 117°W)	1984–2007, 2 sites, (3 m)	Reba et al. (2011 and pers. comm.)
15	−0.008	USA, Massachusetts, Milton (42°N, 71°W)	1885–2009, 1 site, (~15 m)	Iacono (2009 and pers. comm., 2010)
16	−0.026	USA, Massachusetts, Milton (42°N, 71°W)	1960–2009, 1 site, (15 m)	Iacono (2009 and pers. comm., 2010)
17	−0.025	USA, western Nevada (38–39°N, 117–118°W)	2003–2008, 3 sites, (10 m)	Belu and Koracin (2009 and pers. comm.)
18	+0.022	USA, California, Altamont Pass (38°N, 122°W)	1990–2010, 1 site, (10 m)	Rasmussen et al. (2011 and pers. comm., 2011)
19	−0.004	USA, lower 48 states (25–49°N, 65–125°W)	1961–1990, 176 sites, (standardised to 6.1 m using the 1/7 power law, p. 194)	Klink (1999, Table 5)
20	−0.005	USA, lower 48 states (25–49°N, 65–125°W)	1962–1990, 207 sites (standardised to 2 m)	Hobbins (2004, p. 156 update post varying anemometer height correction, pers. comm. Hobbins (2007))
21	−0.019	USA, lower 48 states (25–49°N, 65–125°W)	1973–~2003, 336 sites (10 m)	Pryor and Ledolter (2010, Table 2 averaging p50 data for NCDC 6421_00 and NCDC 6421_12 'original')
22	−0.007	USA, Mid-West, (34–39°N, 84–92°W)	1948–2008, 3 sites, (10 m, pers. comm. Kenner (2010))	Abhishek et al. (2010, Fig. 2), and pers. comm. Kenner (2010)
23	−0.005	USA, California, southern, (34–36°N, 117–119°W)	1979–2000, 2 sites, (10 m)	Rasmussen et al. (2011 and pers. comm. 2011)
24	−0.008	Southern USA and Northern México (25–35°N, 95–115°W)	1973–2003, ~20 sites, (n/s m)	Mahowald et al. (2007, Fig. 18b)
25	−0.031	México, (15–38°N, 87–117°W)	2000–2008, 33 sites, (4 m, pers. comm. Manzano-Agugliaro (2011))	Hernández-Escobedo et al. (2010, Table 1)
26	−0.053	México, Yucatán Peninsula (18–22°N, 87–92°W)	2000–2007, 9 sites, (10 m)	Soler-Bientz et al. (2010) and pers. comm. (2010)
27	+0.017	México, State of Veracruz (18–21°N, 94–97°W)	2001–2006, 5 sites, (10 m)	Cancino-Solórzano and Xiberta-Bernat (2009, Fig. 4)
<b>Europe</b>				
28	−0.038	Estonia, Pakri Peninsula (59°N, 24°E)	1970–1991, 1 site, (10 m)	Keevallik and Soomere (2009, Fig. 2)
29	−0.021	Ireland (51–56°N, 6–11°W)	1961–1978, 12 sites, site trends vary from $+0.049 \text{ m s}^{-1} \text{a}^{-1}$ to $-0.072 \text{ m s}^{-1} \text{a}^{-1}$ , (10–12 m pers. comm.)	Haslett and Raftery (1989) Data from <a href="http://lib.stat.cmu.edu/datasets/">http://lib.stat.cmu.edu/datasets/</a> then calculated
30	+0.043	The Netherlands, De Kooy (53°N, 5°E)	1985–1992, 1 site, (10 m)	Coelingh et al. (1996, Fig. 10)
31	−0.010	Europe (30–75°N, 20°W–40°E)	1979–2008, 276 sites, (10 m)	Vautard et al. (2010, Supplementary Table 1, Row 10)
32	−0.009	The Netherlands, (51–53°N, 4–7°E)	1970–2010, 5 sites, (10 m)	Cusack (2011 and pers. comm. (2011))
33	−0.003	Germany, Dortmund (52°N, 7°E)	1951–2000, 1 site, (10 m)	Gerstengarbe et al. (2004, Table 3.1)
34	−0.025	Germany, Greven (52°N, 8°E)	1982–2005, 1 site, (10 m)	Böwer (2006, Fig. 22)
35	−0.004	Belgium, Saint-Josse-ten-Noode (51°N, 4°E)	1880–2007, 1 site, (10 m)	Brouyaux et al. (2009, Fig. 17)
36	−0.017	Belgium, Zaventem (51°N, 4°E)	1965–2007, 1 site, (10 m)	Brouyaux et al. (2009, Fig. 18)
37	−0.001	Germany (47–55°N, 6–15°E)	1951–2001, 73–113 sites per month, 1 km resolution monthly grids interpolated using Inverse Distance Weighting algorithm elevation corrected, (10 m)	Walter et al. (2006, text discussing Fig. 4)

Table 2 (continued)

Study number	Trend $\text{m s}^{-1} \text{a}^{-1}$	Location (site position/domain)	Study details	Source
38	-0.002	Germany (47–55°N, 6–15°E)	~1888–2006, 6 sites, (10 m)	Bormann (2011, Tables 1 and 2) and pers. comm. (2011)
39	-0.008	Czech Republic (48–51°N, 12–19°E)	1961–2005, 23 sites, (10 m pers. comm. (2010))	Brazdil et al. (2009, Fig. 11c)
40	-0.009	Switzerland (46–48°N, 6–10°E)	1983–2006, 25 sites, trend from 1960–2006 is $+0.007 \text{ m s}^{-1} \text{a}^{-1}$ with a break point in 1983, (10 m)	McVicar et al. (2010, Fig. 2f)
41	-0.005	France (43–51°N, 5°W–8°E)	1984–2003, 51 sites (10 m)	Najac et al. (2011, and pers. comm. (2011))
42	-0.031	Italy, Trieste (45°N, 14°E)	1951–1996, 1 site, (10 m pers. comm.)	Pirazzoli and Tomasin (1999, Fig. 6)
43	-0.009	Spain, north east, Comunidad Foral de Navarra mountainous area (42–43°N, 1–2°W)	1992–2005, 14 sites, (10 m)	Jiménez et al. (2010, Table 1) and pers. comm. (2010)
44	+0.040	Spain, Vigo, Atlantic coast (42°N, 8°W)	1995–2005, 1 site, (n/s m)	Recio et al. (2009, Table 1)
45	+0.017	Spain, north west, Duero Valley (40–43°N, 1–7°W)	1980–2009, 8 sites, (10 m)	Moratiel et al. (2011) and pers. comm. (2011)
46	-0.013	Italy (35–45°N, 9–18°E)	~1955–~1996, 17 sites, break point in 1975; ~-0.026 $\text{m s}^{-1} \text{a}^{-1}$ before and ~-0.002 $\text{m s}^{-1} \text{a}^{-1}$ after break point, (10 m pers. comm.)	Pirazzoli and Tomasin (2003, Table II)
47	-0.022	Greece, Lesvos Island (39°N, 26–27°E)	2003–~2009, 4 sites (10 m)	Palaiologou et al. (2011) and pers. comm. (2011)
48	-0.005	Spain, south, Andalusia area (37–39°N, 1–7°W)	~1967–2005, 8 sites, (10 m)	Espadafor et al. (2011) and pers. comm. (2011)
49	-0.001	Greece (35–41°N, 20–28°E)	1959–2001, 20 sites (2 m)	Papaioannou et al. (2011) and pers. comm. (2011)
50	+0.118	Spain, Malaga, Mediterranean coast (36°N, 4°W)	1991–2006, 1 site, (n/s m)	Recio et al. (2009, Table 1)
51	-0.040	Cyprus (34–35°N, 32–34°E)	~1982–~2002, 5 sites, (~8.5 m)	Jacovides et al. (2002) and pers. comm. (2011)
<b>East Asia</b>				
52	-0.012	East Asia (30–75°N, 100–160°E)	1979–2008, 190 sites, (10 m)	Vautard et al. (2010, Supplementary Table 1, Row 10)
53	-0.029	China, Western Deserts (36–44°N, 80–110°E)	1973–2003, ~25 sites, (n/s m)	Mahowald et al. (2007, Fig. 12b)
54	-0.026	China, Greater Beijing Area (39–41°N, 115–117°E)	1960–2008, 12 sites, (10 m)	Li et al. (2011, Section 3.2 and pers. comm. 2011)
55	-0.010	China, Haihe River Basin (35–43°N, 112–120°E)	1950–2007, 34 sites, (2 m)	Tang et al. (2011, Table 2)
56	-0.014	China, Futuo River Basin (38–40°N, 111–115°E)	1960–2000, 12 sites, (2 m)	Yang and Yang (2011, Fig. 2)
57	-0.014	China, Haihe River Basin (35–42°N, 111–120°E)	1957–2001, 45 sites, (observed at 10 m with a log transform to 2 m with analysis performed at this height)	Zheng et al. (2009, Fig. 6)
58	-0.042	Japan (31–46°N, 129–146°E)	1979–2008, 327 sites, (~7 m, ranges from 6.5 m to 10 m)	Fujibe (2011, Section 5, pers. comm. (2011)) and Fujibe (2009, Table 1)
59	-0.014	China, Loess Plateau (33–42°N, 100–115°E)	1960–2006, 69 sites, (10 m)	McVicar et al. (2010, Fig. 2c)
60	-0.009	China, Yellow River Basin (32–42°N, 96–119°E)	1961–2006, 89 sites, (10 m)	Liu et al. (2010b, Fig. 3)
61	-0.009	China, North China Plain (32–42°N, 113–122°E)	1961–2006, 18 sites, (10 m)	Song et al. (2010, Table 3)
62	-0.022	China (18–54°N, 73–135°E)	1969–2000, 305 sites, (10 m)	Xu et al. (2006c, Fig. 1)
63	-0.011	China (18–54°N, 73–135°E)	1956–2005, 317 sites, break point in 1985; -0.007 $\text{m s}^{-1} \text{a}^{-1}$ before and -0.006 $\text{m s}^{-1} \text{a}^{-1}$ after break point, (10 m)	Cong et al. (2009, Table 1)
64	-0.012	China (18–54°N, 73–135°E)	1956–2004, 535 sites, regional trends vary from -0.020 $\text{m s}^{-1} \text{a}^{-1}$ to 0.000 $\text{m s}^{-1} \text{a}^{-1}$ , (10 m)	Jiang et al. (2010, Fig. 5)
65	-0.018	China (18–54°N, 73–135°E)	1969–2005, 652 sites, break point in 1990; -0.025 $\text{m s}^{-1} \text{a}^{-1}$ before and -0.006 $\text{m s}^{-1} \text{a}^{-1}$ after break point, (10 m)	Guo et al. (2011, Fig. 1)
66	-0.009	China (18–54°N, 73–135°E)	1961–2008, 652 sites, (10 m)	Yin et al. (2010a, Fig. 2b)
67	-0.012	China (18–54°N, 73–135°E)	1971–2008, 603 sites, (10 m)	Yin et al. (2010b, p. 3335)
68	-0.015	China (18–54°N, 73–135°E)	1961–2000, 62 sites, (10 m)	Zuo et al. (2005, Table 1 and pers. comm. (2011))
69	-0.012	China (18–54°N, 73–135°E)	1960–1991, 518 sites, (10 m)	Liu et al. (2011a, Table S2)
70	-0.007	China (18–54°N, 73–135°E)	1992–2007, 518 sites, (10 m)	Liu et al. (2011a, Table S2)
71	-0.013	China (18–54°N, 73–135°E)	1961–2007, 597 sites, (10 m)	Fu et al. (2011, Section 3.1)
72	-0.013	China, Tibet Plateau (26–41°N, 74–104°E)	1961–2000, 101 sites, (10 m)	Shenbin et al. (2006, Table VI)
73	-0.011	South Korea, Jeju Island (33–34°N, 126–127°E)	1978–2007, 3 sites, (10–12 m)	Ko et al. (2010, Figures 2, 3 and 4)
74	-0.017	China, Tibet Plateau (26–39°N, 80–104°E)	1966–2003, 75 sites, (observed at 10 m with a log transform to 2 m with analysis performed at this height; pers. comm. (2010))	Zhang et al. (2007, Fig. 4)
75	-0.018	China, Tibet Plateau (26–39°N, 73–104°E)	1970–2005, 75 sites, (10 m)	Liu et al. (2011b, Fig. 5)
76	-0.008	East Asia (23–40°N, 91–141°E)	1979–1995, 8 sites, (10 m)	Xu (2001, Tables 3 and 5)
77	-0.024	China, Eastern and Central Tibetan Plateau, (26–37°N, 85–101°E)	1980–2005, 71 sites, 63 decreasing, 9 increasing, (10–12 m)	You et al. (2010, Table 1)
78	-0.010	China, Yangtze River Basin (24–36°N, 92–122°E)	1960–2000, 150 sites, (observed at 10 m with a log transform to 2 m with analysis performed at this height; pers. comm.)	Xu et al. (2006a, Table 3)
79	-0.008	China, Central and South-East (17–42°N, 90–125°E)	1956–2005, 202 sites, (10 m)	Cong et al. (2010, Table 3)

(continued on next page)

Table 2 (continued)

Study number	Trend $m\ s^{-1}\ a^{-1}$	Location (site position/domain)	Study details	Source
80	-0.007	China, Yunnan Province (21–29°N, 98–106°E)	1961–2004, 119 sites, 93 decreasing, (10 m)	Fan and Thomas pers. comm. (2010)
<b>South East Asia</b>				
81	-0.011	South East Asia (0–30°N, 99–125°E)	1979–2008, 32 sites, (10 m)	Vautard et al. (2010) pers. comm.
<b>Central Asia</b>				
82	-0.017	Northern Russia (60–74°N, 31–180°E)	1936–2000, 23 sites, (10–12 m)	Mescherskaya et al. (2006, Table 1)
83	-0.016	Russia (40–74°N, 30–180°E)	1936–2006, 64 sites, (10–12 m)	Gruza et al. (2008, Fig. 3.32a) and Mescherskaya pers. comm. (2010)
84	-0.016	Central Asia (30–75°N, 40–100°E)	1979–2008, 96 sites, (10 m)	Vautard et al. (2010, Supplementary Table 1, Row 10)
85	-0.031	Russia, focus on Volga River and Ural region (46–59°N, 37–58°E)	1961–1990, 22 sites, (10–12 m)	Mescherskaya et al. (2004, Table 1)
86	-0.025	Russia, focus on Volga River and Ural region (46–59°N, 37–58°E)	1936–2000, 17 sites, (10–12 m)	Mescherskaya et al. (2004, Table 1)
87	-0.024	Kazakhstan (43–53°N, 51–80°E)	1936–2000, 7 sites, (10–12 m)	Mescherskaya pers. comm. (2010)
88	-0.020	Kazakhstan, southeast, Tujuksu (43°N, 77°E)	1972–2007, 1 site, (5 m pers. comm.)	Thomas pers. comm. (2010)
89	-0.013	Kazakhstan and Uzbekistan, focus on the Aral Sea (36–43°N, 55–73°E)	1973–2003, ~15 sites, (n/s m)	Mahowald et al. (2007, Fig. 20b)
<b>Sub-continent</b>				
90	-0.073	Nepal, Khumba Valley (28°N, 87°E)	~2001–2006, 3 sites, site trends vary from -0.097 $m\ s^{-1}\ a^{-1}$ to -0.039 $m\ s^{-1}\ a^{-1}$ , (5 m pers. comm. (2010))	Vuillermoz et al. (2008, calculated from Section 8)
91	-0.038	India, Rajasthan (25–30°N, 70–76°E)	1951–2007, 10 sites, site trend vary from -0.10 $m\ s^{-1}\ a^{-1}$ to -0.060 $m\ s^{-1}\ a^{-1}$ (2 m)	Choudhary et al. (2009, Table 2) and Jhajharia pers. comm. (2011)
92	-0.022	(North-East) India (centred on Assam State) (23–28°N, 88–93°E)	1979–2000, 11 sites, site trend vary from -0.010 $m\ s^{-1}\ a^{-1}$ to -0.040 $m\ s^{-1}\ a^{-1}$ , (3.05 m)	Jhajharia et al. (2009, Table 6), Jhajharia et al. (2007, Fig. 5) and pers. comm. (2011)
93	-0.027	India, (9–34°N, 69–95°E)	1971–2002, 133 sites in 19 regions, with 113 sites declining and 15 increasing, (2 m, pers. comm.)	Bandyopadhyay et al. (2009, Tables 3 and 4)
94	-0.027	(Peninsular) India, Godavari River Basin (16–23°N, 73–83°E)	1961–2004, 35 sites, site trend vary from -0.10 $m\ s^{-1}\ a^{-1}$ to -0.070 $m\ s^{-1}\ a^{-1}$ , (2 m)	Jhajharia pers. comm. (2010)
95	-0.079	India, Maharashtra State, Phaltan (18°N, 74°E)	1983–2005, 1 site, (n/s m)	Jacob and Rajvanshi (2006, Fig. 8)
<b>Middle East</b>				
96	+0.013	Turkey, Maden-Elazig (39°N, 39°E)	1998–2002, 1 site, (10 m)	Akpinar and Akpinar (2004, Table 1)
97	-0.077	Turkey, Harran-Koruklu (37°N, 39°E)	1979–2001, 1 site, (2 m)	Ozdogan and Salvucci (2004, Fig. 7a)
98	+0.035	Iran, Tehran (36°N, 51°E)	1995–2005, 1 site, (10 m)	Keyhani et al. (2010, Table 1)
99	+0.018	Iran (29–39°N, 46–61°E)	1996–2005, 4 sites, site trends vary from -0.011 $m\ s^{-1}\ a^{-1}$ to +0.047 $m\ s^{-1}\ a^{-1}$ , (2 m)	Sabziparvar et al. (2010, Fig. 2)
100	+0.036	Central Iran, Yazd province (30–36°N, 53–57°E)	~1994–2005, 5 sites, site trends vary from +0.097 $m\ s^{-1}\ a^{-1}$ to -0.053 $m\ s^{-1}\ a^{-1}$ , (10 m – data also provided at 20 m and 40 m)	Mostafaeipour (2010, Figs. 14, 16, 18, 20 and 22)
101	+0.014	Israel, Bet Dagan (32°N, 35°E)	1964–1997, 1 site, (10 m)	Cohen et al. (2002, Table 2, averaged all monthly data via pers. comm. Cohen (2010))
102	0.000	Iran (25–38°N, 46–61°E)	1966–2005, 22 sites, site trends vary from +0.072 $m\ s^{-1}\ a^{-1}$ to -0.038 $m\ s^{-1}\ a^{-1}$ , (10 m)	Dinpashoh (2006) and pers. comm. (2010)
103	-0.016	Iran (25–38°N, 45–61°E)	1960–2005, 32 sites, site trends vary from +0.298 $m\ s^{-1}\ a^{-1}$ to -0.192 $m\ s^{-1}\ a^{-1}$ , (10 m)	Rahimzadeh et al. (2011, Table 3)
104	+0.004	Saudi Arabia, Rafha (30°N, 44°E)	1970–2004, 1 site, (12 m)	Rehman et al. (2007, Fig. 1)
105	-0.087	Jordan, Queira (30°N, 35°E)	1990–2001, 1 site, (10 m)	Hrayshat (2007, Fig. 1)
106	-0.024	Middle East (10–45°N, 28–75°E)	1973–2003, ~130 sites, (n/s m)	Mahowald et al. (2007, Fig. 10b)
107	-0.030	Saudi Arabia (17–33°N, 37–50°E)	~1977–2006, 16 sites, (8–10 m)	Rehman (2010) pers. comm.
108	-0.222	Saudi Arabia, Yanbo (24°N, 38°E)	1970–1983, 1 site, (10 m)	Rehman (2004, Fig. 4)
109	-0.001	Oman (17–26°N, 54–59°E)	1986–1998, 6 sites, (10 m)	Dorvlo and Ampratwum (2002) and pers. comm. (2010)
<b>Africa</b>				
110	-0.116	Libya, Zwara (33°N, 12°E)	1979–1988, 1 site, (n/s m)	El-Osta et al. (1995, Fig. 2)
111	-0.087	Libya, Tripoli (33°N, 13°E)	1993–2002, 1 site, (10 m)	Mohamed and Elmabrouk (2009, Table 2)
112	+0.005	Algeria (28–37°N, 2–15°E)	1973–2003, ~22 sites, (n/s m)	Mahowald et al. (2007, Fig. 8b)
113	-0.091	Algeria (24–37°N, 0–8°E)	2002–2006, 8 sites, (17 m)	Himri et al. (2009, Fig. 2) and pers. comm. (2010)
114	+0.043	Egypt, Raft, Shore of Lake Nasser (24°N, 33°E)	1995–2003, 1 site, (2 m)	Elsawwaf et al. (2010) and pers. comm. (2010)
115	-0.014	North Africa (10–37°N, 15°W–55°E)	1973–2003, ~150 sites, (n/s m)	Mahowald et al. (2007, Fig. 6b)
116	+0.001	Mauritania and Senegal, Atlantic Coast (14–21°N, 15–17°W)	1951–1994, 4 sites, (10 m)	Ozer (1996, Fig. 4)
117	-0.064	Niger, Sadoré, (13°N, 2°E)	1984–1994, 1 site, (10 m)	Michels et al. (1999, Fig. 1)
118	-0.046	Nigeria, North-East Arid Zone (11–12°N, 11–13°E)	~1969–~1982, 2 sites, (n/s m)	Hess, (1998, Fig. 2d)
119	-0.200	Ghana, Manga (11°N, 0°E)	2001–2005, 1 site, (n/s m)	O'Higgins (2007, Fig. 4.4)
120	-0.240	Cameroon, Maroua Salack (10°N, 14°E)	1991–1995, 1 site, (10 m)	Tchinda et al. (2000, Fig. 3)
121	-0.200	Cameroon, Maroua Salack (10°N, 14°E)	1991–1995, 1 site, (10 m)	Nfah and Ngundam (2008, Fig. 2 and pers. comm. (2010))
122	+0.005	Nigeria, (4–13°N, 4–13°E)	1970–2000, 20 sites, (n/s m)	Ogolo (2011, Table 2)
123	-0.029	Cameroon (7–9°N, 13°E)	1990–1999, 2 sites, (10 m)	Tchinda and Kaptoum (2003, Fig. 7)

Table 2 (continued)

Study number	Trend $\text{m s}^{-1} \text{a}^{-1}$	Location (site position/domain)	Study details	Source
124	-0.008	Nigeria, Ibadan, (7°N, 4°E)	1973–2008, 1 site, (10 m)	Oguntunde et al. (2011, Table II)
125	-0.022	Ethiopia, Lake Awassa (7°N, 39°E)	1973–2003, 1 site,	Gebreegziabher (2004, Appendix 2.5)
126	+0.005	Atlantic Coast, (15°S–21°N, 23°W–14°E)	~1955–~1985, 24 sites, (n/s m)	Bigg (1993, Table III)
127	-0.002	Kenya (1°S, 37°E)	1979–2008, 1 site, (10 m)	Vautard et al. (2010) pers. comm.
128	+0.063	Tanzania, Makambako (9°S, 35°E)	2001–2005, 1 site, (2 m)	Kainkwa (2010, Table 3) and pers. comm. (2010)
129	-0.021	South Africa (24–33°S, 20–32°E)	1993–2010, 29 sites, (10 m)	Kruger pers. comm. (2010)
130	-0.019	South Africa, Cape Floristic Region (32–34°S, 18–22°E)	1974–2005, 20 sites, (2 m)	Hoffman et al. (2011, corrections to Table 2, pers. comm.)
<b>Oceania</b>				
131	-0.003	Central Australia (18–32°S, 115–150°E)	1973–2003, ~14 sites, (n/s m)	Mahowald et al. (2007, Fig. 14b)
132	-0.010	Australia (10–45°S, 112–155°E)	1975–2004, 41 sites, (2 m)	Roderick et al. (2007, Table 2)
133	-0.009	Australia (10–45°S, 112–155°E)	1975–2006, area-averaged using 112–194 sites per day 0.01° resolution daily grids interpolated with a spline, (2 m)	McVicar et al. (2008, paragraph [9])
134	-0.010	Australia (10–45°S, 112–155°E)	1980–2006, area-averaged using 112–194 sites per day, 0.05° resolution daily grids interpolated with a TIN, (2 m)	Donohue et al. (2010, Table 3)
135	-0.006	Australia (11–45°S, 112–155°E)	1989–2006, 30 sites, (2 m)	Troccoli et al. (2011, Fig. 5a and pers. comm.)
136	-0.002	Australia (16–45°S, 112–155°E)	1975–2006, 15 sites, (2 m)	Troccoli et al. (2011, Fig. 4a and pers. comm.)
137	+0.035	Australia (20–45°S, 112–155°E)	1975–2006, 14 sites, (10 m)	Troccoli et al. (2011, Fig. 4b and pers. comm.)
138	+0.027	Australia (20–45°S, 112–155°E)	1989–2006, 22 sites, (10 m)	Troccoli et al. (2011, Fig. 5b and pers. comm.)
139	-0.011	New Zealand (36–47°S, 168–175°E)	1975–2002, 5 sites, (2 m)	Roderick et al. (2007, Table 2)
<b>Central and South America</b>				
140	-0.085	Cuba, Villa Clara Province (22–23°N, 79–80°W)	1979–2009, 4 sites, (10 m, pers. comm. Osés-Rodríguez et al. (2010))	Osés-Rodríguez et al. (2010, Table 2)
141	+0.009	Piarco, Trinidad (11°N, 61°W)	1950–1999, 1 site, (n/s m)	Lauckner (2002, Table 2)
142	+0.166	Guyana, Georgetown (7°N, 58°W)	1968–1974, 1 site, (10.67 m)	Persaud et al. (1999, Fig. 4)
143	-0.013	Atlantic Coast and Caribbean, (23°S–22°N, 34°W–98°W)	~1955–~1985, 25 sites, (n/s m)	Bigg (1993, Table III)
144	-0.017	North-eastern Brazil (9°S, 40°W)	1975–2009, 2 sites, (2 m)	da Silva et al. (2010, pp 1857 and pers. comm. (2011))
145	-0.023	Argentina (26–35°S, 56–69°W)	1979–2008, 8 sites, (10 m)	Vautard et al. (2010) pers. comm.
146	-0.027	Argentina and Chile (17–46°S, 60–75°W)	1973–2003, ~6 sites, (n/s m)	Mahowald et al. (2007, Fig. 16b)
<b>Antarctica</b>				
147	+0.001	Dome C, Antarctica (75°S, 123°E)	1984–2003, 1 site (10 m)	Aristidi et al. (2005, Fig. 2)
148	+0.006	Antarctica (65–90°S, 0–360°)	~1960–~2000, 11 sites (10 m pers. comm.)	Turner et al. (2005, Table V)

Exceptions were seen when only long studies (*i.e.*, >50 years) with a high number of sites (*i.e.*, >75 sites) were used, however only two regional studies fulfil this criteria. The results presented in Table 4 are very similar to the average trend of  $-0.011 \text{ m s}^{-1} \text{a}^{-1}$  (with a standard deviation =  $0.026 \text{ m s}^{-1} \text{a}^{-1}$ ) calculated using the 852 stations located across the globe (with bias toward the northern hemisphere extra-tropical region, *i.e.*, >23.5°N, where 760 of the stations are located) from 1979–2010 (Peterson et al., 2011a, Fig. 2.45 and Peterson pers. comm. 2011). This global mean value of  $-0.011 \text{ m s}^{-1} \text{a}^{-1}$  is an arithmetic mean (with no weighting applied) and is thus slightly different to the value of  $-0.0093 \text{ m s}^{-1} \text{a}^{-1}$  reported in Peterson et al. (2011b, paragraph 11) which were weighted according to local station density using a standard National Climatic Data Center area averaging approach (Peterson pers. comm. 2011). The results presented in Table 4 are also similar to the averaged trend ( $-0.010 \text{ m s}^{-1} \text{a}^{-1}$ ) reported in the original stilling paper (Roderick et al., 2007).

### 2.3. Global (terrestrial and oceanic) synthesis

The results presented in Table 2 and Fig. 2 show that declines in terrestrial *u* are geographically wide-spread, with declines being reported in the tropics and mid-latitudes of both hemispheres, and increases reported at high-latitudes (*i.e.*, ~>70° latitude) again

for both hemispheres. This latitudinal dependence of *u* trends qualitatively agrees with model projections showing decreasing *u* at mid-latitudes with increasing *u* at high-latitudes (Seidel et al., 2008; Yin, 2005). In addition to this widespread latitudinal dependence there are two noteworthy exceptions apparent from this review (Table 2 and Fig. 2). Firstly, several coastal studies have experienced increasing *u*, which agrees with increasing observed oceanic *u*, measured by both *in situ* systems (anemometers located on ships or buoys) and remote sensing systems. Examples of increasing observed oceanic *u* trends using *in situ* observational systems include: (i) Flohn and Kapala (1989, Table 1) report *u* increases of  $+0.014 \text{ m s}^{-1} \text{a}^{-1}$  and  $+0.042 \text{ m s}^{-1} \text{a}^{-1}$ , respectively for the Atlantic and Pacific; (ii) Cardone et al. (1990, Fig. 10) document a *u* increase of  $+0.024 \text{ m s}^{-1} \text{a}^{-1}$  over 1965–1985 for the South China Sea shipping lane; and (iii) Thomas et al. (2008, Table II) document a measured height-adjusted *u* trend of  $+0.020 \text{ m s}^{-1} \text{a}^{-1}$  over 1982–2000 and for 1952–2002 report a trend of  $+0.018 \text{ m s}^{-1} \text{a}^{-1}$  (both for the global ocean surface that has ‘well-sampled’ 5° grid cells). Examples of increasing observed oceanic *u* trends using satellite remotely sensed observational systems include: (i) Wentz et al. (2007, p. 244) reported that averaged over the global oceans *u* increased by  $+0.008 \text{ m s}^{-1} \text{a}^{-1}$  from 1987–2006; and (ii) Tokinaga and Xie (2011, Table 3) reported a 1988–2008 global oceanic *u* trend of  $+0.013 \text{ m s}^{-1} \text{a}^{-1}$ . Additionally, projected changes of atmo-

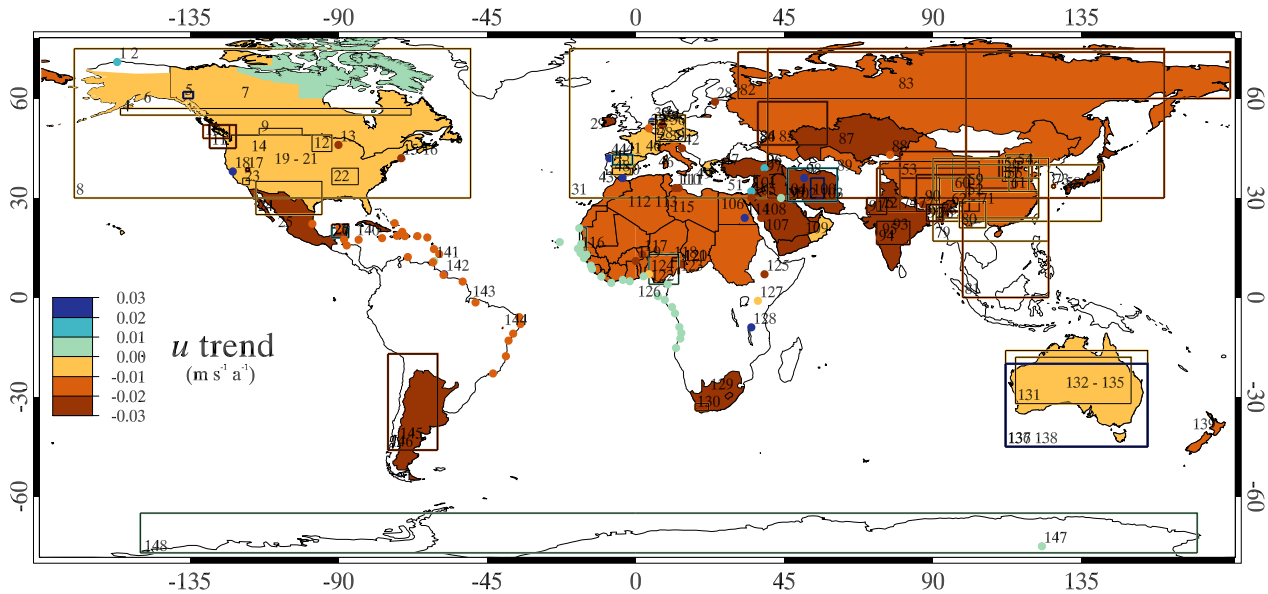


**Fig. 2.** Global distribution of observed *u* trends. The values refer to the study numbers provided in Table 2, either points, geographic domains or countries are identified depending on the level of geographic detail provided in the study. If there are multiple studies for a country (e.g., China) then the average *u* trend for that country is used. A version without the study numbers included is provided as Supplementary material Fig. 1. Versions zoomed to 18°W–150°E and 82°N–0°N, with and without study number labels, are also provided; see Supplementary material Figs. 2 and 3, respectively.

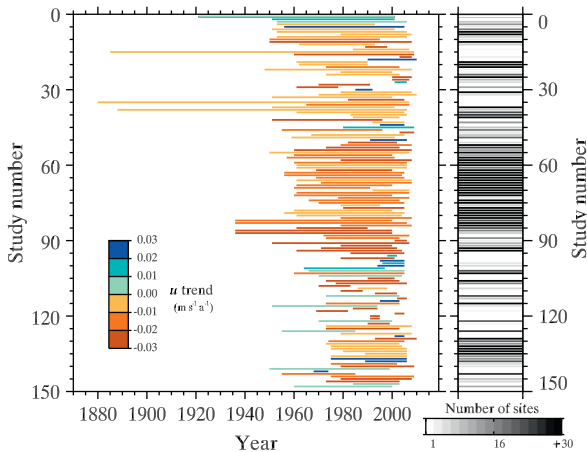


**Fig. 3.** Temporal distribution of observed *u* trends. The values refer to the study numbers provided in Table 2, and the number of sites in each regional study is also shown.

spheric dynamics suggest that both extreme (the highest 5% of winds, Gastineau and Soden, 2009, Fig. 3) and overall wind conditions (Gastineau, pers. comm., 2009) will continue to increase over

the oceans, especially in the Roaring Forties of the southern hemisphere (i.e., 40–60°S). Increasing oceanic *u* will cause a range of impacts including: (i) increasing wave height (e.g., Young et al., 2011); (ii) increasing global oceanic evaporation (e.g., Yu, 2007); and (iii) possibly decreasing the size of ocean sinks for CO<sub>2</sub> (as wind-driven upwelling and the associated ventilation of carbon-rich subsurface waters increases with increasing *u* e.g., Le Quéré et al., 2007), among others. At coastal locations, the relative influence of oceanic or continental winds will depend on the amount of time the wind can be described as on-shore, as compared to off-shore (Griffin et al., 2010; McVicar and Roderick, 2010). The second exception apparent from Table 2 and Fig. 2 are studies within the vicinity of the Mediterranean Sea/Middle East, which have reported both increases and decreases of *u* trends. This is likely a result of complex mesoscale atmospheric circulation in this area (e.g., Evans et al., 2004; Reddaway and Bigg, 1996, and the references therein), with some of the largest increases in oceanic *u* being in the vicinity of the Mediterranean Sea/Middle East (Ward, 1992).

**2.4. Possible causes of stalling**

Several possible reasons might explain the decline in observed near-surface *u* for non-coastal, mid-latitude and tropical locations. These include:

**Table 3**

Comparing *u* trends calculated using ordinary linear regression (OLR – a parametric test) vs. those calculated when temporal autocorrelation is accounted for.

Study details	OLR trend (m s <sup>-1</sup> a <sup>-1</sup> )	Trend when temporal autocorrelation is accounted for (m s <sup>-1</sup> a <sup>-1</sup> )	Source
USA, lower 48 states, ~310 sites 1973–~2003, p50	-0.019	-0.0205 <sup>a</sup>	Pryor and Ledolter (2010, Table 2 using NCDC 6421, p50 averaged for the 2 times)
USA, lower 48 states, ~310 sites 1973–~2003, p90	-0.0305	-0.031 <sup>a</sup>	Pryor and Ledolter (2010, Table 2 using NCDC 6421, p90 averaged for the 2 times)
Australia, 41 sites, 1975–2008	-0.008	-0.008 <sup>b</sup>	Supplementary material Table 2
India, north-east 8 sites, 1979–2000	-0.016	-0.017 <sup>b</sup>	Supplementary material Table 3
India, southern peninsular, 17 sites, 1961–2004	-0.035	-0.035 <sup>b</sup>	Supplementary material Table 4
Iran, 22 sites, 1966–2005	0.000	+0.001 <sup>b</sup>	Supplementary material Table 5

<sup>a</sup> Calculated using a regression model considering first-order autoregressive errors.

<sup>b</sup> Calculated using Theil–Sen’s test (a non-parametric test), after the removal of the significant lag-1 serial correlation effect by applying the “pre-whitening” Mann–Kendall procedure, see Dinpashoh et al. (2011) for full details.

**Table 4**

Results from the meta-analysis by applying number of sites and number of years thresholds to the data presented in Table 2. The average ( $\text{m s}^{-1} \text{a}^{-1}$ ) and number of regional studies (provided in parenthesis) that pass the two thresholds are shown.

Num years Threshold	Number of sites per regional study threshold							
	0	10	20	30	40	50	75	100
0	-0.017 (148)	-0.012 (76)	-0.013 (56)	-0.014 (44)	-0.013 (39)	-0.014 (37)	-0.013 (29)	-0.013 (26)
10	-0.013 (128)	-0.012 (75)	-0.012 (55)	-0.014 (43)	-0.013 (39)	-0.014 (37)	-0.013 (29)	-0.013 (26)
20	-0.013 (110)	-0.012 (68)	-0.014 (50)	-0.014 (41)	-0.014 (37)	-0.014 (35)	-0.013 (28)	-0.013 (25)
30	-0.011 (82)	-0.011 (53)	-0.013 (37)	-0.014 (30)	-0.014 (27)	-0.014 (26)	-0.013 (20)	-0.014 (18)
40	-0.010 (48)	-0.012 (29)	-0.012 (20)	-0.012 (18)	-0.011 (15)	-0.011 (14)	-0.009 (11)	-0.010 (9)
50	-0.010 (18)	-0.013 (8)	-0.012 (6)	-0.011 (5)	-0.012 (4)	-0.012 (4)	-0.003 (2)	-0.005 (1)

- (i) increasing land surface roughness (Vautard et al., 2010) due to increased vegetation cover (with the increasing amount of vegetation cover being primarily caused by the abandonment of agricultural land (Vuichard et al., 2008), increases in air temperatures (e.g., Nemani et al., 2003) and atmospheric  $\text{CO}_2$  concentrations enhancing vegetation growth (e.g., Donohue et al., 2009), large-scale afforestation (Liu et al., 2008) as confirmed by trends of long time series of satellite remote sensing of vegetation cover (Beck et al., 2011, Figs. 4b and 5e and f);
- (ii) mesoscale circulation changes, as examples associated with the strength of El Niño (St. George and Wolfe, 2009) and changes to tropical monsoonal circulation patterns (Vecchi and Soden, 2007; Xu et al., 2006c);
- (iii) poleward expansions of the Hadley cell (Lu et al., 2007; Seidel et al., 2008);
- (iv) the movement of large storms towards polar latitudes (e.g., Frederiksen and Frederiksen, 2007; Lorenz and DeWeaver, 2007; Yin, 2005);
- (v) extracting wind power to generate electricity (e.g., Keith et al., 2004; Miller et al., 2011; Wang and Prinn, 2010);
- (vi) increasing trends in available water (i.e., by precipitation and/or irrigation), so more available energy is partitioned into the latent heat flux and less into the sensible heat flux and associated turbulent transport (e.g., Ozdogan and Salvucci, 2004; Shuttleworth et al., 2009);
- (vii) astronomical changes related to decadal changes in day-length thereby changing the exchange of angular momentum between the solid Earth and the atmosphere, thereby impacting  $u$  (e.g., Lambeck and Cazenave, 1976; Mazzarella, 2007);
- (viii) polar latitudes are heating more rapidly than tropical latitudes (Lorenz and DeWeaver, 2007), with a weakening of the equatorial-polar thermal differential expected to result in decreased equatorial and mid-latitude  $u$  (Ren, 2010); and
- (ix) measurement artefacts including sub-optimal anemometer calibration and data processing protocols (e.g., DeGaetano, 1998; Thomas and Swail, 2011), and poor site selection and site maintenance (Fall et al., 2011, who focus on near-surface air temperature trends, noting that similar analysis is needed for sites measuring  $u$  across the globe).

It is noteworthy that the attribution of independent  $E_{\text{pan}}$  observations suggests that  $u$  trends are not measurement artefacts. In both the northern and southern hemispheres (e.g., Liu et al., 2011a; Roderick et al., 2007; Zheng et al., 2009) independent  $E_{\text{pan}}$  trends have been modelled using forcing meteorological (including  $u$ ) data. The modelled  $E_{\text{pan}}$  trends were in general agreement with observed  $E_{\text{pan}}$  trends, and in several studies  $E_{\text{pan}}$  reductions have been primarily attributed to declining  $u$  (see results in Table 7 'Study type: Attribution'). While it may be possible that measurement artefacts are causing stilling in other studies, we note a general agreement (usually in direction of the  $u$  trend) between many

proximally located studies reviewed herein (Table 2 and Fig. 2). This suggests that: (i) measurement artefacts are not the sole cause; or (ii) that many proximally located studies are affected by measurement artefacts to the same degree. Further research is needed to substantiate the former.

While a full understanding of the process(es) causing the wide-spread terrestrial stilling is currently unresolved, it is noteworthy that Vautard et al.'s (2010) increasing terrestrial surface roughness hypothesis is currently the only possible process that partly explains the previously mentioned increasing oceanic  $u$  and decreasing terrestrial  $u$  that are occurring at the same latitudes (McVicar and Roderick, 2010). We say 'partly' as (Vautard et al., 2010, Fig. 3c) show that stilling can occur even when satellite NDVI (Normalised Difference Vegetation Index) trends are negative (not positive), confirming that stilling cannot be exclusively attributed to increased surface roughness (as per the title of Vautard et al., 2010). We further examine this relationship by regressing long-term (i.e., 1981–2006)  $u$  trends (McVicar et al., 2008) at 41 meteorological sites across Australia (Roderick et al., 2007) against remotely sensed estimates of the fraction of Photosynthetically Active Radiation (fPAR) absorbed by vegetation (Donohue et al., 2008), which is linearly related to fractional green vegetation cover (Lu et al., 2003). At the three scales studied (i.e.,  $\sim 7.5$  km,  $\sim 50$  km and  $\sim 100$  km in one direction centred on the meteorological station), Fig. 4 shows that fPAR trends and  $u$  trends are slightly positively correlated; contrasting previous results (Vautard et al., 2010, Fig. 3c). We also found a slight positive correlation when correlating  $u$  trends with trends of the persistent vegetation component, derived by temporally decomposing the fPAR signal into its recurrent and persistent components (Donohue et al., 2009).

Next we relate our results from Fig. 4 to several recent studies, using a multiple-lines-of-evidence approach. Our findings in Fig. 4 (i.e., that there is no negatively correlated relationship between  $u$  trends and vegetation cover trends) agrees with Shuttleworth et al.'s (2009) findings that large-scale changes in atmospheric circulation exert a greater influence than small-scale surface-atmosphere coupling to determine the resultant declining evaporative demand trends observed across most of Australia for 1975–2004. Shuttleworth et al. (2009) developed an atmospheric boundary layer (ABL) model of area-averaged evaporation that allows the influence of both: (i) large-scale changes in atmospheric water vapour concentrations and circulation (termed Type a); and (ii) small-scale coupling between the surface and ABL (termed Type b) on evaporation rates to be quantified. Using this analysis framework and the  $E_{\text{pan}}$  database developed by Roderick et al. (2007, i.e., 41-sites across Australia, 1975–2004), Shuttleworth et al. (2009, Table 2) show that Type a changes contributed  $-2.08 \text{ mm a}^{-2}$  to the trend of  $E_{\text{pan}}$ , while Type b only contributed  $+0.03 \text{ mm a}^{-2}$ . This analysis suggests that for Australia, for 1975–2004, large-scale changes in atmospheric circulation exert greater influence than small-scale surface-atmosphere coupling to determine the resultant evaporative demand trends.

**Table 5**  
Global summary of observed  $E_{pan}$  trends. Data are grouped by continental regions. Information regarding the pan type is provided in the 'Study Details' column. They are either a: (i) Class A pan (a galvanised metal pan, 120.7 cm diameter, 25.4 cm high mounted 15 cm above ground level); (ii) Chinese micro-pan (a galvanised metal pan, 20-cm diameter, 10 cm high mounted 70 cm above ground level); or (iii) BMO tank (a British Meteorological Office (BMO) tank that is 180 cm × 180 cm × 60 cm, painted black and sunk so that its rim projects 6 cm above the surrounding soil.

Study number	Trend $mm a^{-2}$	Location (site position/domain)	Study details	Source
<b>North America</b>				
1	-0.30 <sup>a</sup>	Canada, (49–51°N, 97–114°W)	4 sites, ~1965–2000, Class A pan <sup>b</sup>	Burn and Hesch (2007, Fig. 8) <sup>c</sup>
2	-2.15	USA, Lower 48 states (25–49°N, 65–125°W)	44 sites (64% are decreasing), 1951–2002, Class A pan <sup>b</sup>	Hobbins et al. (2004, paragraph 6, Fig. 2 and pers. comm. 2011)
3	-0.85 <sup>a</sup>	USA, Lower 48 states (25–49°N, 65–125°W)	228 sites (60% are decreasing), 1951–2002, Class A pan <sup>b</sup>	Hobbins et al. (2004, paragraph 6, Fig. 2 and pers. comm. 2011)
4	-1.44 <sup>a</sup>	USA, Lower 48 states (25–49°N, 65–125°W)	8 regions (from 493 sites), 1948–1998, Class A pan <sup>b</sup>	Lawrimore and Peterson (2000, Table 1)
5	-2.16 <sup>a</sup>	USA, Western (25–49°N, 100–125°W)	746 sites, 1948–1993, Class A pan <sup>b</sup>	Peterson et al. (1995, Figure)
6	-1.90 <sup>a</sup>	USA, Mississippi River Basin (29–51°N, 75–113°W)	1 region (interpolated from 404 sites), 1949–1997, Class A pan <sup>b</sup>	Milly and Dunne (2001, p. 1220 and Fig. 2)
7	+2.71 <sup>a</sup>	USA, Ohio, Coshocton (40°N, 82°W)	1 site, 1956–1997, Class A pan <sup>b</sup>	Golubev et al. (2001, Figure 2)
8	-0.32	México, Zacatecas State (21–25°N, 102–104°W)	40 sites, ~1960–~2005, Class A pan <sup>b</sup>	Blanco-Macias et al. (2011, Table 1)
<b>Europe</b>				
9	-1.30	UK, (50–55°N, 3°W–2°E)	7 sites, ~1908–~1960, BMO tank	Stanhill and Möller (2008, Table 1)
10	+2.10	UK, Central England, Wellesbourne (52°N, 2°W)	1 site, 1957–2004, BMO tank	Stanhill and Möller (2008, Table 1 and Section 3.1)
11	+0.81	Ireland, (52–54°N, 6–10°W)	8 sites, ~1963–2005, Class A pan	Stanhill and Möller (2008, Table 1)
12	+0.56	Ireland, Valentia (52°N, 10°W)	1 site, 1960–2004, Class A pan	Black et al., (2006, Fig. 5)
13	-5.10	Ireland, Kilkenny (53°N, 7°W)	1 site, 1976–2004, Class A pan	Black et al., (2006, Fig. 5)
14	+1.45	Greece (35–41°N, 21–27°E)	14 sites, 1979–1999, Class A pan	Papaioannou et al. (2011) and pers. comm. (2011)
<b>East Asia</b>				
15	-4.91	China, Haihe River Basin (35–42°N, 111–120°E)	45 sites, 1957–2001, Chinese micro-pan	Zheng et al. (2009, Fig. 4 and Table 4)
16	-1.72	China (18–54°N, 73–135°E)	671 sites, 1955–2001, Chinese micro-pan	Liu et al. (2010a, Fig. 3 and Table 5)
17	-1.85	China (18–54°N, 73–135°E)	580 sites, 1951–2000, Chinese micro-pan	Chen et al. (2005, Table 1)
18	-5.43	China (18–54°N, 73–135°E)	518 sites, 1960–1991, Chinese micro-pan	Liu et al. (2011a, Table 1)
19	+7.94	China (18–54°N, 73–135°E)	518 sites, 1992–2007, Chinese micro-pan	Liu et al. (2011a, Table 1)
20	-2.93 <sup>a</sup>	China (18–54°N, 73–135°E)	85 sites, 1955–2000, Chinese micro-pan <sup>b</sup>	Liu et al. (2004, Fig. 2)
21	-3.90	China (18–54°N, 73–135°E)	85 sites, 1955–2000, Chinese micro-pan <sup>b</sup>	Qian et al. (2006, Figure 2 and Paragraph 8)
22	-4.28	China, Yellow River Basin (32–42°N, 96–119°E)	123 sites, 1960–2000, Chinese micro-pan	Liu and Zeng (2004, Fig. 5a)
23	-3.64	China (18–54°N, 73–135°E)	62 sites, 1961–2000, Chinese micro-pan <sup>b</sup>	Zuo et al. (2005, Table 1 and pers. comm. 2011)
24	-2.97	China, Humid zone (32–42°N, 96–119°E)	278 sites, 1955–2001, Chinese micro-pan	Liu et al. (2010a, Fig. 3, Table 5 and pers. comm. 2010)
25	-1.76	China, Semi-humid/semi-arid zone (25–54°N, 80–130°E)	291 sites, 1955–2001, Chinese micro-pan	Liu et al. (2010a, Fig. 3, Table 5 and pers. comm. 2010)
26	-0.55	China, Arid zone (30–50°N, 73–115°E)	102 sites, 1955–2001, Chinese micro-pan	Liu et al. (2010a, Fig. 3, Table 5 and pers. comm. 2010)
27	-1.62	China, Yangtze River Basin (24–36°N, 92–122°E)	115 sites, 1971–2000, Chinese micro-pan <sup>b</sup>	Xu et al. (2006b, Fig. 2 and Table 1)
28	-3.09	China, Yangtze River Basin (24–36°N, 92–122°E)	150 sites, 1960–2000, Chinese micro-pan	Xu et al. (2006a, Table 3)
29	-2.84	China, Yangtze River Basin (24–36°N, 92–122°E)	115 sites, 1961–2000, Chinese micro-pan	Wang et al. (2007, Table 1)
30	-1.81	China, North-West (31–49°N, 73–112°E)	126 sites, 1955–2001, Chinese micro-pan <sup>b</sup>	Shen et al. (2010, Fig. 7 and pers. comm. 2010)
31	-4.57	China, Tibet Plateau (26–39°N, 80–104°E)	75 sites, 1966–2003, Chinese micro-pan	Zhang et al. (2007, Fig. 3)
32	-3.06	China, Tibet Plateau (26–39°N, 73–104°E)	75 sites, 1970–2005, Chinese micro-pan	Liu et al. (2011b, Fig. 5)
33	-2.68	Japan (31–46°N, 129–146°E)	8 sites, 1967–2000, Class A pan	Asanuma and Kamimera (2003, Table 2)
34	-2.85 <sup>a</sup>	Japan (31–46°N, 129–146°E)	14 sites, 1967–2000, Class A pan	Asanuma and Kamimera (2003, Table 2)
<b>South East Asia</b>				
35	-16.63	Thailand (13–20°N, 97–101°E)	8 sites, 1982–2000, (24 of 27 sites are declining), Class A pan <sup>b</sup>	Tebakari et al. (2005, Figures 6 and 7)
<b>Central Asia</b>				
36	-3.76 <sup>a</sup>	Former Soviet Union (49–67°N, 26–44°E)	7 sites, ~1956–~1989, Class A pan <sup>b</sup>	Golubev et al. (2001, Fig. 2)
<b>Sub-continent</b>				
37	-11.78	India, (9–34°N, 69–95°E)	19 sites, 1961–1992, Class A pan	Chattopadhyay and Hulme (1997, Fig. 4)
38	-7.19	India, North-East (centred on Assam State) (23–28°N, 88–93°E)	11 sites, 1965–2000, Class A pan <sup>b</sup>	Jhajharia et al. (2009, Tables 4 and 7)
39	-12.55	India, (9–34°N, 69–95°E)	58 sites, 1971–2000, Class A pan	Jaswal et al. (2008, Fig. 2)
40	-25.27	India, Central (16–23°N, 73–83°E)	7 sites, 1969–2004, Class A pan	Jhajharia pers. comm. (2011)
41	-21.34	India, North-West (25–30°N, 70–76°E)	5 sites, 1977–2007, Class A pan <sup>b</sup>	Choudhary et al. (2009, Table 2) and Jhajharia pers. comm. (2011)

Table 5 (continued)

Study number	Trend $\text{mm a}^{-2}$	Location (site position/domain)	Study details	Source
<b>Middle East<sup>d</sup></b>				
42	+3.67	Israel (32°N, 35°E)	1 site, 1964–1997, Class A pan	Cohen et al. (2002, Fig. 1 caption)
43	+16.08	Iran (33–36°N, 47–50°E)	12 sites, 1982–2003, Class A pan	Tabari and Marofi (2011, Table 3)
<b>Africa</b>				
44	–8.40	Nigeria, Ibadan, (7°N, 4°E)	1 site, 1973–2008, Class A pan	Oguntunde et al. (2011, Table II)
45	–9.06	South Africa, (32–34°S, 18–22°E)	20 sites, 1974–2005, Class A pan	Hoffman et al. (2011, Table 2)
<b>Oceania</b>				
46	–2.00	Australia (10–45°S, 112–155°E)	41 sites, 1975–2004, Class A pan	Roderick et al. (2007, Fig. 2)
47	–2.40	Australia (10–45°S, 112–155°E)	61 sites, 1975–2004, Class A pan	Roderick et al. (2007, Paragraph 14)
48	–4.30	Australia (10–45°S, 112–155°E)	30 sites, 1970–2002, Class A pan	Roderick and Farquhar (2004, Fig. 2)
49	–3.30	Australia (10–45°S, 112–155°E)	61 sites, 1975–2002, Class A pan	Roderick and Farquhar (2004, Figure 4)
50	–2.49	Australia (10–45°S, 112–155°E)	60 sites, 1970–2005, Class A pan	Jovanovic et al. (2008, Fig. 8)
51	–4.00	Australia (10–45°S, 112–155°E)	17 sites, 1975–2004, Class A pan	Rayner (2007, Table 1)
52	–2.80	Australia (10–45°S, 112–155°E)	28 sites, 1970–2004, Class A pan (original data)	Kirono and Jones (2007, Table 2)
53	–0.70	Australia (10–45°S, 112–155°E)	28 sites, 1970–2004, Class A pan (adjusted data)	Kirono and Jones (2007, Table 2)
54	–2.10	New Zealand (36–47°S, 168–178°E)	19 sites, ~1975–~1996, Class A pan	Roderick and Farquhar (2005, Section 3)
<b>Central and South America</b>				
55	+1.41	Brazil, North-East (3–10°S, 35–42°W)	19 sites, ~1965–~1995, Class A pan	da Silva (2004, Table 2)

<sup>a</sup> For these studies the units are  $\text{mm WS}^{-1} \text{a}^{-1}$ ; where WS is an abbreviation for the northern-hemisphere 'Warm Season'. In Asanuma and Kamimera (2003), and Hobbins et al. (2004) it is defined by the months of May to October, inclusive; in Lawrimore and Peterson (2000), Liu et al. (2004), Peterson et al. (1995), and Milly and Dunne (2001) it includes May–September. In Golubev et al. (2001) for the Former Soviet Union sites it primarily includes June to September, and for the USA site it is May through September, and in Burn and Hesch (2007) it includes May through to August (except for Calgary where there are no data for May).

<sup>b</sup> The pan type is not explicitly specified in the paper, so the pan type is assumed (supported by knowledge of the pan type commonly used by the respective national meteorological service).

<sup>c</sup> Burn and Hesch (2007, Figure 7) also report lake evaporation trends, the median values are: (i)  $\sim -1 \text{ mm WS}^{-1} \text{a}^{-1}$  for 48 sites from 1971–2000; (ii)  $\sim -2 \text{ mm WS}^{-1} \text{a}^{-1}$  for 36 sites from 1961–2000; and (iii)  $\sim -0.1 \text{ mm WS}^{-1} \text{a}^{-1}$  for 30 sites from 1951–2000. Here WS = April through to October.

<sup>d</sup> The study from Ozdogan and Salvucci (2004, Fig. 5) is not included as the observed Class A<sup>b</sup> trend of  $-24.14 \text{ mm WS}^{-1} \text{a}^{-1}$  (here WS = 15 June to 15 September) from 1979–2001 is heavily influenced by expanding irrigation on the Harran Plain, Turkey.

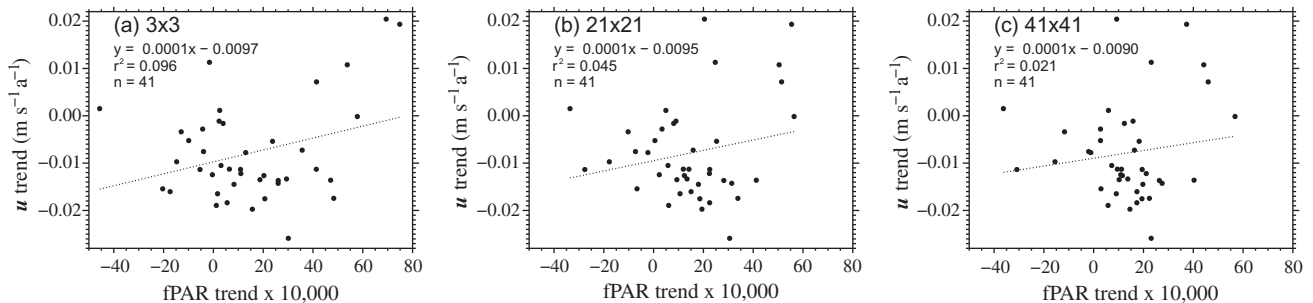


Fig. 4. Relationship between long-term (1981–2006) vegetation trends (as measured by fPAR) and  $u$  trends at 41 sites across Australia. Part (a) shows the relationship for a  $3 \times 3$  grid-cell window centred on the stations, part (b) shows a  $21 \times 21$  grid-cell window, and part (c) a  $41 \times 41$  grid-cell window. Each grid-cell is  $\sim 5 \text{ km}$  resolution and the locations of the 41 sites are provided in (Roderick et al., 2007).

Additionally, when Guo et al. (2011, Fig. 2) stratified their all-China 652-station database into rural and large-urban cases, they reported similar  $u$  trends across the cases: 1969–1990 rural =  $-0.028 \text{ m s}^{-1} \text{a}^{-1}$  and urban =  $-0.031 \text{ m s}^{-1} \text{a}^{-1}$ , and 1991–2005 rural =  $-0.006 \text{ m s}^{-1} \text{a}^{-1}$  and urban =  $-0.004 \text{ m s}^{-1} \text{a}^{-1}$ . This result suggests that in China from 1969–2005 either: (i) surface roughness has been increasing at the same rate for the rural and large-urban cases; or (ii) stilling is not primarily due to local land-cover changes, as suggested by Xu et al. (2006c, Fig. 1). Using 12 stations to study the Greater Beijing Area, China, from 1961–2008, Li et al. (2011) recently suggested that urbanisation contributed one-fifth of the total  $u$  decrease ( $-0.005 \text{ m s}^{-1} \text{a}^{-1}$  of the  $-0.026 \text{ m s}^{-1} \text{a}^{-1}$ ) and noted that changes in strong winds (*i.e.*, wind extremes and winter winds) are influenced by large-scale climatic change. Further research is needed at the global-level, while taking into account any local changes in surface roughness (due to either changes in urbanisation and/or vegetation amounts), and accounting for differing anemometer-based observing systems, to fully

reconcile how near-surface  $u$  observed at similar latitudes could increase over the ocean while decrease over the land.

## 2.5. Implications for other disciplines

Trends in near-surface  $u$  have important implications for disciplines other than hydrology. These include:

- (i) wind energy generation, noting that the near-surface  $u$  results presented in Table 2 need to be reconciled, through either measurement (*e.g.*, Archer and Jacobson, 2003; Rehman et al., 2007) and/or modelling (*e.g.*, Archer and Jacobson, 2005; Pérez et al., 2005), to the height (*i.e.*, 70–100 m) of commercial wind turbines, with 'wind speed-ups' shown to be declining (McVicar et al., 2010);
- (ii) atmospheric circulation modelling, with declines in tropospheric wind (Vautard et al., 2010) and mesospheric wind (Sridharan et al., 2010) being documented;

- (iii) assessing trends in near-surface atmospheric energetics over land (Peterson et al., 2011b);
- (iv) wind erosion (e.g., Alfaro and Gomes, 2001; Shao et al., 1993);
- (v) wind transport, and subsequent deposition, of iron impacting oceanic biogeochemical processes (e.g., Mahowald et al., 2009);
- (vi) wind transport of pollen and seeds (e.g., Friedman and Barrett, 2009; Okubo and Levin, 1989; Riba et al., 2009);
- (vii) wind transport of pollution and associated human health impacts (e.g., Bernard et al., 2001; Chu et al., 2003; Jaffe et al., 1999); and
- (viii) structural engineering (e.g., Cook, 1985).

### 3. Trends in evaporative demand

Even though it is over 60 years since Penman (1948) published his seminal framework combining the radiative and aerodynamic components to quantify evaporation, across the globe over the last

decade or so, several studies have sought to understand the causes of evaporative dynamics without considering  $u$  trends (e.g., Asanuma et al., 2004; da Silva, 2004; Golubev et al., 2001; Lawrimore and Peterson, 2000; Liu et al., 2004; Liu and Zeng, 2004; Moratiel et al., 2010; Papaioannou et al., 2011; Peterson et al., 1995; Tebakari et al., 2005). That is, they implicitly assumed that  $u$  was non-trending, whereas our analysis (i.e., Table 2, Fig. 2 and Table 4) clearly illustrates observed trends in  $u$ . Similarly when assessing long-term trends of some potential evaporation formulations (e.g., Priestly–Taylor or Thornthwaite),  $u$  is implicitly assumed to be non-trending (as wind speed is not a variable in the formulations, see Donohue et al., 2010; McVicar et al., 2007, and the references therein). More recently stilling has been identified as a key factor reducing atmospheric evaporative demand, as measured by  $E_{\text{pan}}$  (Rayner, 2007; Roderick et al., 2007, 2009; Xu et al., 2006a),  $ET_o$  (Gong et al., 2006; Xu et al., 2006a), and  $ET_p$  (Donohue et al., 2010). In this section we review papers that have reported observed trends in  $E_{\text{pan}}$  (Table 5) and  $ET_o$  (Table 6), and finally in Table 7

**Table 6**

Global summary of estimated  $ET_o$  trends. Data are grouped by continental regions, noting trends in  $ET_o$  have not been reported for all continental regions.

Study number	Trend (mm a <sup>-2</sup> )	Location (site position/domain)	Study details	Source
<b>North America</b>				
<b>Europe</b>				
1	+0.01	Spain, Andalusia area (37–39°N, 1–7°W)	8 sites, ~1962–2005	Espadafor et al. (2011) and pers. comm. (2011)
2	+1.27	Greece (35–41°N, 21–27°E)	14 sites, 1979–1999	Papaioannou et al. (2011) and pers. comm. (2011)
<b>East Asia</b>				
3	-2.30	China (18–54°N, 73–135°E)	65 sites, 1954–1993	Thomas (2000, Fig. 2a and Table 2)
4	-1.77	China, Haihe River Basin (35–42°N, 111–120°E)	45 sites, 1957–2001	Zheng et al. (2009, Figs. 4 and 5)
5	-1.00	China, Haihe River Basin (35–43°N, 112–120°E)	34 sites, 1950–2007	Tang et al. (2011, Table 3)
6	-1.69	China, Yangtze River Basin (24–36°N, 92–122°E)	115 sites, 1971–2000	Xu et al. (2006b, Fig. 2 and Table 1)
7	-1.24	China, Yangtze River Basin (24–36°N, 92–122°E)	150 sites, 1960–2000	Xu et al. (2006a, Table 3)
8	-1.37	China, Yangtze River Basin (24–36°N, 92–122°E)	115 sites, 1961–2000	Wang et al. (2007, Table 1)
9	-0.86	China (18–54°N, 73–135°E)	595 sites, 1961–2008	Yin et al. (2010a, Fig. 2 and Table 2)
10	-0.66	China (18–54°N, 73–135°E)	603 sites, 1971–2008	Yin et al. (2010b, Section 3.2 and Table 3)
11	-0.50	China (18–54°N, 73–135°E)	580 sites, 1951–2000	Chen et al. (2005, Table 1)
12	0.00	China, Yellow River Basin (32–42°N, 96–119°E)	89 sites, 1961–2006	Liu et al. (2010b, Tables 3 and 4 and pers. comm. 2010)
13	-1.31	China, Tibet Plateau (26–41°N, 74–104°E)	63 sites, 1961–2000	Shenbin et al. (2006, Fig. 2a and Table 3)
14	-1.05	China, Tibet Plateau (26–39°N, 80–104°E)	75 sites, 1966–2003	Zhang et al. (2007, Fig. 3)
15	-1.41	China, Tibet Plateau (26–39°N, 73–104°E)	75 sites, 1970–2005	Liu et al. (2011b, Fig. 5)
16	-1.49	China, Qinghai–Tibetan Plateau (27–40°N, 76–104°E)	75 sites, 1971–2004	Zhang et al. (2009, Table 3 and pers. comm. 2011)
17	-1.19	China, North China Plain (32–42°N, 113–122°E)	18 sites, 1961–2006	Song et al. (2010, Table 3)
18	-0.90	China Haihe River Basin, (36–42°N, 112–120°E)	34 sites, 1957–2007	Wang et al. (2011, Tables 1 and 2)
<b>South East Asia</b>				
<b>Central Asia</b>				
<b>Sub-continent</b>				
19	-9.36	India, (9–34°N, 69–95°E)	22 sites, 1971–2000	Verma et al. (2008, p. 123)
20	-5.57	India, (9–34°N, 69–95°E)	133 sites, 1971–2002	Bandyopadhyay et al. (2009, Tables 2 and 3)
21	-2.80	India, North-East (22–29°N, 88–97°E)	9 sites, 1979–2000	Jhajharia et al. (in press) and Jhajharia pers. comm. (2011)
<b>Middle East</b>				
22	-0.29	Israel (32°N, 35°E)	1 site, 1964–1997	Cohen et al. (2002, Fig. 1 caption)
23	+1.72	Iran (25–38°N, 45–61°E)	20 sites, 1966–2005	Tabari et al. (2011 and pers. comm. 2010)
24	+0.64	Iran (25–38°N, 45–61°E)	16 sites, 1965–2005	Dinpashoh et al. (2011, Tables 3 and 5)
<b>Africa</b>				
<b>Oceania</b>				
25	-0.94	Australia (10–45°S, 112–155°E)	278,105 grids each 0.05° resolution, 1981–2006	Donohue et al. (2010, pers. comm. 2011)
<b>Central and South America</b>				
26	+0.01	Brazil, North-East (3–10°S, 35–42°W)	19 sites, ~1965–~1995	da Silva (2004, Table 2)

**Table 7**

Global summary of the relative contributions of the four primary meteorological variables to trends in various measures of observed evaporative demand. Studies are grouped by the methodological approach used by others to analyse the relative contribution; units vary between approaches as specified. With Atm. hum. and Rad. being abbreviations for atmospheric humidity and radiation, respectively.

Evaporation type	Trend (mm a <sup>-2</sup> )	Study details	Contribution				Reference
			<i>u</i>	Atm. hum.	Rad.	<i>T<sub>a</sub></i>	
<i>Study type: Stepwise Regression</i> <sup>a</sup>			<i>Units = % (of the total counts-dominance score)</i>				
<i>ET<sub>o</sub></i>	-2.30	65 sites, 1954–1993, China	23.2	27.3	22.6	27.0	Thomas (2000, Fig. 2a and Table 2)
<i>E<sub>pan</sub></i>	-11.78	19 sites, 1961–1992, India	19.3	43.5	19.3	18.0	Chattopadhyay and Hulme (1997, Fig. 4 and Table 3)
<i>ET<sub>p-Penman</sub></i>	-6.02	10 sites, 1976–1990, India	7.7	41.0	34.9	16.4	Chattopadhyay and Hulme (1997, Fig. 7 and Table 3)
<i>ET<sub>o</sub></i>	+0.64	16 sites, 1965–2005, Iran	55.0	19.5	12.0	13.5	Dinpashoh et al. (2011, Tables 3 and 5)
<i>E<sub>pan</sub></i>	-7.19	11 sites, 1965–2000, NE India	27.6	27.6	37.9	6.9	Jhajharia et al. (2009, Tables 4 and 7)
<i>E<sub>pan</sub></i>	-25.27	7 sites, 1969–2004, Central India	36.0	60.0	0.0	4.0	Jhajharia pers. comm. (2011)
<i>E<sub>pan</sub></i>	-21.34	5 sites, 1977–2007, NW India	27.6	62.1	0.0	10.3	Choudhary et al. (2009, Table 2) and Jhajharia pers. comm. (2011)
<i>ET<sub>o</sub></i>	-2.80	9 sites, 1979–2000, NE India	64.1	21.8	0.0	14.1	Jhajharia et al. (in press) and Jhajharia pers. comm. (2011)
<i>Study type: Attribution</i> <sup>b</sup>			<i>Units = mm a<sup>-2</sup></i>				
<i>E<sub>pan</sub></i>	-4.91	45 sites, 1957–2001, Haihe River Basin, China	-5.48	-1.28	-1.47	+3.64	Zheng et al. (2009, Fig. 4 and Table 4)
<i>E<sub>pan</sub></i>	-3.10	54 sites, 1961–2000, China	-2.70	+1.40	-2.60	+0.80	Yang and Yang (in press, Table 3)
<i>E<sub>pan</sub></i>	-5.43	518 sites, 1960–1991, China	-3.50	-0.10	-2.70	+1.30	Liu et al. (2011a, Table 1)
<i>E<sub>pan</sub></i>	+7.94	518 sites, 1992–2007, China	-1.95	+1.65	+0.15	+7.40	Liu et al. (2011a, Table 1)
<i>E<sub>pan</sub></i>	-3.06	75 sites, 1970–2005, Tibetan Plateau, China	-2.81	-1.96	-1.11	+2.73	Liu et al. (2011b, Table 4)
<i>E<sub>pan</sub></i>	-2.00	41 sites, 1975–2004, Australia	-2.70	0.00	+0.60	0.00	Roderick et al. (2007, Fig. 2)
<i>ET<sub>p-Penman</sub></i>	-0.80	278,105 grids each 0.05° resolution, 1981–2006, Australia	-1.30	-0.40	-0.60	+1.50	Donohue et al. (2010, Table 5)
<i>ET<sub>o</sub></i>	-1.00	34 sites, 1950–2007, Haihe River Basin, China	-1.30	-0.50	-0.90	+1.70	Tang et al. (2011, Table 3)
<i>Study type: Regression</i> <sup>c</sup>			<i>Values = r<sup>2</sup> statistics</i>				
<i>E<sub>pan</sub></i>	-1.72	671 sites, 1955–2001, China	0.41	0.02	0.41	0.10	Liu et al. (2010a, Fig. 3 and Table 5)
<i>E<sub>pan</sub></i>	-2.97	278 sites, 1955–2001, humid China	0.56	0.02	0.66	0.01	Liu et al. (2010a, Fig. 3, Table 5 and pers. comm. 2010)
<i>E<sub>pan</sub></i>	-1.76	291 sites, 1955–2001, semi-humid/semi-arid China	0.34	0.03	0.24	0.10	Liu et al. (2010a, Fig. 3, Table 5 and pers. comm. 2010)
<i>E<sub>pan</sub></i>	-0.55	102 sites, 1955–2001, arid China	0.29	0.03	0.14	0.08	Liu et al. (2010a, Fig. 3, Table 5 and pers. comm. 2010)
<i>ET<sub>o</sub></i>	-1.31	63 sites, 1960–2000, Tibetan Plateau, China	0.94	0.46	0.18	0.72	Shenbin et al. (2006, Fig. 2a and Table 3)
<i>E<sub>pan</sub></i>	-2.84	115 sites, 1961–2000, Yangtze River Basin, China	0.49	0.66	0.71	0.27	Wang et al. (2007, Table 1 and Table 4)
<i>ET<sub>o</sub></i>	-1.37	115 sites, 1961–2000, Yangtze River Basin, China	0.54	0.74	0.87	0.20	Wang et al. (2007, Table 1 and Table 4)
<i>ET<sub>o</sub></i>	+0.83	7 sites, 1957–2007, Plateau Haihe River Basin, China	0.03	0.14	0.19	0.07	Wang et al. (2011, Tables 1, 2 and 6)
<i>ET<sub>o</sub></i>	-0.91	8 sites, 1957–2007, Mountains Haihe River Basin, China	0.61	0.45	0.13	0.14	Wang et al. (2011, Tables 1, 2 and 6)
<i>ET<sub>o</sub></i>	-1.53	19 sites, 1957–2007, Plains Haihe River Basin, China	0.38	0.38	0.20	0.19	Wang et al. (2011, Tables 1, 2 and 6)
<i>Study type: Sensitivity Coefficient</i> <sup>d</sup>			<i>Units = mm a<sup>-2</sup></i>				
<i>ET<sub>o</sub></i>	-0.86	595 sites, 1961–2008, China	-1.76	+0.39	-1.00	+1.51	Yin et al. (2010a, Fig. 2 and Table 2)
<i>ET<sub>o</sub></i>	-0.66	603 sites, 1971–2008, China	-2.07	+0.45	-0.26	+1.22	Yin et al. (2010b, Section 3.2 and Table 3)
<i>ET<sub>o</sub></i>	0.00	89 sites, 1961–2006, Yellow River Basin China	-0.63	-0.06	-0.35	+0.68	Liu et al. (2010b, Table 3, Fig. 4 and pers. comm. 2010)
<i>Study type: Significance Testing</i> <sup>e</sup>			<i>Significant (S) or non-significant (NS) and if the variable is causing increasing (↑) or decreasing (↓) evaporation rates</i>				
<i>ET<sub>o</sub></i>	-1.77	45 sites, 1957–2001, Haihe River Basin, China, (0.05)	S↓	S↑	S↓	S↑	Zheng et al. (2009, Figures 4 and 5)
<i>ET<sub>o</sub></i>	-1.69	115 sites, 1971–2000, Yangtze River Basin China, (0.10)	S↓	NS	S↓	S↑	Xu et al. (2006b, Fig. 2 and Table 1)
<i>E<sub>pan</sub></i>	-1.62	115 sites, 1971–2000, Yangtze River Basin China, (0.10)	S↓	NS	S↓	S↑	Xu et al. (2006b, Fig. 2 and Table 1)
<i>E<sub>pan</sub></i>	-1.81	126 sites, 1955–2001, North West China, (0.05)	S↓	Mixed # S↑ > S↓	Not Reported	S↑	Shen et al. (2010, Fig. 7 and pers. comm. 2010)
<i>ET<sub>o</sub></i>	-1.19	18 sites, 1961–2006, North China Plain, China, (0.10)	S↓	NS	S↓	S↑	Song et al. (2010, Table 3)
<i>ET<sub>o</sub></i>	-9.36	22 sites, 1971–2000, India, (0.05)	S↓	S↑	S↓	NS	Verma et al. (2008, p. 123)
<i>ET<sub>o</sub></i>	-5.57	133 sites, 1971–2002 India, (0.05)	S↓	S↑	Mixed # S↓ > S↑	S↑	Bandyopadhyay et al. (2009, Tables 2 and 3)

<sup>a</sup> For the “Stepwise Regression” studies the dominance of each variable was classified into *n* classes by the authors of the papers we review, we scored them as most-dominant = *n* points, next-dominant = *n* – 1 points (and so on depending on the size of *n*) to least-dominant = 1 point, then the number of counts in each dominance class was multiplied by our points and added, then the relative contribution of each meteorological variable to the total “number of counts-dominant score” was expressed as a percentage.

<sup>b</sup> For the “Attribution” group models of evaporation have been formally differentiated, whereas in the “Sensitivity Coefficient” approach Beven’s (1979) relative sensitivity coefficient is combined with the total evaporation change. The sum of the four components does not always add to the observed trend due to errors in rounding and/or measurement error and/or model error and/or other factors driving observed trends.

<sup>c</sup> For the “Regression” study grouping the correlation coefficient (*r*<sup>2</sup>) was determined by correlating evaporative trends with trends of the four primary meteorological variables independently in-turn at the annual time-step.

<sup>d</sup> For the “Sensitivity Coefficient” study group results are the percentage change in the annual evaporation over the study period relative to the annual evaporation at the start of the study period due to the change of each meteorological variable.

<sup>e</sup> For the “Significance Testing” studies the probability (*P*) of the test is provided in brackets at the end of the ‘Study Details’ column, and the symbol # means the number of sites.

we review papers that document the relative contribution that  $u$  trends have made to trends of evaporation, compared to the other three primary meteorological variables (*i.e.*, atmospheric humidity; radiation; and air temperature).

In addition to  $E_{\text{pan}}$  trends reported in units of  $\text{mm a}^{-2}$  (Table 5), other metrics of  $E_{\text{pan}}$  trends have been reported including:

- (i) Golubev et al. (2001, Table 1) from  $\sim 1956\text{--}\sim 1989$  report declining  $E_{\text{pan}}$  trends (significant at the 0.05 level) for seven stations located in European Russia and Latvia;
- (ii) Golubev et al. (2001, Table 1) from 1956–1997 report declining  $E_{\text{pan}}$  trends (significant at the 0.05 level) for Coshocton, Ohio, USA;
- (iii) Golubev et al. (2001, Table 2) from  $\sim 1952\text{--}\sim 1989$  report an average declining  $E_{\text{pan}}$  rate from five regions across much of the Former Soviet Union of  $-0.39\% \text{ a}^{-1}$ , with region-specific values ranging between  $-0.89\% \text{ a}^{-1}$  to  $+0.02\% \text{ a}^{-1}$ ;
- (iv) Golubev et al. (2001, Table 2) from  $\sim 1958\text{--}1998$  report an average declining  $E_{\text{pan}}$  rate from seven regions of the USA (*i.e.*, lower 48 states) of  $-0.07\% \text{ a}^{-1}$ , with region-specific values ranging between  $-0.34\% \text{ a}^{-1}$  to  $+0.30\% \text{ a}^{-1}$ ;
- (v) Groisman et al. (2004, Section 4e, p. 74) for  $\sim 1950\text{--}\sim 2000$  report that warm-season (*i.e.*, May–September)  $E_{\text{pan}}$  totals have decreased over the western two-thirds of the contiguous USA;
- (vi) Asanuma et al. (2004, Fig. 2) for 1967–2000 show that warm-season (*i.e.*, May–October)  $E_{\text{pan}}$  totals have declined for 11 of 13 stations in Japan; and
- (vii) Quintana-Gomez (1998) report for 1951–2000 that annual  $E_{\text{pan}}$  totals have decreased at 14 of the 22 stations over Venezuela (northern-most South America); the declining trend is particularly evident from 1981–1995.

Globally, the majority of measured  $E_{\text{pan}}$  trends are decreasing, with 45 of 55 (or  $\sim 82\%$ ) of regional studies reviewed in Table 5, and all of the ‘other metrics’ studies (summarised above), reporting decreasing  $E_{\text{pan}}$  trends. Assuming that the non-warm season component (*i.e.*, the cold part of the year) is a negligible component to the annual total, the average of the 55  $E_{\text{pan}}$  trend regional studies reviewed in Table 5 is  $-3.19 \text{ mm a}^{-2}$ . The standard deviation, maximum and minimum  $E_{\text{pan}}$  trend are  $6.07 \text{ mm a}^{-2}$ ,  $+16.08 \text{ mm a}^{-2}$  and  $-25.27 \text{ mm a}^{-2}$ , respectively. For Class A pans only ( $n = 35$ ) the trend statistics are: average  $-3.80 \text{ mm a}^{-2}$ ; standard deviation  $7.27 \text{ mm a}^{-2}$ ; maximum

$+16.08 \text{ mm a}^{-2}$ ; and minimum  $-25.27 \text{ mm a}^{-2}$ . For the Class A pan studies with more than 10 sites ( $n = 23$ ) the average is  $-2.50 \text{ mm a}^{-2}$ . For the 18 studies using a 20-cm diameter Chinese micro-pan, the trend statistics are: average  $-2.39 \text{ mm a}^{-2}$ ; standard deviation  $2.89 \text{ mm a}^{-2}$ ; maximum  $+7.94 \text{ mm a}^{-2}$ ; and minimum  $-5.43 \text{ mm a}^{-2}$ .

Globally, the majority of estimated  $ET_o$  trends are decreasing; with 20 of 26 (or 77%) of regional studies reviewed in Table 6 reporting decreasing  $ET_o$  trends. The average of the  $ET_o$  trend regional studies reviewed in Table 6 is  $-1.31 \text{ mm a}^{-2}$ , and the standard deviation, maximum and minimum  $ET_o$  trends are  $2.14 \text{ mm a}^{-2}$ ,  $+1.72 \text{ mm a}^{-2}$  and  $-9.36 \text{ mm a}^{-2}$ , respectively.

Given that  $E_{\text{pan}}$  (Table 5) and  $ET_o$  (Table 6) respond slightly differently to trends in the forcing meteorological data, so the rates of change differ between them (see specifically the following studies where both  $E_{\text{pan}}$  and  $ET_o$  are reported: Cohen et al., 2002; da Silva, 2004; Jhajharia et al., in press; Jhajharia et al., 2009; Tabari and Marofi, 2011; Tabari et al., 2011; Wang et al., 2007; Xu et al., 2006a,b; Zheng et al., 2009). This means that the pan coefficient ( $K_p = ET_o/E_{\text{pan}}$ ), which is widely used across the globe in irrigation areas (especially in developing countries) to transform more commonly available  $E_{\text{pan}}$  observations to  $ET_o$  estimates, is trending. Xu et al. (2006a, Table 3) provide an example of  $K_p$  increasing at a rate of 0.00021  $K_p$  units per annum (though not significant at the  $P = 0.05$  level) from 150 stations over 1960–2000 in the Yangtze River Basin of China, and here we illustrate how  $K_p$  is trending over Australia (Fig. 5a) and north-east India (Fig. 5b). To underpin strategic water resource planning, assessment of long-term observed  $K_p$  trends is urgently needed in those irrigation areas across the globe that use  $E_{\text{pan}}$  measurements to estimate  $ET_o$ . Complimentary to this proposed observational-based assessment, modelled changes in  $K_p$  trends should also be assessed using the theoretical framework developed by Penman and Schofield (1951, Section VI). The Penman and Schofield framework likely requires modification as recent papers illustrate that their assumptions that vapour pressure and  $u$  remains constant during the day are oversimplifications; see McVicar and Jupp (1999, Fig. 5), and Archer and Jacobson (2003, Fig. 2) and Rehman and Ahmad (2004, Fig. 3) for respective examples.

Next we review and summarise over 30 papers that report the relative contributions of the four primary meteorological variables to trends in various measures of evaporative demand (see Table 7).

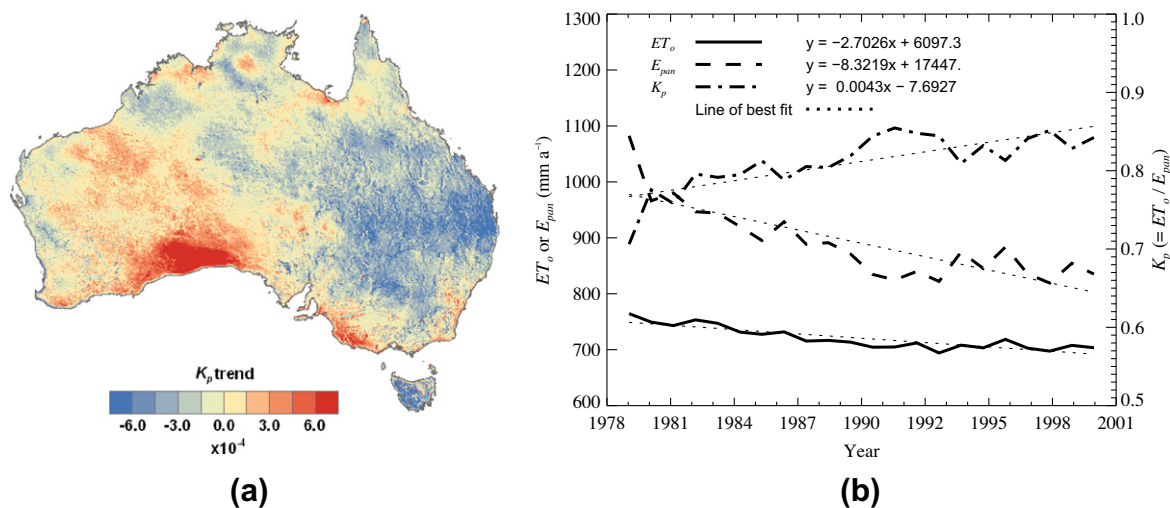


**Fig. 5.** Trends of  $K_p$  for: (a) Australia; and (b) North-East India. Part (a) uses the datasets of Donohue et al. (2010) and  $u$  data of McVicar et al. (2008) for 1981–2006 with  $ET_o$  modelled as per Allen et al. (1998) and  $E_{\text{pan}}$  modelled using PenPan (Rotstajn et al. (2006). The average trend is  $-9.19 \times 10^{-5} K_p$  units per annum, the spatial standard deviation, maximum and minimum are 0.00153, 0.7268 and  $-0.0481 K_p$  units per annum, respectively. There are 278,105 grid cells each  $0.05^\circ$  resolution. For (b) the trends are derived from 1979–2001 for eight sites located in north-east India ( $25\text{--}27^\circ\text{N}$ ,  $88\text{--}96^\circ\text{E}$ ) ranging in elevation from 40 m to 230 m. The 8-site average  $K_p$  trend is 0.0043  $K_p$  units per annum, the slope of the line of best fit is shown on (b).

Results presented in Table 7 show that:

- (i) for the stepwise regression studies  $u$  is commonly in the top two most dominate variables influencing evaporative trends;
- (ii) for the attribution and sensitivity study groupings  $u$  is often the cause for the largest decline of evaporative demand, and in most instances the evaporative decline due to stilling is larger than the evaporative increase due to warming;
- (iii) for the regression studies (which are all conducted in China) the highest correlation between evaporative trends and a meteorological variable is often for  $u$ ; and
- (iv) for the significance testing studies (which are all performed in India and China) all report significant stilling and all but one report significant warming, with radiation in some instances significantly decreasing (likely associated with increasing anthropogenic generated aerosols in those countries which both have rapidly developing economies) with atmospheric moisture generally increasing.

Several other studies have discussed the relative contributions of meteorological variables to evaporative process in a manner that cannot be summarised in the framework used in Table 7. They are:

- (i) Rayner (2007, Fig. 2), from 1975–2004 for 67 stations across Australia, show regressed observed trends in  $E_{\text{pan}}$  ( $X$ -axis) with modelled trends in  $E_{\text{pan}}$  ( $Y$ -axis) derived from Thom et al.'s (1981) model of Class A  $E_{\text{pan}}$ . When using incoming shortwave radiation, actual vapour pressure, and maximum and minimum air temperature, the crossplot of observed vs. modelled  $E_{\text{pan}}$  trends only had a slope 0.14 with an  $r^2 = 0.14$ . When observed  $u$  was added to the model these statistics improved to 0.69 and 0.61, respectively; and
- (ii) Burn and Hesch (2007, Table 4) qualitatively summarised causes for declining trends of open water evaporation ( $E_{\text{ow}}$ ) modelled for the warm season (*i.e.*, April–October) of southern-central Canada from 1971–2000. They show that  $u$  and vapour pressure deficit declines are the primary reasons for  $E_{\text{ow}}$  declining. Actual vapour pressure increased more rapidly than the air-temperature driven increases in saturated vapour pressure, resulting in the vapour pressure deficit decreasing. Interestingly, they also show that the dew point temperature is increasing more rapidly than mean air temperature, confirming that the atmospheric moisture content is increasing and the vapour pressure deficit decreasing.

In summary, results presented in Table 7 clearly show that  $u$  is an important variable effecting evaporative trends, however, the degree of this influence is relative to that of the other primary meteorological variables (Irmak et al., 2006). These all vary spatially, and the degree of this influence likely also depends on temporal extents and analytical method used. Table 7 almost exclusively (*i.e.*, 35 of 36 studies) summarises observed site data. In contrast, Matsoukas et al. (2011) recently used reanalysis output in an attempt to understand the cause(s) of evaporative trends. Matsoukas et al. (2011) concluded that  $ET_p$  trends were primarily a result of change in the radiative component, as opposed to change in the aerodynamic component. We suggest that using reanalysis output rather than observed site data is the likely cause for the contrasting conclusion of Matsoukas et al. (2011) compared to Table 7 (where we show that variables primarily involved in the aerodynamic component often exert greater influence than variables primarily involved in the radiative component). It has been shown that  $u$  trends in reanalysis output demonstrated little similarity to observed  $u$  trends in both the northern (Pryor et al., 2009)

and southern (McVicar et al., 2008) hemispheres. Until this discrepancy is resolved the validity of using reanalysis output to study evaporative trends is questionable (McVicar and Roderick, 2010). Due to the importance of the evaporative process coupling the energy-balance and water-cycle we suggest that all meteorological variables (including  $u$ ) governing evaporative trends need careful long-term observation and assessment.

#### 4. Importance of wind speed to the evaporative process

##### 4.1. Sensitivity analysis

To illustrate the sensitivity of evaporation ( $E$ ) to  $u$  we extracted mid-summer (*i.e.*, January) mean monthly values for an irrigation area in south-eastern Australia (Van Niel and McVicar, 2004) from Australia-wide meteorological grids (Donohue et al., 2010). We calculated three forms of evaporation, being: (i) crop reference evapotranspiration; (ii) Penman potential evapotranspiration; and (iii) Class A pan evaporation.

Following Allen et al. (1998) crop reference evapotranspiration ( $ET_o$ ;  $\text{mm d}^{-1}$ ) is calculated as:

$$ET_o = \frac{0.408\Delta(\mathbf{R}_n - \mathbf{G}) + \gamma \frac{900}{T_a + 273} u_2 D}{\Delta + \gamma(1 + 0.34u_2)} \quad (1)$$

where  $\Delta$  is the slope of the saturation vapour pressure curve ( $\text{kPa } ^\circ\text{C}^{-1}$ );  $\mathbf{R}_n$  is the allwave net radiation at the surface ( $\text{MJ m}^{-2} \text{d}^{-1}$ );  $\mathbf{G}$  is the ground heat flux ( $\text{MJ m}^{-2} \text{d}^{-1}$ );  $\gamma$  is the psychrometric constant ( $\text{kPa } ^\circ\text{C}^{-1}$ );  $T_a$  is the mean daily air temperature, that is  $T_a = (T_{\text{max}} + T_{\text{min}})/2$  ( $^\circ\text{C}$ ), where  $T_{\text{max}}$  and  $T_{\text{min}}$  respectively are the daily maximum and minimum air temperatures ( $^\circ\text{C}$ );  $u_2$  is the daily average wind speed at 2 m above ground level ( $\text{m s}^{-1}$ );  $D$  is the saturation vapour pressure deficit ( $\text{kPa}$ ) =  $e_s - e_a$ ; with  $e_s$  being the saturation vapour pressure ( $\text{kPa}$ ) and  $e_a$  the actual vapour pressure ( $\text{kPa}$ ).

Penman's (1948) potential evapotranspiration ( $E_p$ ;  $\text{mm d}^{-1}$ ), as given in Shuttleworth (1992), is calculated as:

$$E_p = E_{pR} + E_{pA} = \frac{\Delta}{\Delta + \gamma} \mathbf{R}_n + \frac{\gamma}{\Delta + \gamma} \frac{6430(1 + 0.536u_2)D}{\lambda} \quad (2)$$

where  $E_{pR}$  and  $E_{pA}$  represent the radiative and aerodynamic components of the Penman equation, respectively, and  $\lambda$  is the latent heat of vaporisation of water ( $2.45 \times 10^6 \text{ J kg}^{-1}$ ).

PenPan evaporation ( $E_{pp}$ ,  $\text{mm d}^{-1}$ ) is a Penman-based model of Class A pan evaporation (Rotstajn et al., 2006) and is calculated as:

$$E_{pp} = \frac{\Delta R_p + a\gamma D(1.39 \times 10^{-8}(1 + 1.35u_2))86400}{\Delta + a\gamma} \quad (3)$$

where  $R_p$  (in water-equivalent units,  $\text{mm d}^{-1}$ ) is the net radiation of the pan and  $a$  being a dimensionless constant (2.4) related to the different surface areas for heat and mass transfer (see Rotstajn et al., 2006).

Fig. 6a shows that decreasing  $u$  resulted in decreased rates of evaporation; the magnitude of the impact varies depending on the formulation of evaporation, with a change of  $2 \text{ m s}^{-1}$  resulting in a 20% change in the PenPan evaporation rates (Fig. 6b). In addition to the above sensitivity analysis, using a wind tunnel experiment to assess Class A pan evaporation rates, Chu et al. (2010, their Fig. 1) show a  $u$  dependence in the Class A pan evaporation rates. Given widespread stilling (*i.e.*, Table 2, Fig. 2 and Table 4), and the effect this has on evaporation rates (*i.e.*, Table 5–7), this means that changing  $ET_a$  rates will impact rates of streamflow ( $Q$ ) generation to varying degrees. For example, Yang and Yang (2011, paragraph 20) report for the water-limited Futuo River Basin in northern China from 1961–2000 that  $u$  trends had the largest impact among the four primary meteorological variables

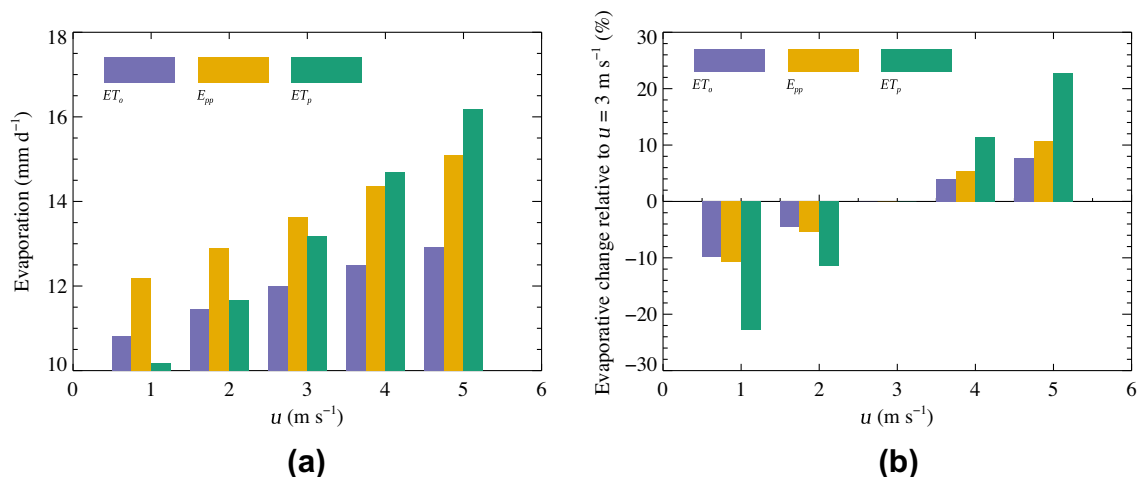


**Fig. 6.** Impact of  $u$  on daily evaporation rates. Part (a) shows the increase of the three common formulations of evaporation with increasing  $u$ , and (b) shows their relative difference of daily evaporation compared to the case when  $u = 3 \text{ m s}^{-1}$ . Values for the three other relevant climate variables are:  $R_n = 32.57 \text{ MJ m}^{-2} \text{ d}^{-1}$ ;  $T_a = 298 \text{ K}$ ; and  $D = 2.15 \text{ kPa}$ .

influencing  $Q$  trends in the catchment. As expected, observed precipitation dominated the resultant  $Q$  trends.

#### 4.2. Relative importance of aerodynamics on evaporation trends

In addition to the summary presented in our Table 7, Chattopadhyay and Hulme (1997, Table 4) clearly highlighted the greater importance of the aerodynamic component over the radiative component when calculating the relative changes in Penman's  $E_p$  given a  $1^\circ\text{C}$  rise in global mean  $T_a$ . Using output from six global climate model experiments by four seasons by three locations (ranging in latitude from  $37.5^\circ\text{N}$  to  $7.5^\circ\text{N}$ ) they report that in 74% (*i.e.*, 53 of the 72 experiment-season-location combinations) of the cases the changes of the aerodynamic component are predicted to be greater than changes of the radiative component (Chattopadhyay and Hulme, 1997). Yin et al. (2010a, Table 3) stratified China into eight regions reporting the relative importance of the four primary meteorological variables to evaporative trends regionally. For seven of the eight regions they show that the changes of  $ET_0$  caused by  $u$  change are larger than that caused by relative humidity change (see Yin et al., 2010a, Table 3).

In this sub-section we discuss the aerodynamic component in three ways. Firstly, we calculate the relative magnitude of the aerodynamic component of  $ET_0$  using a 1961–1990 monthly climatology from a global network of 4367 stations developed by the Agromet Group of the Food and Agriculture Organisation (see Fig. 7). Secondly, we assess the sensitivity of Penman's  $ET_p$  to changes of  $u$ . In this analysis, over a simulated  $u$  range from  $0 \text{ m s}^{-1}$  to  $10 \text{ m s}^{-1}$  using the method of Donohue et al. (2010), we assess the resultant change in Penman's  $ET_p$  given a 5%, 10% and 20% change in  $u$  (see Fig. 8). The upper value (*i.e.*, a 20% change) is based on an analysis presented by Vautard et al. (2010, Supplementary Table 1 Row 10) for Central Asia and Pryor and Ledolter (2010, Table 1) for the USA, lower 48 states. Thirdly, using the methods and data of Donohue et al. (2010) that were applied to all Australia for 1981–2006, we assess the relative contributions the four primary meteorological variables made to trends in evaporative demand for key water-yielding regions in the Murray–Darling Basin, Australia.

As expected, Fig. 7 shows latitudinal banding of the relative importance of the aerodynamic component that is inversely associated with the seasonal cycle radiation maxima. In the mid-latitudes (*i.e.*,  $>35^\circ$ ) in winter the aerodynamics governs  $>80\%$  of the evaporative process, in summer for these latitudes this

reduces to the order of 20–40%. This pattern is clearly seen in data presented by Garcia et al. (2004, Figs. 9 and 10 and Table 4), noting that their site elevations of  $\sim 3800 \text{ m}$  means that the effective latitude is greater (*i.e.*, further south) than the  $17^\circ\text{S}$ . For tropical latitudes (*i.e.*,  $<20^\circ$ ), where there is little annual change in day-length, the aerodynamics governs  $\sim 20\%$  of the evaporative process (as given by  $ET_0$ ). For much of the year in the sub-tropics (*i.e.*, between  $\sim 20^\circ$  to  $\sim 35^\circ$ ) the aerodynamic component varies between 40% and 80% of the total  $ET_0$ . This analysis clearly shows that the relative importance of  $u$  on the evaporative process when water is not limited varies as a function of latitude and season. When considering changes to  $ET_a$ , thereby linking with the terrestrial water balance, an important consideration (in addition to the above two factors: latitude and season) is the availability of water which climatologically limits  $ET_a$  as illustrated in Fig. 1 and Table 1. When dealing with a finer temporal resolution (*i.e.*, from average annual through annual and seasonal to daily) when catchments are energy-limited, changes in  $u$  will result in  $ET_a$  and  $Q$  changes, yet as catchments become more water-limited  $u$  changes will have less impact on  $ET_a$  dynamics. At the shorter time-steps (*i.e.*, monthly to daily) for water-limited locations, precipitation dynamics and water storage (*e.g.*, soil stores and ground-surface water interactions) dynamics are the more dominant factors governing the terrestrial water balance (*e.g.*, Jung et al., 2010; Miralles et al., 2011; Seneviratne et al., 2010).

For a given  $u$  and  $D$  (which is, in turn, dependent on  $T_{max}$  and  $T_{min}$ ) Fig. 8 can be used to determine for a 5%, 10% or 20% change in  $u$  what the resultant relative change in Penman's  $ET_p$  will be, all other factors being constant. For an increase in  $u$  there will be an associated increase in Penman's  $ET_p$  and vice versa. For the important water-supply headwater catchments, that are primarily energy-limited, this change in Penman's  $ET_p$  will be effectively translated to changes in  $ET_a$  and  $Q$ . The importance of  $u$  in mountainous environments has been widely reported (*e.g.*, McVicar et al., 2007, 2010; Wang and Georgakakos, 2007). For water-limited areas the other factors limiting  $ET_a$  require consideration (introduced above when discussing Fig. 7).

Table 8 shows the relative contribution to changes in Penman's  $ET_p$  due to changes in the four primary meteorological variables. For the three high water yielding zones located in the southern Murray–Darling Basin (MBD, *i.e.*, the EHYZ, VHYZ and sHYZ; the abbreviations are explained in the caption) they all show decreasing rates of Penman's  $ET_p$  with the decreases of Penman's  $ET_p$  due to  $u$  and  $e_a$  changes essentially offsetting the rises of Penman's

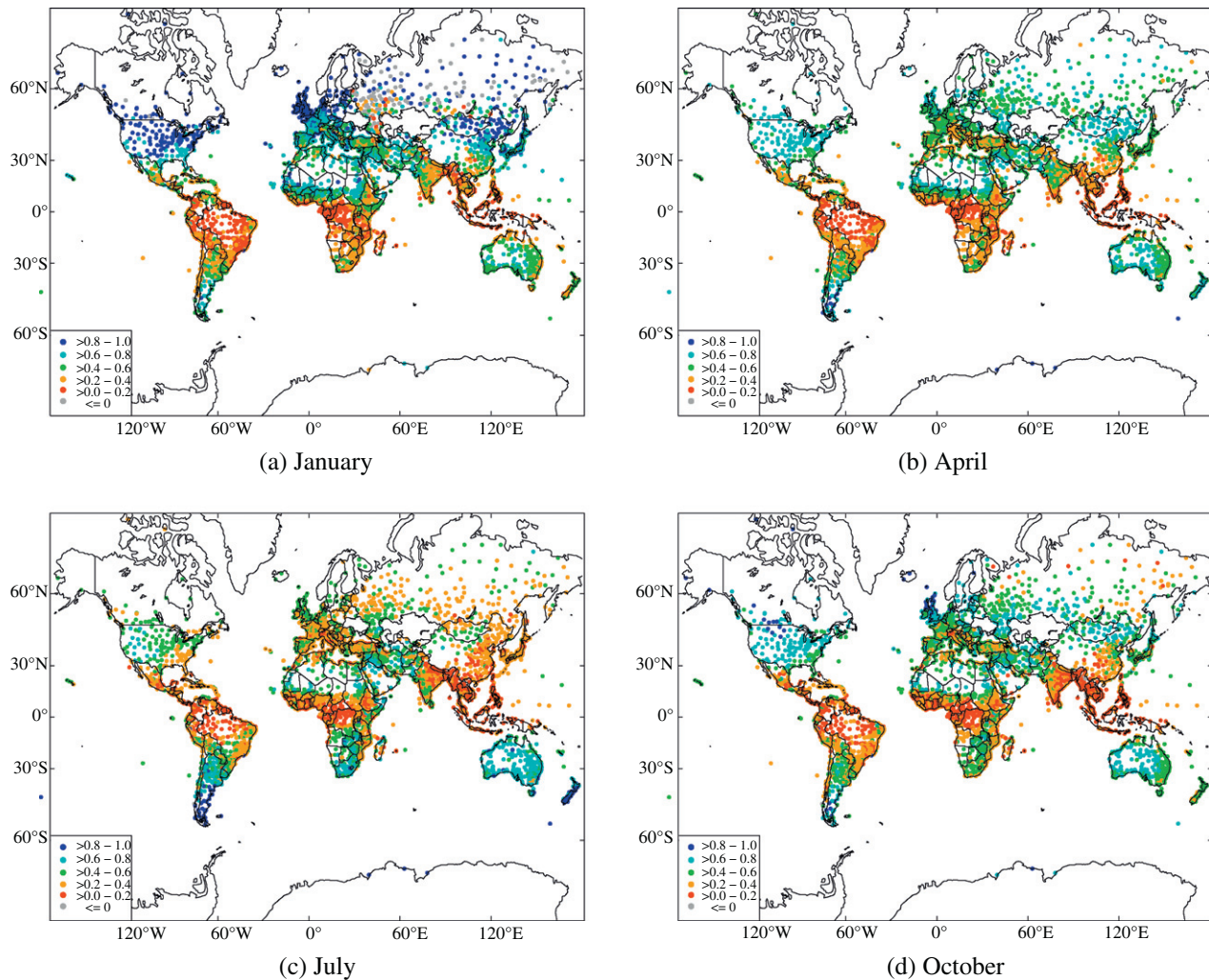


**Fig. 7.** Relative fractional contribution of the aerodynamic component to total  $ET_o$  for the mid-seasonal months. Symbols are larger in the legend to aid readability.

$ET_p$  due to increasing  $T_a$ . For water resource management, including assessing impacts to groundwater recharge (McCallum et al., 2010), it is vital to consider changes of both precipitation and all meteorological variables that govern the evaporative process to better plan for climatic change. This is clearly illustrated by the combined EHYZ, VHYZ and sHYZ, which only cover 8.4% of the MDB yet account for 50% of the  $Q$  generated (Table 8). In these areas Penman's  $ET_p$  is decreasing from 1981–2006 though warming has been experienced during this period, this result only becomes apparent when trends in all four primary meteorological variables are considered. The relative importance of the four primary meteorological variables that control evaporative trends varies spatially (Table 8), and also varies temporally (e.g., Liu et al., 2011a); this means broad generalisations are problematic.

## 5. Conclusion

This global review of 148 studies confirms that near-surface terrestrial  $u$  are declining in both hemispheres for both the tropical and mid-latitudes at a rate of  $-0.014 \text{ m s}^{-1} \text{ a}^{-1}$  (for studies with more than 30 sites observing data for more than 30 years). Assuming a linear trend this constitutes a  $-0.7 \text{ m s}^{-1}$  change in  $u$  over 50 years. At high-latitudes (i.e.,  $>70^\circ$ ), in line with model predictions, observed  $u$  are increasing (again in both hemispheres). While several possible causes have been proposed for the tropical- and

mid-latitudes stilling trend, it is unlikely that one single factor governs the observed trends globally. The combined factors (and their relative influence) governing stilling likely varies spatially and temporally, so successful attribution of the processes governing stilling remains a major challenge. Clearly further research is needed.

We confirmed the declining rates of evaporative demand by reviewing papers reporting trends in  $E_{pan}$  and  $ET_o$  with average results being  $-3.19 \text{ mm a}^{-2}$  ( $n = 55$ ) and  $-1.31 \text{ mm a}^{-2}$  ( $n = 26$ ), respectively. Trends are also shown in  $K_p$  (used to relate  $E_{pan}$  with  $ET_o$ ) and to underpin strategic water resource planning, assessment of long-term  $K_p$  trends is needed in those irrigation areas across the globe that use  $E_{pan}$  measurements to estimate  $ET_o$  and water scheduling.

The contributions to evaporative demand trends made by the four primary meteorological variables (being  $u$ ; atmospheric humidity; radiation; and air temperature) were also assessed. The results from 36 studies highlight the important role that  $u$  trends play in governing evaporative demand trends. We quantified the sensitivity of rates of evaporative demand to changes in  $u$  and globally show how the relative contributions of the aerodynamic and radiative components change seasonally. A series of theoretical calculations showed the relative change in Penman's  $ET_p$  for a given  $u$  (and vapour pressure deficit) change and can be used across the terrestrial global land-surface to estimate the impact of  $u$  changes on evaporative demand.

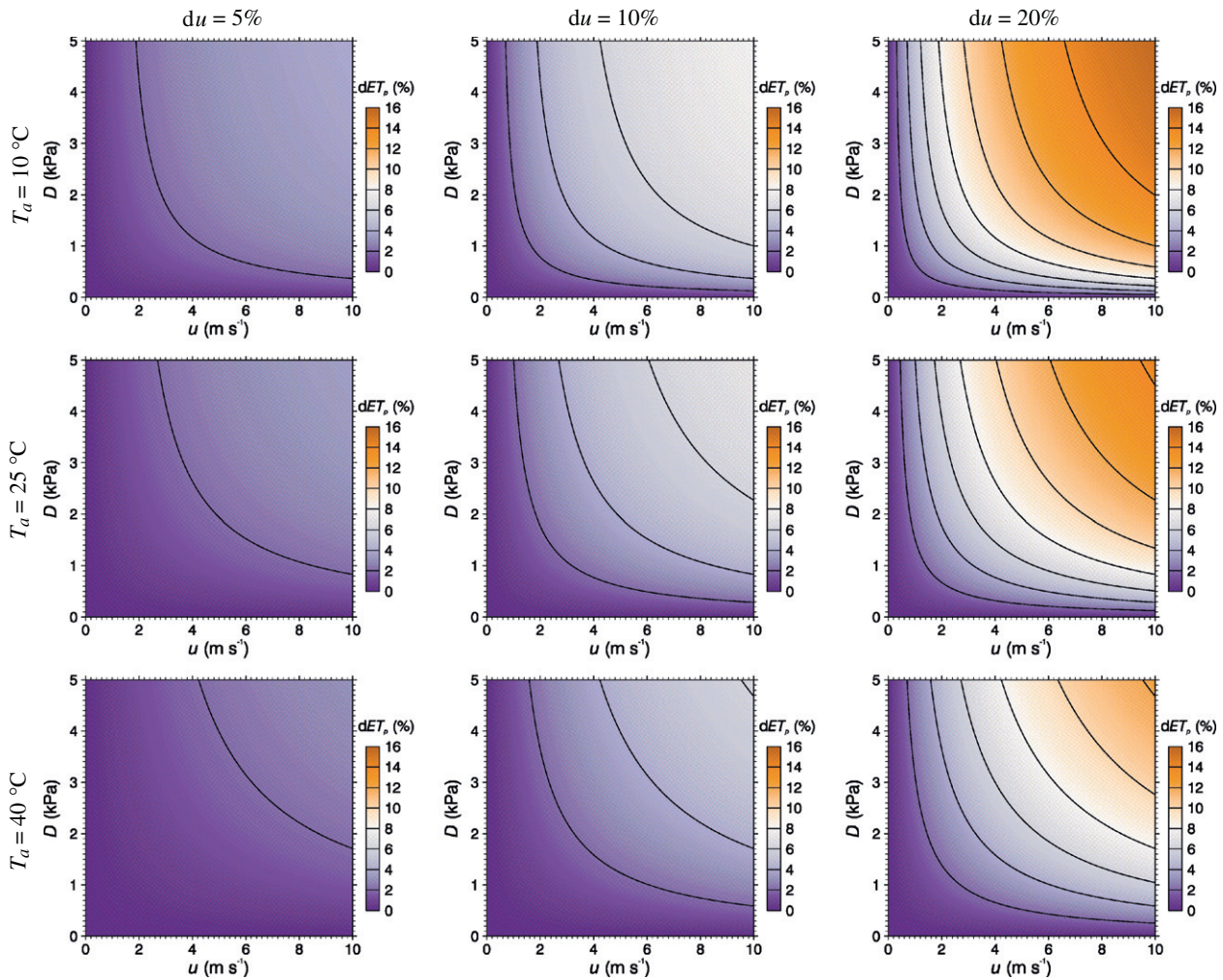


**Fig. 8.** Relative changes in Penman's  $ET_p$  (%) given 5%, 10% and 20% changes in  $u$ . The vapour pressure deficit ( $D$ ) is calculated at three air temperatures which influence  $e_s$ . The black contour lines increment by 2%, increasing from the bottom-left to the top-right of each sub-plot.  $R_n$  is set to  $5.4 \text{ mm d}^{-1}$  ( $=153 \text{ W m}^{-2}$ ). See Supplementary material Table 6 for specific values at the intersections of  $u$  incrementing by  $2 \text{ m s}^{-1}$  and  $D$  incrementing by  $1 \text{ kPa}$  for the nine panels.

**Table 8**  
Annual average Penman's  $ET_p$  (1981–2006), its trend and the contribution of the four primary meteorological variables. These are regionally averaged for Australia, the Murray–Darling Basin (MDB) located in south-east Australia, and for 4 high water yielding zones in the MDB. The extremely high yield zone (EHYZ), very high yield zone (VHYZ), southern high yield zone (sHYZ) and northern high yield zone (nHYZ) are defined and shown in Donohue et al. (2011, Table 1 and Fig. 8, respectively). The method to calculate the contribution of the four primary meteorological variables, using Australia as an example, is provided in Donohue et al. (2010, specifically see Table 5). The area and relative contribution each region makes to MDB annual average (1981–2006) streamflow ( $Q$ ), modelled in Donohue et al. (2011, Table 3), are provided for context. NR stands for not relevant,  $e_a$  is actual vapour pressure,  $R_n$  is net radiation, and  $T_a$  is air temperature.

Region	$ET_p$ ( $\text{mm yr}^{-1}$ )	Trends of $ET_p$ ( $\text{mm yr}^{-2}$ )					Area ( $\text{km}^2 \times 10^3$ ) [% of MDB]	MDB Q ( $\text{GL a}^{-1}$ ) [% of MDB Q]	
		Total	Contribution due to					NR	[100]
			$u$	$e_a$	$R_n$	$T_a$			
Australia	2340	-0.8	-1.3	-0.4	-0.6	+1.5	7694	[NR]	[NR]
MDB	1977	+0.4	-0.9	+0.7	-1.7	+2.3	1065	[100]	29,517 [100]
nHYZ	1739	+2.0	-0.7	-0.1	+0.9	+1.9	43	[4.0]	4588 [16]
sHYZ	1502	-0.3	-1.2	-0.4	-0.6	+1.9	67	[6.3]	6960 [24]
VHYZ	1379	-0.1	-0.7	-0.5	-0.5	+1.6	20	[1.8]	6021 [20]
EHYZ	1248	-0.5	-1.1	-0.5	-0.3	+1.4	3	[0.3]	1765 [6]

Given that we: (i) showed that terrestrial stilling is globally widespread; (ii) confirmed declining rates of evaporative demand; and (iii) highlighted the contribution  $u$  has made to these declining evaporative rates, we advocate that trends in evaporative demand be assessed using all four primary meteorological variables. The relative importance of the four primary meteorological variables governing evaporative demand trends will vary with both their absolute and relative values, which in turn, vary both spatially

and temporally. For example, as  $u$  is now low in China and the rate of stilling has recently declined there (e.g., Guo et al., 2011), other meteorological variables have begun to exert more influence on recent evaporative demand trends in China (e.g., Liu et al., 2011a).

Assessing  $u$  trends and its influence on evaporative demand is important for long-term water resource appraisal in energy-limited catchments (where  $ET_a = ET_p$ ) and in the more humid of the water-limited catchments (where  $ET_a \rightarrow ET_p$ ). This is because

these catchments generate much of the globe's surface water resources and changes in evaporative demand will manifest themselves as complimentary changes in streamflow (all else being equal). In contrast, in severely water-limited catchments  $ET_a$  trends are more closely related with trends in water availability and changes in  $u$  often have little direct impact on the local water balance.

## Acknowledgements

Thanks to: (i) the numerous scientists who provided additional information from their studies; (ii) those who translated material from a variety of languages into English; (iii) Elisa Vuillermoz and Gianni Tartari (Ev-K2-CNR Committee, Bergamo – Italy) for permission to use Stations at High Altitude for Research on the Environment (SHARE) program data; and (iv) the two reviewers, editor and associate editor for comments that helped to improve our paper. MLR acknowledges support from the Australian Research Council Centre of Excellence for Climate System Science (Grant: CE11E0098). Can readers please inform the lead author about new studies, or studies overlooked here, that report  $u$ ,  $E_{pan}$  or  $ET_0$  trends.

## Appendix A. Supplementary material

Supplementary data associated with this article can be found, in the online version, at doi:10.1016/j.jhydrol.2011.10.024.

## References

- Abhishek, A., Lee, J., Keener, T., Yang, Y., 2010. Long-term wind speed variations for three Midwestern US cities. *J. Air Waste Manag. Assoc.* 60 (9), 1057–1064.
- Akpinar, E.K., Akpinar, S., 2004. Determination of the wind energy potential for Maden–Elazig, Turkey. *Energy Convers. Manage.* 45 (18–19), 2901–2914.
- Alfaro, S.C., Gomes, L., 2001. Modeling mineral aerosol production by wind erosion: emission intensities and aerosol size distributions in source areas. *J. Geophys. Res. – Atmos.* 106 (D16), 18075–18084.
- Allen, R.G., Pereira, L.S., Raes, D., Smith, M., 1998. *Crop Evapotranspiration – Guidelines for Computing Crop Water Requirements*. FAO Irrigation and Drainage Paper 56, Rome, Italy.
- Archer, C.L., Jacobson, M.Z., 2003. Spatial and temporal distributions of US winds and wind power at 80 m derived from measurements. *J. Geophys. Res. – Atmos.* 108 (D9), 4289. doi:10.1029/2002JD002076.
- Archer, C.L., Jacobson, M.Z., 2005. Evaluation of global wind power. *J. Geophys. Res. – Atmos.* 110 (D12), D12110. doi:10.1029/2004JD005462.
- Aristidi, E. et al., 2005. An analysis of temperatures and wind speeds above Dome C, Antarctica. *Astron. Astrophys.* 430 (2), 739–746.
- Asanuma, J., Kamimera, H., 2003. Long-term trends of the pan evaporation as an index of the global hydrological change. In: *Proceeding of International Symposium on Disaster Mitigation and Basin-Wide Water Management*. UNESCO, Niigata, Japan.
- Asanuma, J., Kamimera, H., Lu, M.J., 2004. Pan evaporation trends in Japan and its relevance to the variability of the hydrological cycle. *Tenki* 51 (9), 667–678 (in Japanese with an English abstract).
- Bandyopadhyay, A., Bhadra, A., Raghuvanshi, N.S., Singh, R., 2009. Temporal trends in estimates of reference evapotranspiration over India. *J. Hydrol. Eng.* 14 (5), 508–515.
- Barnett, T.P., Adam, J.C., Lettenmaier, D.P., 2005. Potential impacts of a warming climate on water availability in snow-dominated regions. *Nature* 438 (7066), 303–309.
- Beck, H.E. et al., 2011. Global evaluation of four AVHRR-NDVI data-sets: intercomparison and assessment against Landsat imagery. *Remote Sens. Environ.* 115 (10), 2547–2563.
- Belu, R., Koracin, D., 2009. Wind characteristics and wind energy potential in western Nevada. *Renew. Energy* 34 (10), 2246–2251.
- Beniston, M., 2005. Mountain climates and climatic change: an overview of processes focusing on the European Alps. *Pure Appl. Geophys.* 162 (8–9), 1587–1606.
- Bernard, S.M., Samet, J.M., Grambsch, A., Ebi, K.L., Romieu, I., 2001. The potential impacts of climate variability and change on air pollution-related health effects in the United States. *Environ. Health Perspect.* 109 (2), 199–209.
- Even, K., 1979. Sensitivity analysis of the Penman–Monteith actual evapotranspiration estimates. *J. Hydrol.* 44 (3–4), 169–190.
- Bigg, G.R., 1993. Comparison of coastal wind and pressure trends over the tropical Atlantic: 1946–1987. *Int. J. Climatol.* 13 (4), 411–421.
- Black, K. et al., 2006. Long-term trends in solar irradiance in Ireland and their potential effects on gross primary productivity. *Agric. For. Meteorol.* 141 (2–4), 118–132.
- Blanco-Maciás, F., Valdez-Cepeda, R.D., Magallanes-Quintanar, R., 2011. Pan evaporation analysis in central México: trends, self-affinity and important frequencies. *Int. J. Phys. Sci.* 6 (3), 540–549.
- Bormann, H., 2011. Sensitivity analysis of 18 different potential evapotranspiration models to observed climatic change at German climate stations. *Clim. Change* 104 (3–4), 729–753.
- Böwer, C., 2006. *Die Entwicklung des Klimas in Münster/Westfalen*. Diploma Thesis, Westfälischen Wilhelms-Universität Münster, Germany, 74 pp. <http://kli.uni-muenster.de/downloads/2006\_boewer\_dipl.pdf> (last accessed on 4 Nov 2011) (in German).
- Brazdil, R., Chroma, K., Dobrovolny, P., Tolasz, R., 2009. Climate fluctuations in the Czech Republic during the period 1961–2005. *Int. J. Climatol.* 29 (2), 223–242.
- Brouyau, F. et al., 2009. Chapitre 1. L'évolution du climat en Belgique (In French), *Vigilance Climatique*. Publié par l'Institut Royal Météorologique de Belgique, Bruxelles, pp. 6–24. <http://www.meteo.be/meteo/view/fr/69130-Archives.html?view=3236558> (last accessed on 7 Nov 2011).
- Budyko, M.I., 1974. *Climate and Life*. Academic, New York.
- Burn, D.H., Hesch, N.M., 2007. Trends in evaporation for the Canadian prairies. *J. Hydrol.* 336 (1–2), 61–73.
- Cabalar Fuentes, M., 2005. *Los temporales de lluvia y viento en Galicia; Propuesta de clasificación y análisis de tendencias (1961–2001)*. Invest. Geogr. 36, 103–118 (in Spanish).
- Cancino-Solórzano, Y., Xiberta-Bernat, J., 2009. Statistical analysis of wind power in the region of Veracruz (Mexico). *Renew. Energy* 34 (6), 1628–1634.
- Cardone, V.J., Greenwood, J.G., Cane, M.A., 1990. On trends in historical marine wind data. *J. Clim.* 3 (1), 113–127.
- Chattopadhyay, N., Hulme, M., 1997. Evaporation and potential evapotranspiration in India under conditions of recent and future climate change. *Agric. For. Meteorol.* 87 (1), 55–73.
- Chen, D.L., Gao, G., Xu, C.-Y., Guo, J., Ren, G.Y., 2005. Comparison of the Thornthwaite method and pan data with the standard Penman–Monteith estimates of reference evapotranspiration in China. *Clim. Res.* 28 (2), 123–132.
- Choudhary, R.R. et al., 2009. Climate and its variations over Bikaner since 1951–2008. *J. Ind. Geol. Congr.* 1 (2), 79–86.
- Chu, D.A., Kaufman, Y.J., Zibordi, G., Chern, J.D., Mao, J., Li, C., Holben, B.N., 2003. Global monitoring of air pollution over land from the Earth Observing System–Terra Moderate Resolution Imaging Spectroradiometer (MODIS). *J. Geophys. Res. – Atmos.* 108 (D21), 4661. doi:10.1029/2002JD003179.
- Chu, C.R., Li, M.H., Chen, Y.Y., Kuo, Y.H., 2010. A wind tunnel experiment on the evaporation rate of Class A evaporation pan. *J. Hydrol.* 381 (3–4), 221–224.
- Coelingh, J.P., van Wijk, A.J.M., Holtslag, A.A.M., 1996. Analysis of wind speed observations over the North Sea. *J. Wind Eng. Ind. Aerodyn.* 61 (1), 51–69.
- Cohen, S., Ianetz, A., Stanhill, G., 2002. Evaporative climate changes at Bet Dagan, Israel, 1964–1998. *Agric. For. Meteorol.* 111 (2), 83–91.
- Cong, Z.T., Yang, D.W., Ni, G.H., 2009. Does evaporation paradox exist in China? *Hydrol. Earth Syst. Sci.* 13 (3), 357–366.
- Cong, Z.T., Zhao, J.J., Yang, D.W., Ni, G.H., 2010. Understanding the hydrological trends of river basins in China. *J. Hydrol.* 388 (3–4), 350–356.
- Cook, N.J., 1985. *The Designer's Guide to Wind Loading of Building Structures – Part 1: Background, Damage Survey, Wind Data and Structural Classification*. Butterworths, London.
- Cusack, S., 2011. A 100 year record of windstorms in the Netherlands. *Clim. Change*, submitted for publication.
- da Silva, V.D.R., 2004. On climate variability in Northeast of Brazil. *J. Arid Environ.* 58 (4), 575–596.
- da Silva, V.D.R. et al., 2010. Trends in solar radiation in NCEP/NCAR database and measurements in northeastern Brazil. *Sol. Energy* 84 (10), 1852–1862.
- DeGaetano, A.T., 1998. Identification and implications of biases in US surface wind observation, archival, and summarization methods. *Theor. Appl. Climatol.* 60 (1–4), 151–162.
- Dinpashoh, Y., 2006. Study of reference crop evapotranspiration in IR of Iran. *Agric. Water Manage.* 84 (1–2), 123–129.
- Dinpashoh, Y., Jhajharia, D., Fakheri-Fard, A., Singh, V.P., Kahya, E., 2011. Trends in reference crop evapotranspiration over Iran. *J. Hydrol.* 399 (3–4), 422–433. doi:10.1016/j.jhydrol.2011.01.021.
- Donohue, R.J., Roderick, M.L., McVicar, T.R., 2007. On the importance of including vegetation dynamics in Budyko's hydrological model. *Hydrol. Earth Syst. Sci.* 11 (2), 983–995.
- Donohue, R.J., Roderick, M.L., McVicar, T.R., 2008. Deriving consistent long-term vegetation information from AVHRR reflectance data using a cover-triangle-based framework. *Remote Sens. Environ.* 112 (6), 2938–2949.
- Donohue, R.J., McVicar, T.R., Roderick, M.L., 2009. Climate-related trends in Australian vegetation cover as inferred from satellite observations, 1981–2006. *Global Change Biol.* 15 (4), 1025–1039.
- Donohue, R.J., McVicar, T.R., Roderick, M.L., 2010. Assessing the ability of potential evaporation formulations to capture the dynamics in evaporative demand within a changing climate. *J. Hydrol.* 386 (1–4), 186–197. doi:10.1016/j.jhydrol.2010.03.020.
- Donohue, R.J., Roderick, M.L., McVicar, T.R., 2011. Assessing the differences in sensitivities of runoff to changes in climatic conditions across a large basin. *J. Hydrol.* 406 (3–4), 234–244. doi:10.1016/j.jhydrol.2011.07.003.
- Dorvlo, A.S.S., Ampratwum, D.B., 2002. Wind energy potential for Oman. *Renew. Energy* 26 (3), 333–338.

- El-Osta, W., Belhag, M., Klat, M., Fallah, I., Kalifa, Y., 1995. Wind farm pilot project in Libya. *Renew. Energy* 6 (5–6), 639–642.
- Elsawwaf, M., Willems, P., Feyen, J., 2010. Assessment of the sensitivity and prediction uncertainty of evaporation models applied to Nasser Lake, Egypt. *J. Hydrol.* 395 (1–2), 10–22.
- Espadafor, M., Lorite, I.J., Gavilán, P., Berengena, J., 2011. An analysis of the tendency of reference evapotranspiration estimates and other climate variables during the last 45 years in Southern Spain. *Agric. Water Manage.* 98 (6), 1045–1061.
- Evans, J.P., Smith, R.B., Oglesby, R.J., 2004. Middle East climate simulation and dominant precipitation processes. *Int. J. Climatol.* 24 (13), 1671–1694.
- Fall, S. et al., 2011. Analysis of the impacts of station exposure on the US Historical Climatology Network temperatures and temperature trends. *J. Geophys. Res. – Atmos.* 116, D14120. doi:10.1029/2010JD015146.
- Flohn, H., Kapala, A., 1989. Changes of tropical sea air interaction processes over a 30-year period. *Nature* 338 (6212), 244–246.
- Frederiksen, J.S., Frederiksen, C.S., 2007. Interdecadal changes in southern hemisphere winter storm track modes. *Tellus A* 59 (5), 599–617.
- Friedman, J., Barrett, S.C.H., 2009. Wind of change: new insights on the ecology and evolution of pollination and mating in wind-pollinated plants. *Ann. Botany* 103 (9), 1515–1527.
- Fu, G.B. et al., 2011. Temporal variation of wind speed in China for 1961–2007. *Theor. Appl. Climatol.* 104 (3–4), 313–324.
- Fujibe, F., 2009. Relation between long-term temperature and wind speed trends at surface observation stations in Japan. *SOLA (Sci. Online Lett. Atmos.); Meteorological Society of Japan* 5, 81–84.
- Fujibe, F., 2011. Urban warming in Japanese cities and its relation to climate change monitoring. *Int. J. Climatol.* 31 (2), 162–173.
- Fujii, T., 2007. On geographical distributions and decadal changes of the annual maximum wind speeds caused by typhoons in Japan. *J. Nat. Disaster Sci.* 26 (3), 267–277 (in Japanese with an English abstract).
- García, M., Raes, D., Allen, R., Herbas, C., 2004. Dynamics of reference evapotranspiration in the Bolivian highlands (Altiplano). *Agric. For. Meteorol.* 125 (1–2), 67–82.
- Gastineau, G., Soden, B.J., 2009. Model projected changes of extreme wind events in response to global warming. *Geophys. Res. Lett.* 36, L10810. doi:10.1029/2009GL037500.
- Gebregeziabher, Y., 2004. Assessment of the Water Balance of Lake Awassa Catchment, Ethiopia. ITC, Enschede, The Netherlands, 92 pp.
- Gerstengarbe, F.-W., Werner, P.C., Hauf, Y., 2004. Bericht zum Werkvertrag Erstellung regionaler Klimaszenarien für Nordrhein-Westfalen, Nr. 2-53710-2233, 29pp. <[http://www.lanuv.nrw.de/klima/pdf/klimastudie\\_nrw.pdf](http://www.lanuv.nrw.de/klima/pdf/klimastudie_nrw.pdf)> (last accessed on 4 Nov 2011) (in German).
- Golubev, V.S. et al., 2001. Evaporation changes over the contiguous United States and the former USSR: A reassessment. *Geophys. Res. Lett.* 28 (13), 2665–2668.
- Gong, L., Xu, C.Y., Chen, D., Halldin, S., Chen, Y.D., 2006. Sensitivity of the Penman–Monteith reference evapotranspiration to key climatic variables in the Changjiang (Yangtze River) basin. *J. Hydrol.* 329 (3–4), 620–629.
- Griffin, B.J., Kohfeld, K.E., Cooper, A.B., Boenisch, G., 2010. The importance of location for describing typical and extreme wind speed behavior. *Geophys. Res. Lett.* 37, L22804. doi:10.1029/2010GL045052.
- Groisman, P.Y. et al., 2004. Contemporary changes of the hydrological cycle over the contiguous United States: trends derived from in situ observations. *J. Hydrometeorol.* 5 (1), 64–85.
- Gruza, G.V. et al., 2008. Assessment report on climate change and their impact on the territory of the Russian Federation (in Russian), Voeikov Main Geophysical Observatory, Roshydromet (MGO) and Institute of Global Climate and Ecology, Roshydromet and Russian Academy of Sciences (IGCE), Moscow, Russia, pp. 31–87. <<http://climate2008.igce.ru/v2008/v1/v1-3.pdf>> (last accessed on 4 Nov 2011) (Chapter 3).
- Guo, H., Xu, M., Hu, Q., 2011. Changes in near-surface wind speed in China: 1969–2005. *Int. J. Climatol.* 31 (3), 349–358.
- Hartmann, B., Wendler, G., 2005. The significance of the 1976 Pacific climate shift in the climatology of Alaska. *J. Clim.* 18 (22), 4824–4839.
- Haslett, J., Raftery, A.E., 1989. Space-time Modelling with Long-memory dependence: assessing Ireland's wind power resource (with discussion). *Appl. Stat. – J. Roy. Stat. Soc. Ser. C* 38 (1), 1–50.
- Hernández-Escobedo, Q., Manzano-Agugliaro, F., Zapata-Sierra, A., 2010. The wind power of Mexico. *Renew. Sustain. Energy Rev.* 14 (9), 2830–2840.
- Hess, T.M., 1998. Trends in reference evapotranspiration in the North East Arid Zone of Nigeria, 1961–91. *J. Arid Environ.* 38 (1), 99–115.
- Hewston, R., Dorling, S.R., 2011. An analysis of observed daily maximum wind gusts in the UK. *J. Wind Eng. Ind. Aerodyn.* 99 (8), 845–856.
- Hijmans, R.J., Cameron, S.E., Parra, J.L., Jones, P.G., Jarvis, A., 2005. Very high resolution interpolated climate surfaces for global land areas. *Int. J. Climatol.* 25 (15), 1965–1978.
- Himri, Y., Himri, S., Boudghene Stambouli, A., 2009. Assessing the wind energy potential projects in Algeria. *Renew. Sustain. Energy Rev.* 13 (8), 2187–2191.
- Hobbins, M.T., 2004. Regional Evapotranspiration and Pan Evaporation: Complementary Interactions and Long-term Trends Across the Conterminous United States. PhD Thesis. Colorado State University, Fort Collins, CO, USA.
- Hobbins, M.T., Ramírez, J.A., Brown, T.C., 2004. Trends in pan evaporation and actual evapotranspiration across the conterminous US: paradoxical or complementary? *Geophys. Res. Lett.* 31 (13), L13503. doi:10.1029/2004GL019846.
- Hoffman, M.T., Cramer, M.D., Gillson, L., Wallace, M., 2011. Pan evaporation and wind run decline in the Cape Floristic Region of South Africa (1974–2005): implications for vegetation responses to climate change. *Clim. Change* 109 (3–4), 437–452.
- Hrayshat, E.S., 2007. Wind resource assessment of the Jordanian southern region. *Renew. Energy* 32 (11), 1948–1960.
- Huntington, T.G., 2006. Evidence for intensification of the global water cycle: review and synthesis. *J. Hydrol.* 319 (1–4), 83–95.
- Iacono, M.J., 2009. Why is the Wind Speed Decreasing? Blue Hill Meteorological Observatory, Milton, Massachusetts, 3 pp. <[http://www.bluehill.org/climate/200909\\_Wind\\_Speed.pdf](http://www.bluehill.org/climate/200909_Wind_Speed.pdf)> (last accessed on 4 Nov 2011).
- Irmak, S., Payero, J.O., Martin, D.L., Irmak, A., Howell, T.A., 2006. Sensitivity analyses and sensitivity coefficients of standardized daily ASCE–Penman–Monteith equation. *J. Irrig. Drain. Eng.* 132 (6), 564–578.
- Jacob, A., Rajvanshi, A.K., 2006. Long-term Weather Trends in western Maharashtra. Nimbkar Agricultural Research Institute, Phaltan town, Satara district, Maharashtra State, India, 7 pp. <<http://nariphaltan.virtualave.net/weather.pdf>> (last accessed on 04 Nov 2011).
- Jacovides, C.P., Theophilou, C., Tymvios, F.S., Pashiardes, S., 2002. Wind statistics for coastal stations in Cyprus. *Theor. Appl. Climatol.* 72 (3–4), 259–263.
- Jaffe, D. et al., 1999. Transport of Asian air pollution to North America. *Geophys. Res. Lett.* 26 (6), 711–714.
- Jaswal, A.K., Rao, G.S.P., De, U.S., 2008. Spatial and temporal characteristics of evaporation trends over India during 1971–2000. *Mausam* 59 (2), 149–158.
- Jhajharia, D., Roy, S., Ete, G., 2007. Climate and its variation: a case study of Agartala. *J. Soil Water Conserv.* 6 (1), 29–37.
- Jhajharia, D., Shrivastava, S.K., Sarkar, D., Sarkar, S., 2009. Temporal characteristics of pan evaporation trends under the humid conditions of northeast India. *Agric. For. Meteorol.* 149 (5), 763–770.
- Jhajharia, D., Dinpashoh, Y., Kahya, E., Singh, V.P., Fakheri-Fard, A., 2011. Trends in reference evapotranspiration in the humid region of northeast India. *Hydrol. Process.* doi:10.1002/hyp.8140.
- Jiang, Y., Luo, Y., Zhao, Z., Tao, S., 2010. Changes in wind speed over China during 1956–2004. *Theor. Appl. Climatol.* 99 (3–4), 421–430.
- Jiménez, P.A., González-Rouco, J.F., Navarro, J., Montávez, J.P., García-Bustamante, E., 2010. Quality assurance of surface wind observations from automated weather stations. *J. Atmos. Ocean. Technol.* 27 (7), 1101–1122.
- Jovanovic, B., Jones, D.A., Collins, D., 2008. A high-quality monthly pan evaporation dataset for Australia. *Clim. Change* 87 (3–4), 517–535.
- Jung, M. et al., 2010. Recent decline in the global land evapotranspiration trend due to limited moisture supply. *Nature* 467 (7318), 951–954.
- Kainkwa, R.M., 2010. Wind energy development in the African Great Lakes Region to supplement the hydroelectricity in the locality: a case study from Tanzania. *World Acad. Sci. Eng. Technol.* 61, 214–218.
- Kalma, J.D., McVicar, T.R., McCabe, M.F., 2008. Estimating land surface evaporation: a review of methods using remotely sensed surface temperature data. *Surv. Geophys.* 29 (4–5), 421–469.
- Keevallik, S., Soomere, T., 2009. Seasonal and diurnal variations of wind parameters at Pakri. *Est. J. Eng.* 15 (3), 227–239.
- Keimig, F.T., Bradley, R.S., 2002. Recent changes in wind chill temperatures at high latitudes in North America. *Geophys. Res. Lett.* 29 (8), 1163. doi:10.1029/2001GL013228.
- Keith, D.W. et al., 2004. The influence of large-scale wind power on global climate. *Proc. Natl Acad. Sci. USA*, 101 (46), 16115–16120.
- Keyhani, A., Ghasemi-Varnamkhashti, M., Khanali, M., Abbaszadeh, R., 2010. An assessment of wind energy potential as a power generation source in the capital of Iran, Tehran. *Energy* 35 (1), 188–201.
- Kirono, D.G.C., Jones, R.N., 2007. A bivariate test for detecting inhomogeneities in pan evaporation time series. *Aust. Meteorol. Mag.* 56 (2), 93–103.
- Klink, K., 1999. Trends in mean monthly maximum and minimum surface wind speeds in the coterminous United States, 1961–1990. *Clim. Res.* 13 (3), 193–205.
- Klink, K., 2002. Trends and interannual variability of wind speed distributions in Minnesota. *J. Clim.* 15 (22), 3311–3317.
- Ko, K., Kim, K., Huh, J., 2010. Variations of wind speed in time on Jeju Island, Korea. *Energy* 35 (8), 3381–3387.
- Kruger, A.C., Goliger, A.M., Retief, J.V., Sekele, S., 2010. Strong wind climatic zones in South Africa. *Wind Struct.* 13 (1), 37–55.
- Lambeck, K., Cazenave, A., 1976. Long-term variations in length of day and climatic change. *Geophys. J. Roy. Astron. Soc.* 46 (3), 555–573.
- Lauckner, F.B., 2002. Climate change in the Caribbean – the need for immediate research into the expected effects on agricultural production. Caribbean Agricultural Research and Development Institute St. Augustine, Trinidad. <[http://www.gecacs.org/gecacs\\_meetings/2002\\_09\\_19/lauckner\\_paper.pdf](http://www.gecacs.org/gecacs_meetings/2002_09_19/lauckner_paper.pdf)> (last accessed on 4 Nov 2011).
- Lawrimore, J.H., Peterson, T.C., 2000. Pan evaporation trends in dry and humid regions of the United States. *J. Hydrometeorol.* 1 (6), 543–546.
- Le Quéré, C. et al., 2007. Saturation of the Southern Ocean CO<sub>2</sub> sink due to recent climate change. *Science* 316 (5832), 1735–1738.
- Lenters, J.D., Kratz, T.K., Bowser, C.J., 2005. Effects of climate variability on lake evaporation: Results from a long-term energy budget study of Sparkling Lake, northern Wisconsin (USA). *J. Hydrol.* 308 (1–4), 168–195.
- Li, Z., Yan, Z.W., Tu, K., Liu, W.D., Wang, Y.C., 2011. Changes in wind speed and extremes in Beijing during 1960–2008 based on homogenized observations. *Adv. Atmos. Sci.* 28 (2), 408–420.

- Liu, C.M., Zeng, Y., 2004. Changes of pan evaporation in the recent 40 years in the Yellow River Basin. *Water Int.* 29 (4), 510–516.
- Liu, B., Xu, M., Henderson, M., Gong, W., 2004. A spatial analysis of pan evaporation trends in China, 1955–2000. *J. Geophys. Res.* 109, D15102. doi:10.1029/2004JD004511.
- Liu, J.G., Li, S.X., Ouyang, Z.Y., Tam, C., Chen, X.D., 2008. Ecological and socioeconomic effects of China's policies for ecosystem services. *Proc. Natl Acad. Sci. USA* 105 (28), 9477–9482.
- Liu, M., Shen, Y.J., Zeng, Y., Liu, C.M., 2010a. Trend in pan evaporation and its attribution over the past 50 years in China. *J. Geog. Sci.* 20 (4), 557–568.
- Liu, Q., Yang, Z.F., Cui, B.S., Sun, T., 2010b. The temporal trends of reference evapotranspiration and its sensitivity to key meteorological variables in the Yellow River Basin, China. *Hydrol. Process.* 24 (15), 2171–2181.
- Liu, X.M., Luo, Y.Z., Zhang, D., Zhang, M.H., Liu, C.M., 2011a. Recent changes in pan-evaporation dynamics in China. *Geophys. Res. Lett.* 38, L13404. doi:10.1029/2011GL047929.
- Liu, X.M., Zheng, H.X., Zhang, M.H., Liu, C.M., 2011b. Identification of dominant climate factor for pan evaporation trend in the Tibetan Plateau. *J. Geog. Sci.* 21 (4), 594–608.
- Lorenz, D.J., DeWeaver, E.T., 2007. The response of the extratropical hydrological cycle to global warming. *J. Clim.* 20 (14), 3470–3484.
- Lu, H., Raupach, M.R., McVicar, T.R., Barrett, D.J., 2003. Decomposition of vegetation cover into woody and herbaceous components using AVHRR NDVI time series. *Remote Sens. Environ.* 86 (1), 1–18.
- Lu, J., Vecchi, G.A., Reichler, T., 2007. Expansion of the Hadley cell under global warming. *Geophys. Res. Lett.* 34, L06805. doi:10.1029/2006GL028443.
- Lynch, A.H., Curry, J.A., Brunner, R.D., Maslanik, J.A., 2004. Toward an integrated assessment of the impacts of extreme wind events on barrow, Alaska. *Bull. Am. Meteorol. Soc.* 85 (2), 209–221.
- Mahowald, N.M., Ballantine, J.A., Feddes, J., Ramankutty, N., 2007. Global trends in visibility: implications for dust sources. *Atmos. Chem. Phys.* 7 (12), 3309–3339.
- Mahowald, N.M. et al., 2009. Atmospheric iron deposition: global distribution, variability, and human perturbations. *Ann. Rev. Mar. Sci.* 1, 245–278.
- Matsoukas, C. et al., 2011. Potential evaporation trends over land between 1983–2008: driven by radiative fluxes or vapour-pressure deficit? *Atmos. Chem. Phys.* 11 (15), 7601–7616.
- Mazzarella, A., 2007. The 60-year solar modulation of global air temperature: the Earth's rotation and atmospheric circulation connection. *Theor. Appl. Climatol.* 88 (3–4), 193–199.
- McCallum, J.L., Crosbie, R.S., Walker, G.R., Dawes, W.R., 2010. Impacts of climate change on groundwater in Australia: a sensitivity analysis of recharge. *Hydrogeol. J.* 18 (7), 1625–1638.
- McKenney, M.S., Rosenber, N.J., 1993. Sensitivity of some potential evapotranspiration estimation methods to climate change. *Agric. For. Meteorol.* 64, 81–110.
- McVicar, T.R., Jupp, D.L.B., 1999. Estimating one-time-of-day meteorological data from standard daily data as inputs to thermal remote sensing based energy balance models. *Agric. For. Meteorol.* 96 (4), 219–238.
- McVicar, T.R., Roderick, M.L., 2010. Atmospheric science: winds of change. *Nat. Geosci.* 3 (11), 747–748.
- McVicar, T.R. et al., 2007. Spatially distributing monthly reference evapotranspiration and pan evaporation considering topographic influences. *J. Hydrol.* 338 (3–4), 196–220.
- McVicar, T.R. et al., 2008. Wind speed climatology and trends for Australia, 1975–2006: capturing the stilling phenomenon and comparison with near-surface reanalysis output. *Geophys. Res. Lett.* 35, L20403. doi:10.1029/2008GL035627.
- McVicar, T.R. et al., 2010. Observational evidence from two mountainous regions that near-surface wind speeds are declining more rapidly at higher elevations than lower elevations: 1960–2006. *Geophys. Res. Lett.* 37, L06402. doi:10.1029/2009GL042255.
- Mescherskaya, A.V., Getman, I.F., Borisenko, M.M., Shevkunova, E.I., 2004. Monitoring of wind-speed in the Volga River catchment and the Ural region in the twentieth century. *Russ. Meteorol. Hydrol.* 3, 83–97 (in Russian).
- Mescherskaya, A.V., Eremin, V.V., Baranova, A.A., Maystrova, V.V., 2006. Change in wind speed in northern Russia in the second half of the twentieth century, from surface and upper air data. *Russ. Meteorol. Hydrol.* 9, 46–58 (in Russian).
- Michels, K., Potter, K.N., Williams, J.R., 1999. Calibration of EPIC for the simulation of wind erosion damage to pearl millet in West Africa. In: Skidmore, E.L., Tatarko, J. (Eds.), *Proceedings Wind Erosion – An International Symposium/Workshop, 3–5 June 1997* (on CD-ROM). USDA-ARS Wind Erosion Research Unit, Kansas State University, Manhattan, Kansas, USA, p. 12.
- Miller, L.M., Gans, F., Kleidon, A., 2011. Estimating maximum global land surface wind power extractability and associated climatic consequences. *Earth Syst. Dynam.* 2 (1), 1–12.
- Milly, P.C.D., Dunne, K.A., 2001. Trends in evaporation and surface cooling in the Mississippi River basin. *Geophys. Res. Lett.* 28 (7), 1219–1222.
- Miralles, D.G., De Jeu, R.A.M., Gash, J.H., Holmes, T.R.H., Dolman, A.J., 2011. Magnitude and variability of land evaporation and its components at the global scale. *Hydrol. Earth Syst. Sci.* 15 (3), 967–981.
- Mohamed, A.A., Elmbrouk, A.M., 2009. Assessment of the wind energy potential on the coast of Tripoli. pp. 10. [http://www.ontario-sea.org/Storage/27/1865\\_Assessment\\_of\\_the\\_wind\\_Energy\\_Potential\\_on\\_the\\_Coast\\_of\\_Tripoli.pdf](http://www.ontario-sea.org/Storage/27/1865_Assessment_of_the_wind_Energy_Potential_on_the_Coast_of_Tripoli.pdf). (accessed on 4 Nov 2011).
- Moratiel, R., Durán, J.M., Snyder, R.L., 2010. Responses of reference evapotranspiration to changes in atmospheric humidity and air temperature in Spain. *Clim. Res.* 44 (1), 27–40.
- Moratiel, R., Snyder, R.L., Durán, J.M., Tarquis, A.M., 2011. Trends in climatic variables trends and future reference evapotranspiration in Duero Valley (Spain). *Nat. Haz. Earth Syst. Sci.* 11 (6), 1795–1805.
- Morton, F.I., 1983. Operational estimates of areal evapotranspiration and their significance to the science and practice of hydrology. *J. Hydrol.* 66 (1–4), 1–76.
- Mostafaeipour, A., 2010. Feasibility study of harnessing wind energy for turbine installation in province of Yazd in Iran. *Renew. Sustain. Energy Rev.* 14 (1), 93–111.
- Najac, J., Lac, C., Terray, L., 2011. Impact of climate change on surface winds in France using a statistical-dynamical downscaling method with mesoscale modelling. *Int. J. Climatol.* 31 (3), 415–430.
- Nemani, R.R. et al., 2003. Climate-driven increases in global terrestrial net primary production from 1982 to 1999. *Science* 300 (5625), 1560–1563.
- Nfah, E.M., Ngundam, J.M., 2008. Modelling of wind/diesel/battery hybrid power systems for far North Cameroon. *Energy Convers. Manage.* 49 (6), 1295–1301.
- Nicholls, N., 2001. The insignificance of significance testing. *Bull. Am. Meteorol. Soc.* 82 (5), 981–986.
- Ogolo, E.O., 2011. Spatial and temporal trends of pan evaporation in differential climatic environments in Nigeria: 1970–2000. *Ind. J. Radio Space Phys.* submitted for publication.
- Oguntunde, P.G., Abiodun, B.J., Olukunle, O.J., Olufayoa, A.A., 2011. Trends and variability in pan evaporation and other climatic variables at Ibadan, Nigeria, 1973–2008. *Meteorol. Appl.* doi:10.1002/met.281.
- O'Higgins, R.C., 2007. Savannah woodland degradation assessments in Ghana: integrating ecological indicators with local perceptions. *Earth Environ.* 3, 246–281.
- Okubo, A., Levin, S.A., 1989. A theoretical framework for data-analysis of wind dispersion of seeds and pollen. *Ecology* 70 (2), 329–338.
- Osés-Rodríguez, R., Saura-González, G., Pedraza-Martínez, A., Otero-Martín, M., 2010. Impacto climático hasta el 2059 del viento en la provincia de Villa Clara, Cuba. Technical Report from Centro Meteorológico Provincial (CMP), Villa Clara, Cuba, 5 pp. <<http://eventos.fim.uclv.edu.cu/comec/new/cd2010/AutoPlay/Docs/ponencias/c1/c1.49.pdf>> (last accessed on 4 Nov 2011) (in Spanish).
- Ozdogan, M., Salvucci, G.D., 2004. Irrigation-induced changes in potential evapotranspiration in southeastern Turkey: test and application of Bouchet's complementary hypothesis. *Water Resour. Res.* 40, W04301. doi:10.1029/2003WR002822.
- Ozer, P., 1996. Evolution des directions et des vitesses des vents de 1951 à 1994 sur la façade Atlantique de l'Afrique de l'Ouest du sud du Senegal au nord de la Mauritanie. *Publ. Assoc. Int. Climatol.* 9, 479–486 (in French with an English Abstract).
- Palaiologou, P., Kalabokidis, K., Haralambopoulos, D., Feidas, H., Polatidis, H., 2011. Wind characteristics and mapping for power production in the Island of Lesbos, Greece. *Comput. Geosci.* 37 (7), 962–972.
- Papaioannou, G., Kitsara, G., Athanasatos, S., 2011. Impact of global dimming and brightening on reference evapotranspiration in Greece. *J. Geophys. Res.* – Atmos. 116, D09107. doi:10.1029/2010JD015525.
- Penman, H.L., 1948. Natural evaporation from open water, bare soil and grass. *Proc. Roy. Soc., Lond.* A193, 120–145.
- Penman, H.L., Schofield, R.K., 1951. Some Physical Aspects of Assimilation and Transpiration, Carbon Dioxide Fixation and Photosynthesis Symposium Number V Society of Experimental Biology. Cambridge University Press, Cambridge, pp. 115–129.
- Pérez, I.A., García, M.A., Sánchez, M.L., de Torre, B., 2005. Analysis and parameterisation of wind profiles in the low atmosphere. *Sol. Energy* 78 (6), 809–821.
- Persaud, S., Flynn, D., Fox, B., 1999. Potential for wind generation on the Guyana coastlands. *Renew. Energy* 18 (2), 175–189.
- Peterson, T.C., Golubev, V.S., Groisman, P.Y., 1995. Evaporation losing its strength. *Nature* 377 (6551), 687–688.
- Peterson, T.C., Vautard, R., McVicar, T.R., Thépaut, J.-N., Berrisford, P., 2011a. Surface winds over land. *Bull. Am. Meteorol. Soc.* 92 (6), S57.
- Peterson, T.C., Willett, K.M., Thorne, P.W., 2011b. Observed changes in surface atmospheric energy over land. *Geophys. Res. Lett.* 38, L16707. doi:10.1029/2011GL048442.
- Philip, J.R., 1957. Evaporation, and moisture and heat fields in the soil. *J. Meteorol.* 14 (4), 354–366.
- Pinard, J.-P., 2007. Wind climate of the Whitehorse area. *Arctic* 60 (3), 227–237.
- Pirazzoli, P.A., Tomasin, A., 1999. Recent abatement of easterly winds in the northern Adriatic. *Int. J. Climatol.* 19 (11), 1205–1219.
- Pirazzoli, P.A., Tomasin, A., 2003. Recent near-surface wind changes in the central Mediterranean and Adriatic areas. *Int. J. Climatol.* 23 (8), 963–973.
- Postel, S.L., 1998. Water for food production: will there be enough in 2025? *Bioscience* 48 (8), 629–637.
- Postel, S.L., Daily, G.C., Ehrlich, P.R., 1996. Human appropriation of renewable fresh water. *Science* 271 (5250), 785–788.
- Priestley, C.H.B., Taylor, R.J., 1972. On the assessment of surface heat flux and evaporation using large-scale parameters. *Mon. Weather Rev.* 100 (2), 81–92.
- Pryor, S.C., Ledolter, J., 2010. Addendum to “Wind speed trends over the contiguous United States”. *J. Geophys. Res.* – Atmos. 115, D10103. doi:10.1029/2009JD013281.
- Pryor, S.C. et al., 2009. Wind speed trends over the contiguous United States. *J. Geophys. Res.* – Atmos. 114, D14105. doi:10.1029/2008JD011416.
- Pryor, S.C., Barthelmie, R.J., Riley, E.S., 2007. Historical evolution of wind climates in the USA. *Journal of Physics: Conference Series* 75 – The Science of Making Torque from Wind, Copenhagen, Denmark, doi:10.1088/1742-6596/75/1/012065.

- Qian, Y., Kaiser, D.P., Leung, L.R., Xu, M., 2006. More frequent cloud-free sky and less surface solar radiation in China from 1955 to 2000. *Geophys. Res. Lett.* 33: L01812. doi:10.1029/2005GL024586.
- Quintana-Gomez, R.A., 1998. Changes in evaporation patterns detected in northernmost South America, homogeneity testing. In: 7th International Meeting on Statistical Climatology (25–29 May). National Research Center for Statistics and the Environment. Whistler, BC, Canada, p. 97. <http://ccma.seos.ubic.ca/jmsc/proceedings/7IMSC.pdf>. (accessed on 4 Nov 2011).
- Rahimzadeh, F., Noorian, A.M., Pedram, M., Kruk, M.C., 2011. Wind speed variability over Iran and its impact on wind power potential: a case study for Esfahan Province. *Meteorol. Appl.* 18 (2), 198–210.
- Rasmussen, D.J., Holloway, T., Nemet, G.F., 2011. Opportunities and challenges in assessing climate change impacts on wind energy – a critical comparison of wind speed projections in California. *Environ. Res. Lett.* 6, 024008. doi:10.1088/1748-9326/6/2/024008.
- Rayner, D.P., 2007. Wind run changes: the dominant factor affecting pan evaporation trends in Australia. *J. Clim.* 20 (14), 3379–3394.
- Reba, M.L. et al., 2011. A long-term data set for hydrologic modeling in a snow-dominated mountain catchment. *Water Resour. Res.* 47, W07702. doi:10.1029/2010WR010030.
- Recio, M., Rodriguez-Rajo, F.J., Jato, M.V., Trigo, M.M., Cabezudo, B., 2009. The effect of recent climatic trends on Urticaceae pollination in two bioclimatically different areas in the Iberian Peninsula: Malaga and Vigo. *Clim. Change* 97 (1–2), 215–228.
- Reddaway, J.M., Bigg, G.R., 1996. Climatic change over the Mediterranean and links to the more general atmospheric circulation. *Int. J. Climatol.* 16 (6), 651–661.
- Rehman, S., 2004. Wind energy resources assessment for Yanbo, Saudi Arabia. *Energy Convers. Manage.* 45 (13–14), 2019–2032.
- Rehman, S., Ahmad, A., 2004. Assessment of wind energy potential for coastal locations of the Kingdom of Saudi Arabia. *Energy* 29 (8), 1105–1115.
- Rehman, S. et al., 2007. Wind power resource assessment for Rafha, Saudi Arabia. *Renew. Sustain. Energy Rev.* 11 (5), 937–950.
- Ren, D., 2010. Effects of global warming on wind energy availability. *J. Renew. Sustain. Energy* 2, 052301. doi:10.1063/1.3486072.
- Riba, M. et al., 2009. Darwin's wind hypothesis: does it work for plant dispersal in fragmented habitats? *New Phytol.* 183 (3), 667–677.
- Ritchie, J.T., 1972. Model for predicting evaporation from a row crop with incomplete cover. *Water Resour. Res.* 8 (5), 1204–1213.
- Roderick, M.L., Farquhar, G.D., 2004. Changes in Australian pan evaporation from 1970 to 2002. *Int. J. Climatol.* 24 (9), 1077–1090.
- Roderick, M.L., Farquhar, G.D., 2005. Changes in New Zealand pan evaporation since the 1970s. *Int. J. Climatol.* 25 (15), 2031–2039.
- Roderick, M.L., Rotstayn, L.D., Farquhar, G.D., Hobbins, M.T., 2007. On the attribution of changing pan evaporation. *Geophys. Res. Lett.* 34, L17403. doi:10.1029/2007GL031166.
- Roderick, M.L., Hobbins, M.T., Farquhar, G.D., 2009. Pan evaporation trends and the terrestrial water balance II. Energy balance and interpretation. *Geogr. Compass* 3 (2), 761–780.
- Rotstayn, L.D., Roderick, M.L., Farquhar, G.D., 2006. A simple pan-evaporation model for analysis of climate simulations: evaluation over Australia. *Geophys. Res. Lett.* 33, L17715. doi:10.1029/2006GL027114.
- Sabziparvar, A.A., Tabari, H., Aeni, A., Ghafouri, M., 2010. Evaluation of Class A pan coefficient models for estimation of reference crop evapotranspiration in cold semi-arid and warm arid climates. *Water Resour. Manage.* 24 (5), 909–920.
- Seidel, D.J., Fu, Q., Randel, W.J., Reichler, T.J., 2008. Widening of the tropical belt in a changing climate. *Nat. Geosci.* 1 (1), 21–24.
- Seneviratne, S.I. et al., 2010. Investigating soil moisture–climate interactions in a changing climate: a review. *Earth-Sci. Rev.* 99 (3–4), 125–161.
- Shao, Y., Raupach, M.R., Findlater, P.A., 1993. Effect of saltation bombardment on the entrainment of dust by wind. *J. Geophys. Res.* – Atmos. 98 (D7), 12719–12726.
- Shen, Y.J., Liu, C.M., Liu, M., Zeng, Y., Tian, C.Y., 2010. Change in pan evaporation over the past 50 years in the arid region of China. *Hydrol. Process.* 24 (2), 225–231.
- Shenbin, C., Yunfeng, L., Thomas, A., 2006. Climatic change on the Tibetan Plateau: potential evapotranspiration trends from 1961–2000. *Clim. Change* 76 (3–4), 291–319.
- Shuttleworth, W.J., 1992. Evaporation. In: Maidment, D.R. (Ed.), *Handbook of Hydrology*, pp. 4.1–4.53 (Chapter 4).
- Shuttleworth, W.J., Serrat-Capdevila, A., Roderick, M.L., Scott, R.L., 2009. On the theory relating changes in area-average and pan evaporation. *Quart. J. Roy. Meteorol. Soc.* 135 (642), 1230–1247.
- Smits, A., Klein Tank, A.M.G., Können, G.P., 2005. Trends in storminess over the Netherlands, 1962–2002. *Int. J. Climatol.* 25 (10), 1331–1344.
- Soler-Bientz, R., Watson, S., Infield, D., 2010. Wind characteristics on the Yucatán Peninsula based on short term data from meteorological stations. *Energy Convers. Manage.* 51 (4), 754–764.
- Song, Z.W., Zhang, H.L., Snyder, R.L., Anderson, F.E., Chen, F., 2010. Distribution and trends in reference evapotranspiration in the North China Plain. *J. Irrig. Drain. Eng.* 136 (4), 240–247.
- Sridharan, S., Tsuda, T., Gurubaran, S., 2010. Long-term tendencies in the mesosphere/lower thermosphere mean winds and tides as observed by medium-frequency radar at Tirunelveli (8.7 degrees N, 77.8 degrees E). *J. Geophys. Res.* – Atmos. 115, D08109. doi:10.1029/2008JD011609.
- St. George, S., Wolfe, S.A., 2009. El Niño stills winter winds across the southern Canadian Prairies. *Geophys. Res. Lett.* 36, L23806. doi:10.1029/2009GL01282.
- Stanhill, G., Möller, M., 2008. Evaporative climate change in the British Isles. *Int. J. Climatol.* 28 (9), 1127–1137.
- Sweeney, J., 2000. A three-century storm climatology for Dublin 1715–2000. *Irish Geogr.* 33 (1), 1–14.
- Tabari, H., Marofi, S., 2011. Changes of pan evaporation in the West of Iran. *Water Resour. Manage.* 25 (1), 97–111.
- Tabari, H., Marofi, S., Aeni, A., Talae, P.H., Mohammadi, K., 2011. Trend analysis of reference evapotranspiration in the western half of Iran. *Agric. For. Meteorol.* 151 (2), 128–136.
- Tang, B., Tong, L., Kang, S., Zhang, L., 2011. Impacts of climate variability on reference evapotranspiration over 58 years in the Haihe river basin of north China. *Agric. Water Manage.* 98 (10), 1660–1670.
- Tchinda, R., Kaptoum, E., 2003. Wind energy in Adamaoua and North Cameroon provinces. *Energy Convers. Manage.* 44 (6), 845–857.
- Tchinda, R., Kendjio, J., Kaptoum, E., Njomo, D., 2000. Estimation of mean wind energy available in far north Cameroon. *Energy Convers. Manage.* 41 (17), 1917–1929.
- Tebakari, T., Yoshitani, J., Suvanpimol, C., 2005. Time-space trend analysis in pan evaporation over Kingdom of Thailand. *J. Hydrol. Eng.* 10 (3), 205–215.
- Thom, A.S., Thony, J.-L., Vauclin, M., 1981. On the proper employment of evaporation pans and atmometers in estimating potential transpiration. *Quart. J. Roy. Meteorol. Soc.* 107 (453), 711–736.
- Thomas, A., 2000. Spatial and temporal characteristics of potential evapotranspiration trends over China. *Int. J. Climatol.* 20 (4), 381–396.
- Thomas, B.R., Swail, V.R., 2011. Buoy wind inhomogeneities related to averaging method and anemometer type: application to long time series. *Int. J. Climatol.* 31 (7), 1040–1055.
- Thomas, B.R., Kent, E.C., Swail, V.R., Berry, D.I., 2008. Trends in ship wind speeds adjusted for observation method and height. *Int. J. Climatol.* 28 (6), 747–763.
- Thorntonwaite, C.W., 1948. An approach toward a rational classification of climate. *Geogr. Rev.* 38, 55–94.
- Tokinaga, H., Xie, S.P., 2011. Wave and anemometer-based sea-surface wind (WASWind) for climate change analysis. *J. Clim.* 24 (1), 267–285.
- Troccoli, A. et al., 2011. Long term wind trends over Australia. *J. Clim.* doi: 10.1175/2011JCLI4198.1.
- Tuller, S.E., 2004. Measured wind speed trends on the west coast of Canada. *Int. J. Climatol.* 24 (11), 1359–1374.
- Turner, J. et al., 2005. Antarctic climate change during the last 50 years. *Int. J. Climatol.* 25 (3), 279–294.
- Van Niel, T.G., McVicar, T.R., 2004. Determining temporal windows of crop discrimination with remote sensing: a case study in south-eastern Australia. *Comput. Electron. Agric.* 45 (1–3), 91–108.
- Vautard, R., Cattiaux, J., Yiou, P., Thépaut, J.-N., Ciais, P., 2010. Northern hemisphere atmospheric stilling partly attributed to increased surface roughness. *Nat. Geosci.* 3 (11), 756–761.
- Vecchi, G.A., Soden, B.J., 2007. Global warming and the weakening of the tropical circulation. *J. Clim.* 20 (17), 4316–4340.
- Verma, I.J., Jadhav, V.N., Erande, R.S., 2008. Recent variations and trends in potential evapotranspiration (PET) over India. *Mausam* 59 (1), 119–128.
- Viviroli, D., Durr, H.H., Messerli, B., Meybeck, M., Weingartner, R., 2007. Mountains of the world, water towers for humanity: typology, mapping, and global significance. *Water Resour. Res.* 43 (7), W07447. doi:10.1029/2006WR005653.
- Viviroli, D. et al., 2011. Climate change and mountain water resources: overview and recommendations for research, management and policy. *Hydrol. Earth Syst. Sci.* 15 (2), 471–504.
- Vuichard, N., Ciais, P., Belelli, L., Smith, P., Valentini, R., 2008. Carbon sequestration due to the abandonment of agriculture in the former USSR since 1990. *Global Biogeochem. Cycles* 22 (4), GB4018. doi:10.1029/2008GB003212.
- Vuillermoz, E., Cabini, E., Verza, G.P., Tartari, G., 2008. Summary Report 1994–2006 of Pyramid Meteorological Network, Khumbu Valley, Nepal, SHARE Project, EvK2-CNR Committee, Bergamo, Italy.
- Walser, A. et al., 2006. A high resolution reference data set of German wind velocity 1951–2001 and comparison with regional climate model results. *Meteorol. Z.* 15 (6), 585–596.
- Wan, H., Wang, X.L., Swail, V.R., 2010. Homogenization and trend analysis of Canadian near-surface wind speeds. *J. Clim.* 23 (5), 1209–1225.
- Wang, C., Prinn, R.G., 2010. Potential climatic impacts and reliability of very large-scale wind farms. *Atmos. Chem. Phys.* 10 (4), 2053–2061.
- Wang, J.Z., Georgakakos, K.P., 2007. Estimation of potential evapotranspiration in the mountainous Panama Canal watershed. *Hydrol. Process.* 21 (14), 1901–1917.
- Wang, Y., Jiang, T., Bothe, O., Fraedrich, K., 2007. Changes of pan evaporation and reference evapotranspiration in the Yangtze River basin. *Theor. Appl. Climatol.* 90 (1–2), 13–23.
- Wang, W.G. et al., 2011. Spatial and temporal characteristics of reference evapotranspiration trends in the Haihe River basin, China. *J. Hydrol. Eng.* 16 (3), 239–252.
- Ward, M.N., 1992. Provisionally corrected surface wind data, worldwide ocean atmosphere surface fields, and Sahelian rainfall variability. *J. Clim.* 5 (5), 454–475.
- Wentz, F.J., Ricciardulli, L., Hilburn, K., Mears, C., 2007. How much more rain will global warming bring? *Science* 317 (5835), 233–235.
- Xu, J.Q., 2001. An analysis of the climatic changes in Eastern Asia using the potential evaporation. *J. Jpn. Soc. Hydrol. Water Resour.* 14 (2), 151–170 (in Japanese with English abstract and captions).
- Xu, J.Q., Haginoya, S., Saito, K., Motoya, K., 2005. Surface heat balance and pan evaporation trends in Eastern Asia in the period 1971–2000. *Hydrol. Process.* 19 (11), 2161–2186.

- Xu, C.Y., Gong, L., Jiang, T., Chen, D., Singh, V.P., 2006a. Analysis of spatial distribution and temporal trend of reference evapotranspiration and pan evaporation in Changjiang (Yangtze River) catchment. *J. Hydrol.* 327 (1–2), 81–93.
- Xu, C.Y., Gong, L.B., Tong, J., Chen, D.L., 2006b. Decreasing reference evapotranspiration in a warming climate – a case of Changjiang (Yangtze) River catchment during 1970–2000. *Adv. Atmos. Sci.* 23 (4), 513–520.
- Xu, M. et al., 2006c. Steady decline of East Asian monsoon winds, 1969–2000: evidence from direct ground measurements of wind speed. *J. Geophys. Res. – Atmos.* 111, D24111. doi:10.1029/2006JD007337.
- Yang, H., Yang, D., 2011. Derivation of climate elasticity of runoff to assess the effects of climate change on annual runoff. *Water Resour. Res.* 47, W07526. doi:10.1029/2010WR009287.
- Yang, H.B., Yang, D.W., in press. Climatic factors influencing changing pan evaporation across China from 1961–2001. *J. Hydrol.* doi:10.1016/j.jhydrol.2011.10.043.
- Yin, J.H., 2005. A consistent poleward shift of the storm tracks in simulations of 21st century climate. *Geophys. Res. Lett.* 32, L18701. doi:10.1029/2005GL023684.
- Yin, Y., Wu, S., Chen, G., Dai, E., 2010a. Attribution analyses of potential evapotranspiration changes in China since the 1960s. *Theor. Appl. Climatol.* 101 (1–2), 19–28.
- Yin, Y.H., Wu, S.H., Dai, E.F., 2010b. Determining factors in potential evapotranspiration changes over China in the period 1971–2008. *Chin. Sci. Bull.* 55 (29), 3329–3337.
- You, Q.L. et al., 2010. Decreasing wind speed and weakening latitudinal surface pressure gradients in the Tibetan Plateau. *Clim. Res.* 42 (1), 57–64.
- Young, I.R., Zieger, S., Babanin, A.V., 2011. Global trends in wind speed and wave height. *Science* 332 (6028), 451–455.
- Yu, L., 2007. Global variations in oceanic evaporation (1958–2005): the role of the changing wind speed. *J. Clim.* 20 (21), 5376–5390.
- Zhang, Y.Q., Liu, C.M., Tang, Y.H., Yang, Y.H., 2007. Trends in pan evaporation and reference and actual evapotranspiration across the Tibetan Plateau. *J. Geophys. Res. – Atmos.* 112, D12110. doi:10.1029/2006JD008161.
- Zhang, X., Y. Ren, Y., Yin, Z.-Y., Lin, Z., Zheng, D., 2009. Spatial and temporal variation patterns of reference evapotranspiration across the Qinghai–Tibetan Plateau during 1971–2004. *J. Geophys. Res. – Atmos.* 114, D15105. doi:10.1029/2009JD011753.
- Zheng, H., Liu, X., Liu, C., Dai, X., Zhu, R., 2009. Assessing contributions to pan evaporation trends in Haihe River Basin, China. *J. Geophys. Res. – Atmos.* 114, D24105. doi:10.1029/2009JD012203.
- Zomer, R.J., Trabucco, A., Bossio, D.A., Verchot, L.V., 2008. Climate change mitigation: a spatial analysis of global land suitability for clean development mechanism afforestation and reforestation. *Agric. Ecosyst. Environ.* 126 (1–2), 67–80.
- Zuo, H.C., Li, D.L., Y.Q., H., Bao, Y., Lü, S.H., 2005. Characteristics of climatic trends and correlation between pan-evaporation and environmental factors in the last 40 years over China. *Chin. Sci. Bull.* 50 (12), 1235–1241.

## Supplementary Material

### **Global review and synthesis of trends in observed terrestrial near-surface wind speeds: Implications for evaporation**

McVicar, T.R., Roderick, M.L., Donohue, R.J., Li, L.T., Van Niel, T.G., Thomas, A., Grieser, J., Jhajharia, D., Himri, Y., Mahowald, N.M., Mescherskaya, A.V., Kruger, A.C., Rehman, S., and Dinpashoh, Y. (2012) Global review and synthesis of trends in observed terrestrial near-surface wind speeds: Implications for evaporation. *Journal of Hydrology*. 416-417, 182-205, doi:10.1016/j.jhydrol.2011.10.024

24 January 2012

Supplementary Material Table 1. Percent areas of all 169 countries  $> 5,000 \text{ km}^2$  (in descending order of size) that are climatologically energy-limited (*i.e.*, moist). The water-limited areas are the compliment, *i.e.*, water limited areas can be calculated as  $100 - \text{energy-limited percent area}$ . The energy-limited areas are where long-term (1950-2000) annual average  $P / \text{annual average } ET_p$  is  $> 1.0$ , using  $P$  and  $ET_p$  data from Hijmans et al. (2005) and Zomer et al. (2008), respectively. Ann represents the annual time-step, with DJF referring to the season defined by December, January and February (and so on for the remaining seasons), and the 12 months are listed. Values assume that precipitation is the only source of water and do not account for water storage dynamics. The continents are abbreviated as: As = Asia; NA = North America; Eu = Europe; Af = Africa; SA = South America; Oc = Oceania. The country areas were derived from a map of countries provided with IDL Version 6.4 (filename is Country.SHP), this has a Mercator projection, linear units are meters, and the geographic coordinate system and datum are both WGS 1984.

Seq	Country	Area* 1000 ( $\text{km}^2$ )	Continent	ANN	DJF	MAM	JJA	SON	Jan	Feb	Mar	Apr	May	Jun	Jul	Aug	Sep	Oct	Nov	Dec
1	Russia	16897.3	As,Eu	42	100	27	3	93	100	100	88	47	3	1	3	16	67	93	100	100
2	Canada	9832.9	NA	40	100	37	5	94	100	100	95	56	8	2	3	19	75	93	99	100
3	United States	9426.3	NA,Oc	22	75	15	3	52	77	68	60	19	3	2	3	15	27	45	69	79
4	China	9366.2	As	18	30	12	30	14	36	28	12	12	15	24	34	32	23	12	16	26
5	Brazil	8493.1	SA	53	77	64	23	26	77	78	76	63	42	30	22	14	13	30	54	69
6	Australia	7694.3	Oc	3	9	5	10	1	11	14	9	4	9	13	11	7	3	1	1	3
7	India	3153.0	As	17	6	7	67	26	7	6	5	5	10	28	75	73	69	24	5	6
8	Kazakhstan	2832.8	As,Eu	0	90	1	0	2	91	77	6	1	0	0	0	0	0	14	71	95
9	Argentina	2776.9	SA	3	0	15	23	1	1	1	5	18	29	39	28	10	4	3	0	0
10	Sudan	2496.3	Af	0	0	0	20	0	0	0	0	0	3	8	27	34	9	2	0	0
11	Congo, DRC	2336.5	Af	40	61	66	32	73	55	48	73	79	47	25	30	38	53	72	82	68
12	Algeria	2323.5	Af	0	6	0	0	0	6	4	1	0	0	0	0	0	0	0	5	6
13	Greenland	2118.1	NA	95	100	97	69	100	100	100	100	100	80	65	61	84	100	100	100	100
14	Mexico	1953.9	NA	7	3	0	30	20	3	1	0	0	1	24	34	34	40	15	5	5
15	Saudi Arabia	1936.7	As	0	0	0	0	0	0	0	0	0	0	0	0	0	0	0	0	0
16	Indonesia	1847.0	As	97	99	97	73	82	99	97	97	96	94	80	69	63	69	75	91	99
17	Iran	1680.1	As	1	28	0	0	2	37	22	7	2	0	0	0	0	2	2	6	27
18	Libya	1627.0	Af	0	1	0	0	0	1	1	0	0	0	0	0	0	0	0	0	2

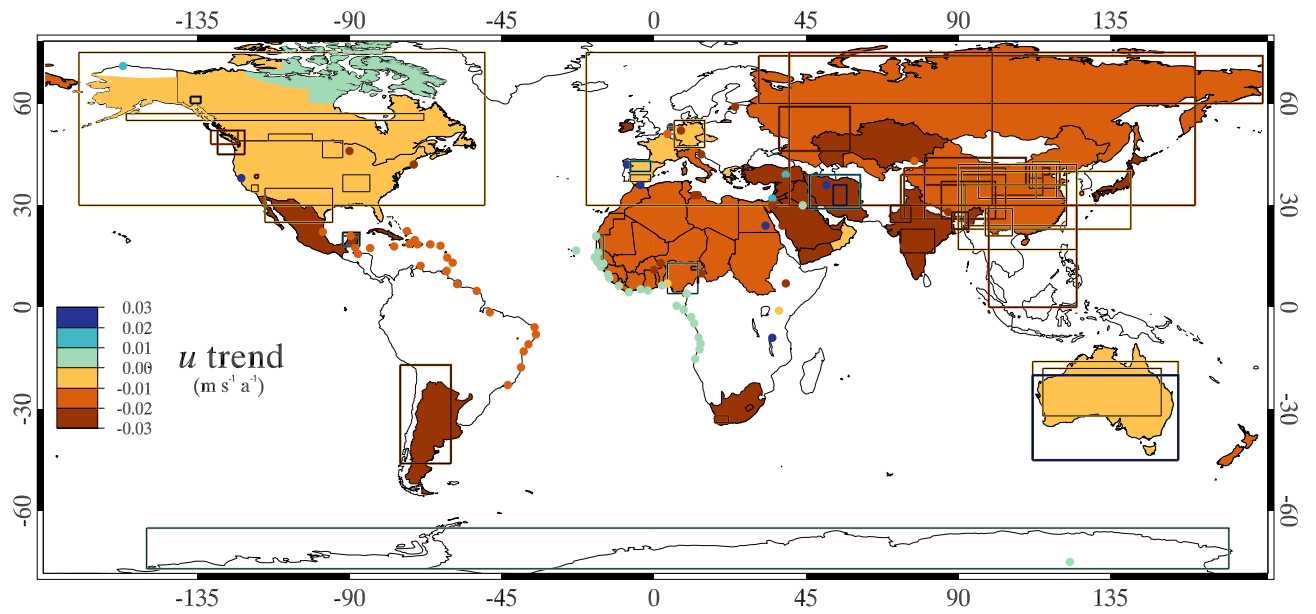
Seq	Country	Area* 1000 (km <sup>2</sup> )	Continent	ANN	DJF	MAM	JJA	SON	Jan	Feb	Mar	Apr	May	Jun	Jul	Aug	Sep	Oct	Nov	Dec
19	Mongolia	1557.3	As	0	65	0	0	1	75	54	8	0	0	0	1	1	0	1	20	67
20	Peru	1296.6	SA	48	73	58	25	47	73	79	82	57	36	31	24	19	27	45	53	59
21	Chad	1270.8	Af	0	0	0	21	0	0	0	0	0	0	2	23	33	14	0	0	0
22	Mali	1258.0	Af	0	0	0	18	0	0	0	0	0	0	1	20	27	15	0	0	0
23	Angola	1252.9	Af	0	56	17	0	5	54	61	73	40	0	0	0	0	0	6	48	55
24	South Africa	1219.9	Af	0	3	1	3	0	3	5	3	0	2	4	3	2	0	0	1	2
25	Niger	1184.4	Af	0	0	0	0	0	0	0	0	0	0	0	0	5	0	0	0	0
26	Colombia	1143.0	NA,SA	89	33	90	86	97	24	34	48	91	96	89	82	86	92	99	89	46
27	Ethiopia	1134.2	Af	5	0	4	40	7	0	0	0	12	15	22	45	45	29	6	0	0
28	Bolivia	1090.6	SA	17	57	24	1	5	62	62	47	20	6	3	1	0	0	5	29	50
29	Mauritania	1038.3	Af	0	0	0	0	0	0	0	0	0	0	0	0	0	0	0	0	0
30	Egypt	1000.9	Af	0	0	0	0	0	0	0	0	0	0	0	0	0	0	0	0	0
31	Tanzania	942.5	Af	4	53	40	0	1	48	50	64	62	10	0	0	0	0	0	12	53
32	Venezuela	913.5	SA	53	12	37	89	62	8	5	9	35	70	90	89	86	71	62	46	27
33	Nigeria	913.4	Af	13	0	11	87	25	0	0	2	9	32	60	90	94	76	27	2	0
34	Pakistan	880.2	As	2	16	6	1	0	19	18	13	7	1	0	3	4	0	0	2	12
35	Namibia	827.9	Af	0	0	0	0	0	0	0	0	0	0	0	0	0	0	0	0	0
36	Mozambique	794.0	Af	2	69	16	0	0	70	77	58	8	0	0	0	0	0	0	0	50
37	Turkey	778.6	As, Eu	2	100	11	0	5	100	98	61	15	1	0	0	0	0	10	85	100
38	Zambia	753.9	Af	0	97	3	0	0	98	99	52	2	0	0	0	0	0	0	14	93
39	Chile	722.5	SA	45	20	52	64	34	17	23	34	50	63	66	65	62	50	31	23	20
40	Myanmar	659.6	As	63	0	8	91	90	0	0	0	4	69	91	90	93	99	95	5	0
41	Afghanistan	641.4	As	7	63	15	0	1	69	64	40	20	7	0	0	0	0	3	11	52
42	Somalia	637.9	Af	0	0	0	0	0	0	0	0	1	0	0	0	0	0	0	0	0
43	Central African Republic	619.9	Af	0	0	1	98	46	0	0	0	2	38	86	98	99	97	67	1	0
44	Ukraine	593.8	Eu	3	100	1	1	45	100	100	55	1	1	1	0	0	0	38	100	100
45	Madagascar	591.7	Af	25	83	26	12	0	87	82	72	16	10	13	13	10	2	0	9	78
46	Kenya	584.7	Af	1	0	11	4	2	0	0	1	24	14	4	4	4	1	2	16	1
47	Botswana	579.8	Af	0	0	0	0	0	0	0	0	0	0	0	0	0	0	0	0	0
48	Turkmenistan	552.5	As	0	9	0	0	0	16	7	2	0	0	0	0	0	0	0	0	12
49	France	547.0	Eu	31	100	12	2	99	100	100	64	10	6	3	1	3	19	99	100	100

Seq	Country	Area* 1000 (km <sup>2</sup> )	Continent	ANN	DJF	MAM	JJA	SON	Jan	Feb	Mar	Apr	May	Jun	Jul	Aug	Sep	Oct	Nov	Dec
50	Thailand	515.4	As	26	5	5	77	80	3	0	0	2	61	60	76	86	98	63	15	9
51	Spain	503.3	Eu,Af	14	87	12	0	27	87	66	29	14	3	1	0	1	4	33	91	97
52	Cameroon	466.4	Af	39	0	48	77	75	0	0	18	50	81	81	65	77	94	75	28	0
53	Papua New Guinea	458.7	As,Oc	98	99	100	77	87	100	100	100	100	97	82	77	72	80	85	86	98
54	Yemen	455.1	As	0	0	0	0	0	0	0	0	0	0	0	0	0	0	0	0	0
55	Uzbekistan	446.6	As	1	32	4	0	1	53	18	10	4	1	0	0	0	0	2	6	61
56	Sweden	442.2	Eu	92	100	13	7	100	100	100	100	20	1	0	9	30	100	100	100	100
57	Iraq	434.8	As	0	18	2	0	0	19	15	11	3	0	0	0	0	0	0	8	20
58	Morocco	406.5	Af	0	29	0	0	0	28	19	7	0	0	0	0	0	0	0	25	41
59	Paraguay	401.2	SA	14	0	41	18	13	1	4	3	46	45	34	16	3	5	18	20	3
60	Zimbabwe	391.5	Af	1	45	1	0	0	49	44	2	0	0	0	0	0	0	0	1	40
61	Japan	370.7	As	100	99	93	93	100	99	100	99	92	63	80	90	90	100	100	100	99
62	Germany	355.2	Eu	46	100	10	4	98	100	100	83	8	3	4	2	6	20	100	100	100
63	Congo	345.4	Af	57	49	96	17	88	42	43	77	94	86	17	12	21	63	83	94	57
64	Finland	331.0	Eu	98	100	1	0	100	100	100	100	4	0	0	0	29	100	100	100	100
65	Malaysia	328.5	As	100	96	97	88	100	94	84	87	91	98	87	85	88	99	100	100	98
66	Vietnam	322.7	As	88	6	8	89	84	5	1	0	4	82	83	90	91	100	68	43	13
67	Cote d'Ivory	321.1	Af	13	0	20	74	38	0	0	1	12	38	81	58	55	91	39	12	0
68	Poland	312.1	Eu	11	100	1	1	96	100	100	31	1	1	2	1	1	15	91	100	100
69	Oman	310.3	As	0	0	0	0	0	0	0	0	0	0	0	0	0	0	0	0	0
70	Norway	305.9	Eu	100	100	76	47	100	100	100	100	79	30	26	44	85	100	100	100	100
71	Italy	301.1	Eu	34	100	24	8	87	100	99	76	29	11	9	6	11	23	96	100	100
72	Philippines	281.0	As	98	58	41	99	99	52	32	22	26	80	97	99	97	98	99	91	80
73	Burkina Faso	274.1	Af	0	0	0	64	0	0	0	0	0	0	1	71	91	46	0	0	0
74	Western Sahara	268.2	Af	0	0	0	0	0	0	0	0	0	0	0	0	0	0	0	0	0
75	New Zealand	267.2	Oc	86	36	97	100	74	31	35	76	97	100	100	100	100	90	73	49	44
76	Gabon	263.0	Af	85	67	100	0	100	57	64	100	100	89	2	0	0	35	98	100	74
77	Ecuador	254.8	SA	63	74	84	48	46	73	86	87	88	65	55	48	44	45	47	46	53
78	Uganda	245.6	Af	7	3	29	18	14	0	3	12	59	51	5	18	35	17	24	24	6
79	Guinea	245.5	Af	38	0	0	100	76	0	0	0	2	20	94	100	100	100	66	2	0

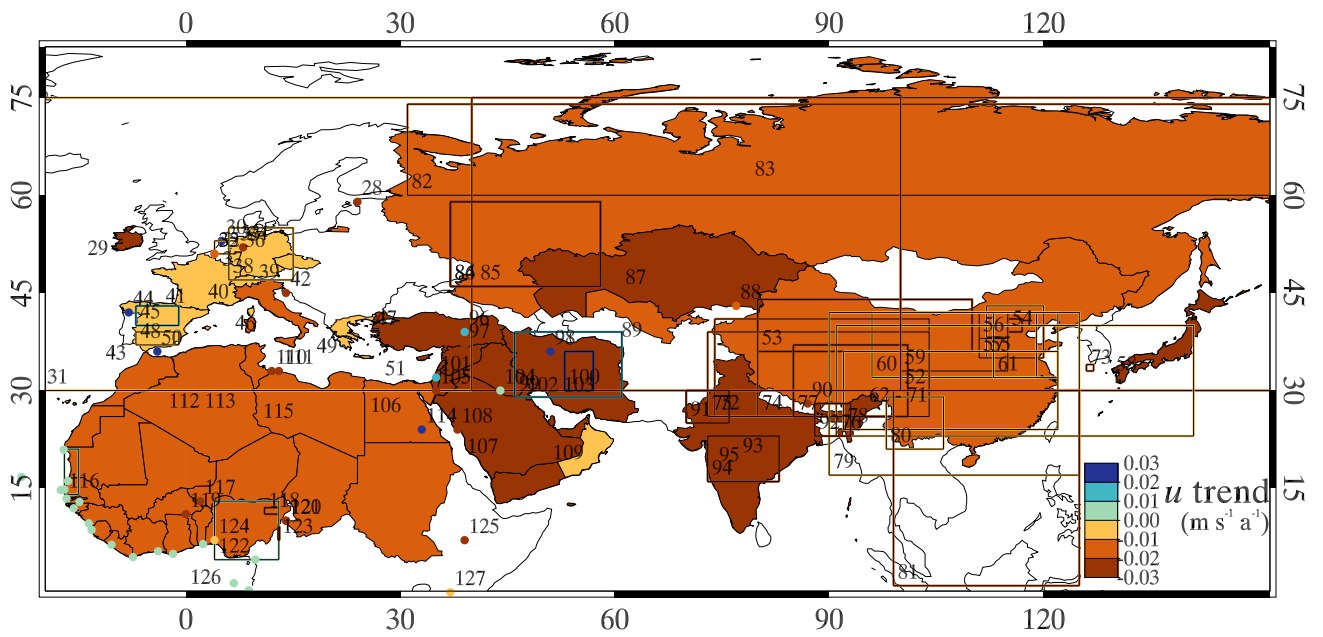
Seq	Country	Area* 1000 (km <sup>2</sup> )	Continent	ANN	DJF	MAM	JJA	SON	Jan	Feb	Mar	Apr	May	Jun	Jul	Aug	Sep	Oct	Nov	Dec
80	Ghana	240.3	Af	9	0	22	92	30	0	0	2	18	48	82	85	45	91	51	5	0
81	United Kingdom	238.1	Eu	80	100	57	14	100	100	100	99	50	11	6	9	45	77	100	100	100
82	Romania	237.1	Eu	12	100	7	4	13	100	100	13	6	5	9	3	1	1	11	100	100
83	Laos	231.0	As	75	0	9	100	59	0	0	0	1	97	100	100	100	100	23	4	0
84	Guyana	210.3	SA	83	51	89	100	16	57	36	30	79	100	100	100	91	9	8	35	54
85	Belarus	206.0	Eu	5	100	0	0	100	100	100	95	0	0	0	0	0	29	100	100	100
86	Kyrgyzstan	200.6	As	8	94	26	0	8	96	93	64	25	14	0	0	0	0	18	71	94
87	Senegal	197.4	Af	0	0	0	40	2	0	0	0	0	0	2	45	73	63	0	0	0
88	Syria	190.0	As	1	38	1	0	0	49	25	7	1	0	0	0	0	0	0	6	41
89	Cambodia	181.9	As	58	0	10	98	100	0	0	0	2	80	94	98	98	100	100	14	0
90	Uruguay	178.4	SA	3	0	99	100	0	0	0	14	99	100	100	100	90	84	11	0	0
91	Azerbaijan	164.1	As,Eu	3	69	6	0	10	72	47	25	4	5	1	0	0	5	20	54	81
92	Tunisia	156.7	Af	0	20	0	0	0	21	17	2	0	0	0	0	0	0	1	8	21
93	Nepal	148.3	As	65	18	1	96	45	26	17	15	0	11	67	99	99	88	9	0	5
94	Tajikistan	143.9	As	32	99	62	0	19	100	95	85	62	42	1	0	0	0	33	68	97
95	Suriname	143.2	SA	100	89	100	100	0	96	95	89	100	100	100	100	69	0	0	1	77
96	Bangladesh	135.7	As	92	0	23	100	100	0	0	0	12	82	100	100	100	100	97	1	0
97	Nicaragua	129.8	NA	72	47	7	94	100	55	7	0	1	66	100	84	92	100	100	70	58
98	Greece	125.5	As,Eu	7	100	2	0	34	100	95	57	3	0	0	0	0	0	47	100	100
99	North Korea	122.8	As	81	63	1	97	70	71	43	9	2	0	21	93	100	89	8	96	85
100	Eritrea	119.9	Af	0	0	0	2	0	0	0	0	0	0	0	16	22	0	0	0	0
101	Benin	118.5	Af	0	0	0	92	0	0	0	0	0	8	48	92	86	93	4	0	0
102	Malawi	117.4	Af	6	99	32	0	0	100	99	79	30	2	0	0	0	0	0	0	94
103	Honduras	113.0	NA	50	29	0	91	97	29	12	0	0	38	94	80	86	100	99	55	42
104	Bulgaria	110.5	As,Eu	2	100	3	0	6	100	100	17	3	0	0	0	0	0	1	100	100
105	Guatemala	109.8	NA	68	23	8	98	96	24	5	1	2	51	100	94	89	100	97	58	39
106	Cuba	107.9	NA	11	3	3	59	89	3	1	0	0	78	83	28	53	90	99	14	4
107	Yugoslavia	102.7	Eu	27	100	23	0	42	100	100	39	22	10	1	0	0	17	41	100	100
108	Iceland	99.9	Eu	100	100	100	79	100	100	100	100	100	78	58	62	100	100	100	100	100
109	Liberia	95.7	Af	99	13	82	100	100	5	11	26	80	96	100	100	100	100	100	61	20
110	South Korea	94.8	As	96	85	18	100	87	84	82	27	35	6	64	100	100	100	11	83	70

Seq	Country	Area* 1000 (km <sup>2</sup> )	Continent	ANN	DJF	MAM	JJA	SON	Jan	Feb	Mar	Apr	May	Jun	Jul	Aug	Sep	Oct	Nov	Dec
111	Hungary	92.2	Eu	0	100	0	0	11	100	100	0	0	0	0	0	0	0	4	100	100
112	Portugal	90.4	Eu,Af	27	100	24	0	54	100	100	55	24	1	0	0	0	1	70	100	100
113	Jordan	87.4	As	0	9	0	0	0	12	7	0	0	0	0	0	0	0	0	0	9
114	French Guiana	83.7	SA	100	100	100	100	0	100	100	100	100	100	100	100	34	0	0	34	100
115	Austria	82.9	Eu	77	100	61	57	90	100	100	83	56	47	57	54	59	66	88	100	100
116	Czech Republic	78.3	Eu	18	100	5	2	76	100	100	42	3	1	3	1	4	7	70	100	100
117	Panama	73.7	NA,SA	95	20	57	99	100	14	5	4	28	98	100	97	99	100	100	100	54
118	Sierra Leone	73.1	Af	97	0	15	100	100	0	0	0	5	99	100	100	100	100	100	76	0
119	Georgia	69.7	As,Eu	62	96	59	23	69	95	96	75	60	38	38	10	20	42	74	98	97
120	United Arab Emirates	68.2	As	0	0	0	0	0	0	0	0	0	0	0	0	0	0	0	0	0
121	Ireland	67.6	Eu	100	100	87	10	100	100	100	100	64	9	1	4	59	100	100	100	100
122	Latvia	64.7	Eu	99	100	0	0	100	100	100	100	0	0	0	0	0	100	100	100	100
123	Sri Lanka	64.7	As	64	80	33	22	100	61	34	18	58	32	24	21	20	25	99	100	100
124	Lithuania	64.4	Eu	44	100	0	0	100	100	100	100	0	0	0	0	0	80	100	100	100
125	Svalbard	60.1	Eu	100	100	100	13	100	100	100	100	100	28	1	2	93	100	100	100	100
126	Togo	56.2	Af	1	0	2	83	6	0	0	0	2	25	77	82	78	90	8	0	0
127	Croatia	53.5	Eu	57	100	29	0	94	100	100	60	34	6	2	0	0	34	93	100	100
128	Costa Rica	52.9	NA	94	44	60	100	100	39	26	17	47	97	100	96	100	98	100	89	60
129	Bosnia & Herzegovina	51.4	Eu	78	100	54	0	99	100	100	84	60	7	1	0	0	31	98	100	100
130	Slovakia	48.6	Eu	34	100	18	12	72	100	100	45	13	12	19	5	12	16	61	100	100
131	Dominican Republic	47.3	NA	29	16	16	26	70	10	4	0	6	70	33	19	32	55	81	56	32
132	Estonia	45.5	Eu	100	100	0	0	100	100	100	100	0	0	0	0	0	100	100	100	100
133	Switzerland	41.9	Eu	99	100	90	74	100	100	100	100	89	73	75	56	88	97	100	100	100
134	Denmark	41.1	Eu	100	100	1	0	100	100	100	100	0	0	0	0	10	100	100	100	100
135	Bhutan	39.4	As	59	0	39	80	50	0	0	0	20	54	74	92	96	74	36	0	0
136	Taiwan	36.7	As	99	48	87	100	76	43	57	65	69	100	100	100	100	96	59	33	40
137	Netherlands	34.7	Eu	100	100	3	0	100	100	100	100	13	0	0	0	0	79	100	100	100
138	Moldova	33.5	Eu	0	100	0	0	0	100	100	0	0	0	0	0	0	0	0	100	100
139	Guinea-Bissau	31.4	Af	29	0	0	100	99	0	0	0	0	0	56	100	100	100	83	0	0

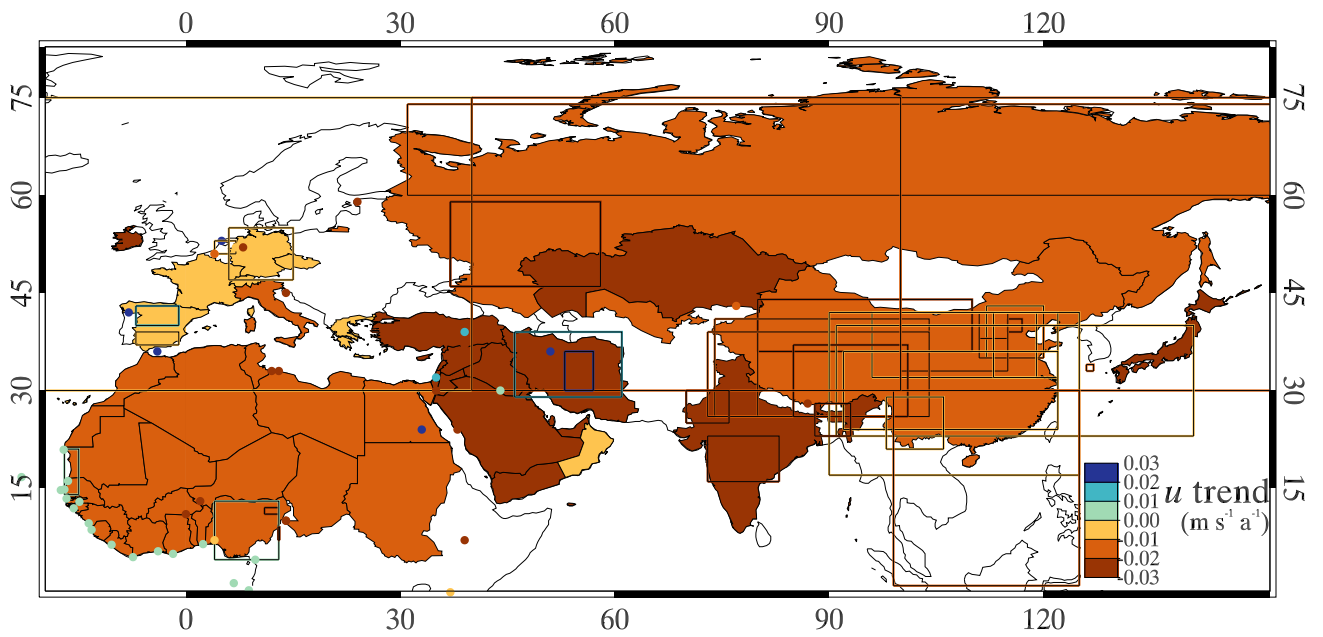
Seq	Country	Area* 1000 (km <sup>2</sup> )	Continent	ANN	DJF	MAM	JJA	SON	Jan	Feb	Mar	Apr	May	Jun	Jul	Aug	Sep	Oct	Nov	Dec
140	Lesotho	30.8	Af	2	10	3	0	2	10	15	16	3	0	0	0	0	2	9	6	
141	Belgium	30.7	Eu	97	100	23	1	100	100	100	19	0	0	1	3	42	100	100	100	
142	Armenia	30.2	As	0	83	28	0	0	89	81	51	19	26	0	0	0	2	75	86	
143	Albania	28.8	Eu	89	100	68	0	100	100	100	73	5	0	0	0	15	100	100	100	
144	Haiti	27.9	NA	42	7	38	58	86	6	2	0	30	85	65	17	65	84	91	43	16
145	Burundi	27.1	Af	8	70	88	0	5	53	67	84	100	13	0	0	0	4	75	79	
146	Equatorial Guinea	26.7	Af	100	45	100	7	100	20	65	97	100	100	59	7	7	100	100	100	47
147	Macedonia	25.3	Eu	11	100	11	0	33	100	93	37	11	2	0	0	0	37	100	100	
148	Rwanda	25.0	Af	16	23	59	0	23	16	26	38	100	53	0	0	4	26	45	25	
149	Israel	22.7	As,Af	0	44	0	0	0	46	38	2	0	0	0	0	0	0	21	45	
150	Belize	22.7	NA	80	58	3	100	100	69	4	0	0	16	100	100	85	100	100	95	76
151	Solomon Is.	21.6	Oc	100	100	100	98	99	100	100	100	100	100	97	99	97	95	99	100	100
152	Slovenia	20.6	Eu	93	100	72	16	100	100	100	91	71	28	26	9	23	88	100	100	100
153	Djibouti	20.5	Af	0	0	0	0	0	0	0	0	0	0	0	0	0	0	0	0	0
154	El Salvador	19.9	NA	63	0	0	100	100	0	0	0	0	86	100	100	100	100	100	0	0
155	New Caledonia	17.9	Oc	82	96	98	87	3	97	99	100	89	85	100	86	39	7	0	8	58
156	Fiji	17.8	Oc	100	100	100	95	97	100	100	100	100	100	99	92	71	95	91	100	100
157	Swaziland	16.8	Af	1	29	0	0	0	30	36	14	0	0	0	0	0	0	20	23	
158	Kuwait	16.7	As	0	0	0	0	0	0	0	0	0	0	0	0	0	0	0	0	0
159	East Timor	15.5	As	74	99	94	3	1	99	99	98	91	88	66	1	0	0	29	98	
160	Jamaica	11.0	NA	86	45	78	77	100	38	25	1	54	92	83	39	86	98	100	93	61
161	Lebanon	10.8	As	15	100	13	0	0	100	100	85	6	0	0	0	0	0	90	100	
162	The Bahamas	10.7	NA	18	0	0	46	82	0	9	0	0	3	63	11	40	66	86	15	0
163	Qatar	10.6	As	0	0	0	0	0	0	0	0	0	0	0	0	0	0	0	0	0
164	Falkland Is.	10.2	SA	37	0	100	100	0	0	0	15	100	100	100	100	100	43	0	0	0
165	The Gambia	10.0	Af	0	0	0	86	0	0	0	0	0	0	0	96	100	100	0	0	0
166	Cyprus	9.9	As	0	100	0	0	0	100	69	19	0	0	0	0	0	0	30	100	
167	Puerto Rico	9.1	NA	72	37	40	70	94	37	3	1	28	78	59	58	80	88	99	89	62
168	Vanuatu	8.5	Oc	100	100	100	94	77	100	100	100	100	100	100	94	66	69	62	92	90
169	Brunei	6.1	As	100	100	100	100	100	100	100	100	100	100	100	100	100	100	100	100	100



Supplementary Material Figure 1. Global distribution of observed  $u$  trends. Either points, geographic domains or countries are identified depending on the level of geographic detail provided in each study. If there are multiple studies for a country (*e.g.*, China) then the average  $u$  trend for that country is used.



Supplementary Material Figure 2. Distribution of observed  $u$  trends for Europe to East Asia. The values refer to the study numbers provided in Table 2, either points, geographic domains or countries are identified depending on the level of geographic detail provided in each study. If there are multiple studies for a country (e.g., China) then the average  $u$  trend for that country is used. This zoomed area is bounded by 18°W to 150°E and 82°N to 0°N.



Supplementary Material Figure 3. Distribution of observed  $u$  trends for Europe to East Asia. Either points, geographic domains or countries are identified depending on the level of geographic detail provided in each study. If there are multiple studies for a country (*e.g.*, China) then the average  $u$  trend for that country is used. This zoomed area is bounded by  $18^{\circ}\text{W}$  to  $150^{\circ}\text{E}$  and  $82^{\circ}\text{N}$  to  $0^{\circ}\text{N}$ .

Supplementary Material Table 2. Comparing trend and significance test results for parametric and non-parametric statistical tests. Under the column ‘Trends’ OLR (an abbreviation of ordinary linear regression) is a parametric test while the Theil-Sen’s test is a non-parametric test. Sites are from Australia from 1975-2008 using the data presented in McVicar et al. (2008). Long and lat are abbreviations for longitude and latitude, respectively.

Site Information					Trends ( $\text{m s}^{-1} \text{a}^{-1}$ )	
N	Site ID	Name	Long (DD)	Lat (DD)	OLR	Theil-Sen’s
1	2012	Halls Creek Airport	127.7	-18.2	-0.008	-0.011
2	2014	Kimberley Res. Station	128.7	-15.7	-0.009	-0.010
3	3003	Broome Airport	122.2	-18.0	-0.012	-0.011
4	4032	Port Hedland Airport	118.6	-20.4	-0.019	-0.017
5	5007	Learmonth Airport	114.1	-22.2	-0.002	-0.004
6	6011	Carnarvon Airport	113.7	-24.9	-0.008	-0.009
7	7045	Meekatharra Airport	118.5	-26.6	-0.019	-0.017
8	8051	Geraldton Airport	114.7	-28.8	0.000	0.012
9	9592	Pemberton	116.0	-34.5	-0.007	-0.007
10	9741	Albany Airport	117.8	-34.9	0.002	0.001
11	9789	Esperance	121.9	-33.8	0.002	0.003
12	12038	Kalgoorlie-Boulder Airport	121.5	-30.8	-0.010	-0.011
13	13017	Giles Meteorological Office	128.3	-25.0	0.004	0.001
14	14015	Darwin Airport	130.9	-12.4	-0.013	-0.015
15	15135	Tennant Creek Airport	134.2	-19.6	-0.011	-0.011
16	15590	Alice Springs Airport	133.9	-23.8	0.008	0.001
17	16001	Woomera Aerodrome	136.8	-31.2	0.004	0.004
18	18012	Ceduna Amo	133.7	-32.1	-0.005	-0.005
19	18139	Polda (Gum View)	135.3	-33.5	-0.011	-0.013
20	23343	Rosedale (Turretfield Research)	138.8	-34.6	-0.009	-0.010
21	26021	Mount Gambier Aero	140.8	-37.8	-0.027	-0.025
22	29127	Mount Isa Aero	139.5	-20.7	-0.008	-0.007
23	31011	Cairns Aero	145.8	-16.9	0.011	0.013
24	36031	Longreach Aero	144.3	-23.4	-0.005	-0.005
25	39083	Rockhampton Aero	150.5	-23.4	-0.001	-0.002
26	44021	Charleville Aero	146.3	-26.4	-0.008	-0.010
27	48027	Cobar Mo	145.8	-31.5	-0.006	-0.006
28	59040	Coffs Harbour Mo	153.1	-30.3	-0.027	-0.028
29	61078	Williamstown RAAF	151.8	-32.8	-0.022	-0.022
30	61089	Scone SCS	150.9	-32.1	-0.012	-0.012
31	61242	Cessnock (Nulkaba)	151.4	-32.8	-0.018	-0.018
32	63005	Bathurst Agricultural Station	149.6	-33.4	-0.016	-0.015
33	66037	Sydney Airport AMO	151.2	-33.9	-0.013	-0.014
34	70014	Canberra Airport	149.2	-35.3	-0.011	-0.010
35	72150	Wagga Wagga AMO	147.5	-35.2	-0.006	-0.007
36	76031	Mildura Airport	142.1	-34.2	-0.016	-0.018
37	82039	Rutherglen Research	146.5	-36.1	-0.009	-0.010
38	85072	East Sale Airport	147.1	-38.1	-0.015	-0.016
39	88023	Lake Eildon	145.9	-37.2	-0.001	-0.003
40	91104	Launceston Airport Comparison	147.2	-41.5	0.004	0.004
41	94069	Grove (Comparison)	147.1	-43.0	0.015	0.016
Averages for Trends					-0.008	-0.008

Supplementary Material Table 3. Comparing trend and significance test results for parametric and non-parametric statistical tests. Under the column ‘Trends’ OLR (an abbreviation of ordinary linear regression) is a parametric test while the Theil-Sen’s test is a non-parametric test. Sites are from north-east India from 1979-2000 using the data presented in Jhajharia et al (2011). NR is not relevant, as the source of data, Tocklai Tea Research Centre, do not use identification codes. Long and lat are abbreviations for longitude and latitude, respectively.

N	Site Information				Trends ( $\text{m s}^{-1} \text{a}^{-1}$ )	
	Site ID	Name	Long (DD)	Lat (DD)	OLR	Theil-Sen’s
1	NR	Jorhat	94.2	26.8	-0.009	-0.009
2	NR	Silcoorie	92.8	24.8	-0.009	-0.008
3	NR	Margherita	95.5	27.3	-0.012	-0.012
4	NR	Nagrakata	88.9	26.9	-0.012	-0.013
5	NR	Thakurbari	92.7	26.8	-0.025	-0.024
6	NR	Nagrifarm	88.2	26.9	-0.035	-0.031
7	NR	Gungaram	88.8	26.6	-0.023	-0.021
8	NR	Chuapara	89.5	26.7	-0.011	-0.011
Averages for Trends					-0.016	-0.017

Supplementary Material Table 4. Comparing trend and significance test results for parametric and non-parametric statistical tests. Under the column ‘Trends’ OLR (an abbreviation of ordinary linear regression) is a parametric test while the Theil-Sen’s test is a non-parametric test. Trends from 1961-2004 are provided for 17 sites located in the southern peninsular of India (specifically in the Godavari river basin). Long and lat are abbreviations for longitude and latitude, respectively.

N	Site Information				Trends ( $\text{m s}^{-1} \text{ a}^{-1}$ )	
	Site ID	Name	Long (DD)	Lat (DD)	OLR	Theil-Sen’s
1	43009	Ahmednagar	74.8	19.1	-0.034	-0.033
2	42933	Akola	77.0	20.7	-0.047	-0.027
3	42937	Amraoti	77.8	20.9	-0.040	-0.039
4	43014	Aurangabad	75.4	19.9	-0.043	-0.047
5	43125	Bidar	77.5	17.9	-0.030	-0.035
6	42931	Buldana	76.2	20.5	-0.020	-0.017
7	43029	Chandrapur	79.3	20.0	-0.018	-0.022
8	43128	Hyderabad	78.5	17.5	-0.023	-0.025
9	43041	Jagdapur	82.0	19.1	-0.020	-0.022
10	42925	Malegaon	74.5	20.6	-0.070	-0.064
11	42867	Nagpur	79.1	21.1	-0.039	-0.042
12	43021	Nanded	77.3	19.1	-0.020	-0.025
13	43081	Nizamabad	78.1	18.7	-0.040	-0.039
14	42920	Ozar	72.9	20.4	-0.050	-0.044
15	43017	Parbhani	76.8	19.3	-0.040	-0.039
16	43086	Ramagundam	79.4	18.8	-0.026	-0.030
17	42943	Yeotmal	75.2	20.4	-0.039	-0.040
Averages for Trends					-0.035	-0.035

Supplementary Material Table 5. Comparing trend and significance test results for parametric and non-parametric statistical tests. Under the column ‘Trends’ LReg (an abbreviation of linear regression) is a parametric test while the Theil-Sen’s test is a non-parametric test. Sites are from Iran from 1966-2005 using the data obtained from the Islamic Republic of Iran Meteorological Organization (IRIMO). Long and lat are abbreviations for longitude and latitude, respectively.

Site Information					Trends (m s <sup>-1</sup> a <sup>-1</sup> )	
N	Site ID	Name	Long (DD)	Lat (DD)	LReg	Theil-Sen’s
1	40831	Abadan	48.3	30.4	-0.012	-0.014
2	40800	Esfahan	51.7	32.6	-0.026	-0.023
3	40718	Anzali	49.5	37.5	+0.009	+0.012
4	40811	Ahwaz	48.7	31.3	-0.010	-0.003
5	40809	Birjand	59.2	32.9	-0.024	-0.025
6	40706	Tabriz	46.3	38.1	+0.000	+0.007
7	40762	Torbate H.	59.2	35.3	+0.006	-0.000
8	40754	Tehran	51.3	35.7	-0.007	-0.007
9	40898	Chabahar	60.6	25.3	+0.033	+0.022
10	40829	Zabol	61.5	31.0	+0.079	+0.077
11	40856	Zahedan	60.9	29.5	-0.003	-0.002
12	40729	Zanjan	48.5	36.7	+0.043	+0.043
13	40743	Sabzevar	57.7	36.2	-0.015	+0.005
14	40757	Semnan	53.6	35.6	+0.015	+0.007
15	40747	Sanandaj	47.0	35.3	+0.001	+0.000
16	40848	Shiraz	52.6	29.5	-0.014	-0.014
17	40859	Fassa	53.7	29.0	-0.036	-0.038
18	40731	Qazvin	50.0	36.3	-0.029	-0.027
19	40841	Kerman	57.0	30.3	-0.038	-0.026
20	40738	Gorgan	54.3	36.9	+0.017	+0.012
21	40745	Mashhad	59.6	36.3	+0.025	+0.026
22	40767	Hamadan (nojeh)	48.7	35.2	-0.008	-0.006
Averages for Trends					+0.000	+0.001

Supplementary Material Table 6. Relative changes in Penman's  $ET_p$  (%) given 5%, 10% and 20% changes in  $u$ . The vapor pressure deficit ( $D$ ) is calculated at three air temperatures which influence the saturation vapor pressure ( $e_s$ ). Values are calculated at the intersections of  $u$  incrementing by 2  $m\ s^{-1}$  and  $D$  incrementing by 1 kPa for the 9 panels shown in Figure 8.

$u$ ( $m\ s^{-1}$ )	$D$ (kPa)	$du = 5\%$						$du = 10\%$						$du = 20\%$					
		0.1	2	4	6	8	10	0.1	2	4	6	8	10	0.1	2	4	6	8	10
$T_a = 10\ ^\circ C$	5	0.17	2.07	2.93	3.40	3.69	3.90	0.34	4.14	5.86	6.80	7.39	7.80	0.68	8.29	11.72	13.59	14.78	15.59
	4	0.16	1.97	2.83	3.31	3.61	3.83	0.32	3.95	5.66	6.62	7.23	7.65	0.63	7.89	11.32	13.23	14.46	15.30
	3	0.14	1.83	2.68	3.17	3.49	3.71	0.28	3.66	5.36	6.34	6.98	7.42	0.56	7.31	10.71	12.67	13.95	14.85
	2	0.11	1.59	2.42	2.92	3.26	3.50	0.23	3.19	4.84	5.84	6.52	7.01	0.46	6.38	9.67	11.68	13.04	14.01
	1	0.07	1.15	1.87	2.37	2.73	3.00	0.15	2.31	3.75	4.73	5.45	6.00	0.30	4.61	7.49	9.47	10.90	11.99
	0.1	0.01	0.19	0.37	0.54	0.69	0.83	0.02	0.38	0.74	1.07	1.38	1.67	0.04	0.77	1.48	2.14	2.76	3.33
$T_a = 25\ ^\circ C$	5	0.12	1.65	2.49	2.99	3.32	3.56	0.24	3.31	4.97	5.97	6.64	7.12	0.48	6.62	9.94	11.95	13.28	14.24
	4	0.11	1.52	2.33	2.83	3.18	3.43	0.21	3.03	4.66	5.67	6.35	6.85	0.43	6.07	9.31	11.33	12.71	13.71
	3	0.09	1.33	2.11	2.61	2.96	3.23	0.18	2.67	4.21	5.22	5.93	6.45	0.36	5.33	8.42	10.44	11.85	12.90
	2	0.07	1.07	1.77	2.25	2.61	2.89	0.13	2.15	3.54	4.51	5.22	5.78	0.27	4.29	7.07	9.01	10.45	11.55
	1	0.04	0.68	1.19	1.60	1.93	2.20	0.08	1.35	2.39	3.20	3.85	4.39	0.16	2.71	4.77	6.40	7.71	8.79
	0.1	0.00	0.09	0.17	0.26	0.34	0.41	0.01	0.18	0.35	0.51	0.67	0.83	0.02	0.35	0.70	1.03	1.35	1.66
$T_a = 40\ ^\circ C$	5	0.08	1.20	1.93	2.43	2.79	3.06	0.15	2.39	3.86	4.86	5.57	6.12	0.31	4.79	7.73	9.71	11.15	12.23
	4	0.07	1.06	1.74	2.23	2.58	2.86	0.13	2.11	3.49	4.45	5.17	5.72	0.26	4.22	6.97	8.91	10.34	11.45
	3	0.05	0.88	1.50	1.96	2.31	2.58	0.11	1.76	3.00	3.91	4.61	5.17	0.21	3.53	6.00	7.82	9.23	10.34
	2	0.04	0.66	1.17	1.57	1.90	2.17	0.08	1.33	2.34	3.14	3.79	4.33	0.15	2.65	4.68	6.29	7.59	8.66
	1	0.02	0.38	0.71	0.99	1.24	1.46	0.04	0.76	1.41	1.98	2.48	2.92	0.08	1.52	2.83	3.96	4.95	5.83
	0.1	0.00	0.04	0.09	0.13	0.17	0.21	0.00	0.09	0.17	0.26	0.34	0.42	0.01	0.18	0.35	0.52	0.68	0.85